ABSTRACT

CARBON AND OXYGEN PRODUCTION DURING THE HELIUM BURNING PHASE IN INTERMEDIATE MASS STARS

by

Lawrence Edward Turner, Jr.

Stars of 5.0 M_o, 7.0 M_o, and 15.0 M_o are evolved from a homogeneous initial composition of extreme population I until core helium burnout. Helium burning reactions through neon-alpha are considered. The carbon-alpha reaction rate is obtained from an R-matrix model of the 1^- states in ^{16}O. The equation of state includes ionization and degeneracy. Neutrino cooling is computed in hydrogen free regions.

The evolution of the 7.0 M_o star is repeated with a different value of the carbon-alpha reaction rate. This is used to test the feasibility of evolving only the core of the star to investigate further the effects of the reaction rates on the end abundances.

The evolutions of the core agree quite well with the evolutionary sequences of the entire star. The core takes about 1/12 the computer time that is needed for the entire star.

The uncertainties in the triple-alpha rate lead to an uncertainty in the final abundance of carbon of about 20 percent. A large range of the carbon-alpha reaction rate is considered. The reduced level width of the 7.12 MeV state is varied from 0.005 to 0.10 MeV. The effect is to change the final carbon abundance from about 0.66 to 0.03. The effect of the different conditions due to the mass of the star is quite small.

A large uncertainty does arise from the growing convective core. This is due to the exact method by which convection is handled. No semi-convection is considered in this investigation. The maximum effect is estimated to reduce the final carbon abundance by about 20 percent.

The conditions of helium burning are such as to produce a constant density and a constant energy generation rate situation. This is a better approximation than constant density and temperature. The fixed conditions that best reproduce the end abundances are those that occur when the energy generation rates due to the triple-alpha and the carbon-alpha reactions are equal.

CARBON AND OXYGEN PRODUCTION DURING THE HELIUM BURNING PHASE IN INTERMEDIATE MASS STARS

by

Lawrence Edward Turner, Jr.

A THESIS

Submitted to
Michigan State University
in partial fulfillment of the requirements
for the degree of

DOCTOR OF PHILOSOPHY

Department of Physics

1971

to my Anita

ACKNOWLEDGMENTS

I first wish to express my thanks to Dr. Erik Zimmermann who advised me throughout this research. It was he who provided the code that served as a basis for the program used and made the largest contribution to my understanding of stellar structure and evolution.

I am also grateful to Dr. Sam Austin whose knowledge of nuclear physics and reaction rates was invaluable and whose course in nuclear astrophysics suggested the topic for this project.

I am thankful to Dr. F. Barker for his development of the R-matrix model of the oxygen nucleus.

I acknowledge the support of a National Science Foundation traineeship for the past two years. Use of the Michigan State University computing facilities was also made possible, in part, through support from the National Science Foundation.

Both the departments of Astronomy and Physics at Michigan State University provided every possible opportunity and the inspiration for study and learning.

I am very appreciative of the encouragement I have received from my family, my committee, and all my friends at Michigan State University and elsewhere.

And most importantly, I wish to express a special thanks to my wife, Anita, to whom this work is gratefully dedicated.

TABLE OF CONTENTS

APPENDIX Page

LIST OF TABLES

TABLE Page

LIST OF FIGURES

CHAPTER I

INTRODUCTION

Knowest thou the ordinances of heaven? canst thou set the dominion thereof in the earth? Job 38:33

I-1. General effects of nuclear burning

During the helium burning phase of stellar evolution several different elements are synthesized. The main products are those elements whose nuclei can be thought of as containing an integer multiple of alpha particles: ^{12}C, ^{16}O, ^{20}Ne, ^{24}Mg, and possibly ^{28}Si. These are produced through the chain of reactions:

$$3\,^4He \rightarrow {}^{12}C \qquad \text{triple-alpha,}$$

$$^{12}C + {}^4He \rightarrow {}^{16}O \qquad \text{carbon-alpha,}$$

$$^{16}O + {}^4He \rightarrow {}^{20}Ne \qquad \text{oxygen-alpha,}$$

$$^{20}Ne + {}^4He \rightarrow {}^{24}Mg \qquad \text{neon-alpha,}$$

$$^{24}Mg + {}^4He \rightarrow {}^{28}Si \qquad \text{magnesium-alpha.}$$

There is also the possibility of alpha reactions on ^{14}N, which is left over from the hydrogen burning via the CNO cycle. The nitrogen-alpha reaction leads to the production of ^{18}O and ^{22}Ne.

The energy released by the above reactions serve temporarily to halt the gravitational contraction of the star and provide a relatively long quasi-static situation. The temperature dependence of the energy generation rate per unit mass, ε, may be extracted as

$$\epsilon = ST^n \tag{1.1}$$

where T is the temperature and S contains the cross-section factors and the density and composition dependence. The exponent n also contains part of the cross-section dependence and changes with the temperature. For the triple-alpha process n varies from 40 to 20 as the temperature varies between 10^8 and 2×10^8 °K, the approximate range in which helium burning takes place. For the carbon-alpha reaction n≈20 over the range.

Nearly all the helium burning takes place in a very small region of the star. The numerical value of ϵ is determined by the luminosity of the star, which depends largely on the opacity through the bulk of the star. For moderate changes in S the star will adjust itself to give approximately the same energy generation rate by an extremely small change in the temperature.

The rate of change of the helium concentration, which determines the time scale for the helium burning phase, is proportional to the energy generation rate. Thus

$$\frac{dY}{dt} = - E\epsilon \tag{1.2}$$

where Y is the fractional abundance by mass of helium and E is the reciprocal of the energy released per unit mass of the interacting nuclei. If S is changed, the star will adjust its structure to produce approximately the same ϵ, and dY/dt will be roughly unchanged.

If two or more reactions are competing, then the term on the right in equation (1.2) must be replaced by a summation over all contributing reactions. Now if one of the reaction rates is changed, the star will adjust to give the same total ϵ, but the values of the individual contributions will be altered, and since E is not the same for all reactions

dY/dt will be changed. This alteration in the time scale will not be large since all the reactions destroy helium and the E's are not greatly different.

Thus the structure and immediate evolution of the stars are relatively insensitive to the values of the reaction rates chosen. However, the relative abundances of the various end products are extremely dependent on the relative reaction rates. For an element heavier than helium, there are both reactions that destroy it and reactions that create it. If, for example, the destruction rate is increased, then the elements heavier than it will be enhanced at its expense.

The relative values of the reaction rates will depend not only on the specific parameters chosen but on the conditions where the nuclear burning is taking place. The reaction rates have different density dependence as well as different temperature dependence. In a massive star the center is less dense and hotter than in a light star. Thus there may be a difference in the final abundances due to the mass of the star.

Unfortunately, these reaction rates are not extremely well known. The values of the cross-sections can not be measured in the laboratory in the same range of energies that are important to the production of energy in the interiors of stars. One must be content in devising a model of the reaction process that can be checked by laboratory measurements and then extrapolate to the range of astrophysical interest.

There are uncertainties in the laboratory measurements as well as an uncertainty in the model itself. Thus there is a range of possible values for the parameters of each reaction rate. To get a clear picture of the helium burning phase several evolutionary sequences must be made at different masses and with the different possible values of the

reaction rate parameters. However, one need not consider all possible values for all the reactions that may take place during helium burning. The oxygen-alpha reaction is very small compared to the carbon-alpha, thus very little oxygen will be destroyed. A large error in the final abundance of neon or the heavier elements will have a negligible effect on the further evolution of the star since the maximum abundance of these elements is extremely small.

I-2. Historical

The most obvious helium burning reaction of $^4He + {}^4He \rightarrow {}^8Be$ gave rise to much puzzlement in early investigators. This isotope is unstable and spontaneously decays back into two alpha particles. Salpeter (1952) showed that even though the decay was rapid a sufficient equilibrium concentration of ^8Be would exist to allow an additional alpha particle to interact to produce ^{12}C. Once this step was over, then succeeding alpha captures would produce ^{16}O and the rest of the alpha elements.

The effect of the reaction rates on nucleosynthesis was studied by Cameron (1957) by assuming that the temperature and density were constant. The reaction rates then become dependent only on the abundances themselves and can be numerically integrated. In the interior of a star both the temperature and the density change slowly. However, the largest changes are near the beginning of the helium burning where no carbon has been produced so the only reaction is the triple-alpha and near the end where the very small helium abundance greatly reduces the triple-alpha. Thus for most of the helium burning phase where there is competition between the triple-alpha and the carbon-alpha reactions there are also only small changes in the density and the temperature.

An early evolutionary calculation was made by Hayashi, Hoshi, and Sugimoto (1962). They constructed by semi-analytical methods the evolutionary tracks for a number of stars with different mass and different values of the carbon-alpha reaction rate. The most likely value of this rate produced approximately 50 percent carbon in a 15.6 solar mass star. The carbon abundance slowly increased as the mass of the star was decreased.

Cox and Salpeter (1964) and Deinzer and Salpeter (1964) approached the problem by constructing a series of hydrogen-free models. They used an integration method for solving the structure equations and considered the production of elements through silicon. The evolution was approximated by neglecting the gravitational contribution to the energy equation and by assuming that all of the nuclear burning took place in a convective core.

The total mass of these stars must be matched with the mass of the cores in ordinary stars which have large hydrogen rich envelopes to get a correct comparison. But the abundance of carbon produced was approximately the same as that calculated by Hayashi, et al. (1962) for the more massive stars. Below about one solar mass the final abundance of carbon decreased with decreasing mass. Virtually no neon or heavier elements were produced for stars with less mass than about 8 solar masses which would correspond to an ordinary star of perhaps 30 solar masses.

Hofmeister (1967) carried through the evolutionary tracks of a 5 and a 9 solar mass star for both an extreme population I and a median population I composition. The calculation was done with a differencing method based on the work of Henyey, et al. (1959). Again approximately 50 percent carbon was produced and virtually no neon.

Iben in a series of papers, (1965a, 1965b, 1966a, 1966b, and 1966c), presented the results of computations by the Henyey method for stars of 3, 5, 9, and 15 solar masses. The composition was a median population I. Neutrino cooling was included but without the pair-annihilation process which becomes an important part of the total neutrino cooling in the more massive stars near the end of core helium burning. The evolution was carried to near the end of the core helium burning phase for two different values of the carbon-alpha reaction rate. He included the weak screening contribution to the reaction rates and the nitrogen-alpha reaction which ignited sometime before the triple-alpha process and thus was a major influence on the evolution of the star for a short period of time. The oxygen-alpha reaction was not included.

The tracks in the HR diagram were altered slightly during the core helium burning phase and the time scale was decreased slightly when the carbon-alpha reaction rate was decreased by a factor of 10. For the value of the reaction rate that is most reasonable approximately 50 percent carbon was produced with a less amount in the more massive stars.

I-3. Research purpose

The purpose of the present investigation is to determine the effect of the uncertainties in the triple-alpha and the carbon-alpha reaction rates on the relative abundances of the various end products of the core helium burning phase in upper main sequence stars. These are the stars that make the most contribution to the nuclcosynthesis of carbon and oxygen. Stars with a mass less than about 5 solar masses have such a long lifetime that they do not contribute greatly. Their structure is

such that large amounts of computer time are necessary to follow them through the helium burning phase. Above about 15 solar masses the number of stars decreases rapidly so that the contribution to the observed abundances is again small.

The oxygen-alpha reaction also contains large uncertainties but because it is small very little neon will be produced. The major end products of helium burning will be ^{12}C and ^{16}O. The relative abundances of these two elements will depend on the relative values of the triple-alpha and the carbon-alpha reaction rates.

The initial composition will be taken as the extreme population I with

$$X = 0.602, \qquad Y = 0.354, \qquad Z = 0.044$$

where X, Y, and Z represent the fractional abundance by mass of hydrogen, helium, and the heavier elements respectively. The initial star will be taken to be homogeneous and static.

Recent work by Upton and Bohannan (1971) and Turner and Zimmermann (1971) indicate that this value of Z most closely agrees with the observed mass-radius relationship for these stars. The value of Y is perhaps large but opacity tables for this composition are available. In the core during the helium burning there is no hydrogen present. The exact amount of hydrogen in the envelope can affect the evolutionary track of the star in the H-R diagram (Robertson 1971), but the effect on the core should be very small.

With this value of Z there should be a substantial amount of ^{14}N left over from the CNO cycle. Each ^{14}N nucleus leads to the destruction of two alphas, but because the nitrogen nucleus is so much more massive than the alpha the maximum helium that could be consumed is about 1.5

percent. Iben found that the nitrogen-alpha reaction ignited before the triple-alpha, but recent measurements by Parker (1968) indicate that the value used by Iben was many times too large. This conclusion is still very uncertain, but one may expect that the actual value is somewhere between these two limits. Probably all the nitrogen will react with the helium sometime during the course of helium burning, but it will change the helium available to the triple-alpha and the carbon-alpha reactions by a very small amount. Only if the nitrogen-alpha reaction ignites before the triple-alpha will it have a major influence on the star, and then it will be before the main phase of helium burning so that there will be little effect on the relative abundances of carbon and oxygen. The nitrogen-alpha reaction will not be included in the present investigation.

There are various approximations that may be made to investigate this problem. However, to determine the validity of these approximations one must compare them to a complete evolutionary sequence. Several different evolutionary sequences will be computed at different masses. At least two will be done at one mass but with different values of the reaction rate parameters. This will serve as a basis for comparing various approximations. These approximations, if they are reasonable, may be used to investigate the problem more thoroughly than would be possible using only complete evolutionary sequences.

One approximation that will be examined is that of evolving only the core of a star, using as outer boundary conditions the values of the structure variables at the edge of the core obtained from the evolutionary sequence of the entire star. The approximation is that the structure of the star is relatively insensitive to the reaction rates.

If the central conditions of the star are known during the helium burning phase, then the effects of the convective core that is present during most of the helium burning may be isolated by integrating the reaction rates assuming that no mixing is taking place. Again, these conditions can only be obtained from the complete evolutionary sequence of a star.

CHAPTER II

STELLAR STRUCTURE

II-1. Introduction

The structure of a star is the solution to a set of coupled first-order differential equations. These time-dependent equations are best solved by the Henyey method, a differencing method introduced by Henyey and his co-workers (1959, 1964). This method is described most readably by Kippenhahn, Weigert, and Hofmeister (1967). The particular choice of transformed variables is due to Zimmermann (1970). The development below will closely follow his presentation.

II-2. Structure equations

The equations of stellar structure, under the assumption of spherical symmetry and hydrostatic equilibrium, are given by Schwarzchild (1958). Writing them in the Lagrangian form with mass as the independent variable one obtains:

$$\frac{\partial L_r}{\partial M_r} = \varepsilon_n - \varepsilon_\nu + \varepsilon_g \qquad \text{energy equation,} \qquad (2.1)$$

$$\frac{\partial P}{\partial M_r} = -\frac{GM_r}{4\pi r^4} \qquad \text{hydrostatic equation,} \qquad (2.2)$$

$$\frac{\partial r}{\partial M_r} = \frac{1}{4\pi r^2 \rho} \qquad \text{continuity equation,} \qquad (2.3)$$

$$\frac{\partial T}{\partial M_r} = \begin{cases} -\dfrac{3\kappa L_r}{64\pi^2 acr^4 T^3} & \text{radiative transport,} \quad (2.4a) \\ \dfrac{\partial P}{\partial M_r}\dfrac{T}{P}\nabla_a & \text{convective transport.} \quad (2.4b) \end{cases}$$

where the symbols are defined as:

r is the distance from the center of the star,

M_r is the mass interior to a shell of radius r,

L_r is the luminosity at the shell M_r,

P is the pressure at shell M_r,

T is the temperature at shell M_r,

ε_n is the nuclear energy generation rate,

ε_ν is the neutrino cooling rate,

ε_g is the gravitational energy generation rate,

ρ is the density,

κ is the opacity,

∇_a is the adiabatic temperature gradient $\left(\frac{d \ln T}{d \ln P}\right)$,

G is the gravitation constant,

a is the radiation density constant,

c is the speed of light.

The above equations are in CGS units. The correct transport equation, equation (2.4a) or (2.4b), is the one that gives the smallest absolute value temperature gradient at that point.

In addition to these four structure equations several auxiliary equations must be specified:

$$\rho = \rho(P,T,\{X_i\}) \qquad \text{equation of state,} \qquad (2.5)$$

$$\varepsilon_n = \varepsilon_n(\rho,T,\{X_i\}) \qquad \text{nuclear energy generation,} \qquad (2.6)$$

$$\epsilon_\nu = \epsilon_\nu(\rho,T,\{X_i\}) \qquad \text{neutrino cooling rate,} \qquad (2.7)$$

$$\kappa = \kappa(\rho,T,\{X_i\}) \qquad \text{opacity equation,} \qquad (2.8)$$

$$\nabla_a = \nabla_a(\rho,T,\{X_i\}) \qquad \text{adiabatic gradient.} \qquad (2.9)$$

where $\{X_i\}$ is the set of composition variables, X_i being defined as the fractional abundance by mass of element i. These auxiliary equations will be considered in detail in a subsequent chapter.

The gravitational energy term is not included above. It is the only quantity that involves time derivatives. It is convenient to introduce it explicitly at this point. The gravitational energy term is

$$\epsilon_g = -C_p \frac{\partial T}{\partial t} + \frac{\delta}{\rho} \frac{\partial P}{\partial t} \qquad (2.10)$$

where C_p is the specific heat at constant pressure. And δ is defined as

$$\delta = -\left(\frac{\partial \ln \rho}{\partial \ln T}\right)_p. \qquad (2.11)$$

The subscript p indicates that the derivative is taken at constant pressure.

Then equation (2.1) becomes

$$\frac{\partial L_r}{\partial M_r} = \epsilon_n - \epsilon_\nu - C_p \frac{\partial T}{\partial t} + \frac{\delta}{\rho} \frac{\partial P}{\partial t}. \qquad (2.12)$$

These structure equations are extremely non-linear and the structure variables vary over many orders of magnitude between the center and the surface of a star. They must be solved by numerical means, hence it is desirable to make them as linear as possible. To achieve this define the following transformed variables:

$$\xi = \ln\left(1-M_r/M\right) = \ln(1-q), \qquad (2.13)$$

$$p = \ln P, \qquad (2.14)$$

$$\theta = \ln T, \tag{2.15}$$

$$x = \ln r, \tag{2.16}$$

$$\ell = (L_r/L_o)^{1/5}, \tag{2.17}$$

$$y = \ln \rho, \tag{2.18}$$

$$K = \ln \kappa. \tag{2.19}$$

Here M is the total mass of the star and L_o is a constant taken to be 10^{34} erg/sec. If a temperature inversion appears in the star, L_r would be negative and thus a logarithmic variable is prohibited.

The structure equations, equations (2.2) through (2.4b) and (2.12), may now be written in terms of these transformed variables:

$$5L_o\ell^4 \frac{\partial \ell}{\partial \xi} = -Me^{\xi}\left(\varepsilon_n - \varepsilon_\nu - C_p \frac{\partial e^{\theta}}{\partial t} + \delta e^{-y} \frac{\partial e^{p}}{\partial t}\right), \tag{2.20}$$

$$\frac{\partial p}{\partial \xi} = \frac{GM^2}{4\pi}\left(1-e^{\xi}\right)e^{\xi} - 4x - p, \tag{2.21}$$

$$\frac{\partial x}{\partial \xi} = -\frac{M}{4\pi} e^{\xi} - 3x - y, \tag{2.22}$$

$$\frac{\partial \theta}{\partial \xi} = \begin{cases} \dfrac{3ML_o}{64\pi^2 ac} \ell^5 e^{\xi} + K - 4\theta - 4x & \text{radiative,} \quad (2.23a) \\ \dfrac{\partial p}{\partial \xi} \nabla_a & \text{convective.} \quad (2.23b) \end{cases}$$

II-3. Boundary conditions

To completely specify the star suitable boundary conditions must be imposed. The structure equations become singular at both the center and the surface of the star.

At the center of the star r is zero and thus M_r is also zero. L_r is also taken to be zero, but T and P take on finite values designated

as T_c and P_c respectively. The singularities in the structure equations may be removed by expanding them over a small region M_r with the auxiliary variables assumed constant. This will then be the smallest shell for which the structure equations themselves are applied. From Kippenhahn, Weigert, and Hofmeister (1967), these conditions become:

$$L_r = M_r (\varepsilon_n - \varepsilon_\nu + \varepsilon_g)_c, \tag{2.24}$$

$$P = P_c - \tfrac{1}{2}\left(\frac{4\pi}{3}\right)^{1/3} G\rho_c^{4/3} M_r^{2/3}, \tag{2.25}$$

$$r = \left(\frac{3}{4\pi}\right)^{1/3} \left(\frac{M_r}{\rho_c}\right)^{1/3}, \tag{2.26}$$

$$\frac{d \ln T}{d \ln P} = \begin{cases} \left(\dfrac{3}{16\pi acG} \dfrac{\kappa L_r P}{M_r T^4}\right)_c & \text{radiative,} \quad (2.27a) \\ \nabla_{a,c} & \text{convective.} \quad (2.27b) \end{cases}$$

Here M_r is the mass of a suitably chosen small sphere about the center.

These can be immediately written in terms of the transformed variables:

$$L_o \ell^5 = M_r (\varepsilon_n - \varepsilon_\nu + \varepsilon_g)_c, \tag{2.28}$$

$$p = p_c + \ln\left[1 - \tfrac{1}{2}\left(\frac{4\pi}{3}\right)^{1/3} GM_r e^{4y_c/3 - p_c}\right], \tag{2.29}$$

$$\ln M_r = \ln\left(\frac{4\pi}{3}\right) + y_c + 3x, \tag{2.30}$$

$$\frac{d\theta}{dp} = \begin{cases} \dfrac{3}{16\pi acG} \dfrac{L_o}{M_r} \ell^5 \left(e^{K + p_c - 4\theta_c}\right) & \text{radiative,} \quad (2.31a) \\ \nabla_{a,c} & \text{convective.} \quad (2.31b) \end{cases}$$

The outer boundary of the star presents more problems. Immediately

$$M_r = M, \quad L_r = L, \quad \text{and} \quad r = R \tag{2.32}$$

where R is the radius of the star and L is the total luminosity of the

star. The effective temperature of the star can be easily derived from the radius and luminosity, assuming the star radiates as a blackbody. But both the temperature and the pressure vary by many orders of magnitude near the surface, in a very small region of the star.

To handle the surface in a reasonable way the usual method is to compute separately a grid of envelope models covering the outer few percent of the mass for various values of the effective temperature and luminosity. These integrations then give the values of radius, luminosity, temperature, and pressure at the given fitting point M_f. The exact nature of these envelope calculations will be discussed in a subsequent chapter.

The outer boundary conditions then become expressed in terms of a simple interpolation formula, (Kippenhahn, Weigert, and Hofmeister, 1967),

$$\ln r_f = \alpha_1 \ln P_f + \beta_1 \ln T_f + \gamma_1 \tag{2.33}$$

$$\ln L_f = \alpha_2 \ln P_f + \beta_2 \ln T_f + \gamma_2 \tag{2.34}$$

The coefficients are obtained from three envelope models chosen to bracket the actual surface conditions of the star. The subscript f refers to the fitting point, chosen for the present work to be M_f=0.97M.

One additional set of parameters must be given to specify the star, and these are the set of composition parameters. Initially the star is homogeneous,but it rapidly becomes very inhomogeneous due to nuclear reactions and convective mixing. This point will be discussed in a subsequent chapter. For the present it will be assumed that the composition and the auxiliary variables are given.

II-4. Difference equations

To solve the above structure equations a differencing technique is adopted. Divide the star into concentric shells, each denoted by a subscript j and with a specific value of the mass variable ξ_j. Shells are numbered inward from j=1 at the fitting point, M_f, to j=m at the center of the star.

The transformed structure equations (2.20) through (2.23b) may be written in the form of difference equations as:

$$G_{1j} = 5L_o \ell^4_{j+\frac{1}{2}} \frac{\ell_{j+1} - \ell_j}{\xi_{j+1} - \xi_j} + Me^{\xi_{j+\frac{1}{2}}} \left(\epsilon_{n,j+\frac{1}{2}} - \epsilon_{\nu,j+\frac{1}{2}} + \epsilon_{g,j+\frac{1}{2}}\right), \tag{2.35}$$

$$G_{2j} = \frac{p_{j+1} - p_j}{\xi_{j+1} - \xi_j} - \frac{GM^2}{4\pi} \left(1 - e^{\xi_{j+\frac{1}{2}}}\right) e^{\xi_{j+\frac{1}{2}} - 4x_{j+\frac{1}{2}} - p_{j+\frac{1}{2}}}, \tag{2.36}$$

$$G_{3j} = \frac{x_{j+1} - x_j}{\xi_{j+1} - \xi_j} + \frac{M}{4\pi} e^{\xi_{j+\frac{1}{2}} - 3x_{j+\frac{1}{2}} - y_{j+\frac{1}{2}}}, \tag{2.37}$$

$$G_{4j} = \begin{cases} \dfrac{\theta_{j+1} - \theta_j}{\xi_{j+1} - \xi_j} - \dfrac{3ML_o}{64\pi^2 ac} \ell^5_{j+\frac{1}{2}} e^{\xi_{j+\frac{1}{2}} + K_{j+\frac{1}{2}} - 4\theta_{j+\frac{1}{2}} - 4x_{j+\frac{1}{2}}}, & (2.38a) \\ \dfrac{\theta_{j+1} - \theta_j}{\xi_{j+1} - \xi_j} - \left(\dfrac{\partial p}{\partial \xi}\right)_{j+\frac{1}{2}} \nabla_{a,j+\frac{1}{2}}. & (2.38b) \end{cases}$$

The variables at the half-integer points are defined by

$$\epsilon_{n,j+\frac{1}{2}} = \left(\epsilon_{n,j} \times \epsilon_{n,j+1}\right)^{\frac{1}{2}}, \tag{2.39}$$

$$\epsilon_{\nu,j+\frac{1}{2}} = \left(\epsilon_{\nu,j} \times \epsilon_{\nu,j+1}\right)^{\frac{1}{2}}, \tag{2.40}$$

$$\epsilon_{g,j+\frac{1}{2}} = - C_{p,j+\frac{1}{2}} \frac{e^{\theta_{j+\frac{1}{2}}} - e^{\theta^*_{j+\frac{1}{2}}}}{\Delta t} + \delta_{j+\frac{1}{2}} e^{-y_{j+\frac{1}{2}}} \frac{e^{p_{j+\frac{1}{2}}} - e^{p^*_{j+\frac{1}{2}}}}{\Delta t}, \tag{2.41}$$

$$v_{j+\frac{1}{2}} = \tfrac{1}{2}(v_j + v_{j+1}) \tag{2.42}$$

where v is any variable other than the ε's. The quantities p* and θ* are the values taken from the previous model with an age of Δt before the present one. These difference equations are to be applied to all the shells down to j=m-2. For the j=m-1 shell the inner boundary conditions, equations (2.28) through (2.31b), are written in the form of difference equations:

$$G_{1,m-1} = L_o \ell_{m-1}^5 - M\left(1-e^{\xi_{m-1}}\right)\left(\varepsilon_{n,m-\frac{1}{2}} - \varepsilon_{\nu,m-\frac{1}{2}} + \varepsilon_{g,m-\frac{1}{2}}\right), \tag{2.43}$$

$$G_{2,m-1} = p_{m-1} - p_m - \ln\left[1 - \tfrac{1}{2}\left(\frac{4\pi}{3}\right)^{1/3} GM^{2/3}\left(1-e^{\xi_{m-1}}\right)^{2/3} e^{4y_m/3} - p_m\right], \tag{2.44}$$

$$G_{3,m-1} = \ln\left(\frac{3M}{4\pi}\right) + \ln\left(1-e^{\xi_{m-1}}\right) - y_m - 3x_{m-1}, \tag{2.45}$$

$$G_{4,m-1} = \begin{cases} \dfrac{\theta_m - \theta_{m-1}}{p_m - p_{m-1}} - \dfrac{3}{32\pi acG}\dfrac{L_o}{M}\ell_{m-1}^5 \dfrac{e^{K_{m-1} + p_{m-1} - 4\theta_{m-1}}}{\left(1-e^{\xi_{m-\frac{1}{2}}}\right)}, & (2.46a) \\ \dfrac{\theta_m - \theta_{m-1}}{p_m - p_{m-1}} - \nabla_{a,m-\frac{1}{2}}\,. & (2.46b) \end{cases}$$

A factor of $\frac{1}{2}$ appears in the second term of equation (2.46a) since a better average is obtained by averaging ∇_r, the radiative gradient, rather then using equation (2.31a) exactly as written.

For the outer boundary conditions only two equations are given. These become:

$$R_1 = \alpha_1 p_1 + \beta_1 \theta_1 + \gamma_1 - x_1, \tag{2.47}$$

$$R_2 = \alpha_2 p_1 + \beta_2 \theta_1 + \gamma_2 - \ln L_o - 5 \ln \ell_1. \tag{2.48}$$

The G_{ij}'s and the R_k's represent how badly the structure equations are violated. Evidently for a correct model

$$G_{ij} = 0 \qquad \text{for } i = 1,2,3,4 \text{ and } j = 1,2,\ldots,m-1, \tag{2.49}$$

$$R_k = 0 \qquad \text{for } k = 1,2. \tag{2.50}$$

With equations (2.35) through (2.50) the structure of the star is specified in the form

$$R_k(x_1,\ell_1,p_1,\theta_1) = 0, \qquad k = 1,2; \tag{2.51}$$

$$G_i(x_j,\ell_j,p_j,\theta_j,x_{j+1},\ell_{j+1},p_{j+1},\theta_{j+1}) = 0, \quad i = 1,2,3,4; \tag{2.52}$$

$$G_i(x_{m-1},\ell_{m-1},p_{m-1},\theta_{m-1},p_m,\theta_m) = 0, \qquad i = 1,2,3,4. \tag{2.53}$$

II-5. Solution

These equations are non-linear and can not be solved analytically. The Henyey method solves them by iterating with a Newton-Raphson method. If an approximate model is given with estimates of the structure variables for each shell j, the above equations will not generally be satisfied. Corrections to the structure variables (δx_j, $\delta \ell_j$, δp_j, and $\delta \theta_j$) are sought such that all R_k's and G_{ij}'s will vanish after the corrections are applied. That is, the desired corrections will produce variations in R_k and G_{ij} such that

$$R_k + \delta R_k = 0 \qquad \text{and} \qquad G_{ij} + \delta G_{ij} = 0 \tag{2.54}$$

Expanding G_{ij} to first order:

$$\delta G_{ij} = \frac{\partial G_{ij}}{\partial x_j}\delta x_j + \frac{\partial G_{ij}}{\partial \ell_j}\delta \ell_j + \frac{\partial G_{ij}}{\partial p_j}\delta p_j + \frac{\partial G_{ij}}{\partial \theta_j}\delta \theta_j + \frac{\partial G_{ij}}{\partial x_{j+1}}\delta x_{j+1}$$

$$+ \frac{\partial G_{ij}}{\partial \ell_{j+1}}\delta \ell_{j+1} + \frac{\partial G_{ij}}{\partial p_{j+1}}\delta p_{j+1} + \frac{\partial G_{ij}}{\partial \theta_{j+1}}\delta \theta_{j+1} \tag{2.55}$$

with similar equations for R_k.

Then from equations (2.54)

$$-R_k = \frac{\partial R_k}{\partial x_1}\delta x_1 + \frac{\partial R_k}{\partial \ell_1}\delta \ell_1 + \frac{\partial R_k}{\partial p_1}\delta p_1 + \frac{\partial R_k}{\partial \theta_1}\delta \theta_1, \quad k = 1,2; \tag{2.56}$$

$$-G_{ij} = \frac{\partial G_{ij}}{\partial x_j}\delta x_j + \ldots + \frac{\partial G_{ij}}{\partial \theta_{j+1}}\delta \theta_{j+1}, \quad i=1,2,3,4, \quad j=1,\ldots,m-2; \tag{2.57}$$

$$-G_{i,m-1} = \frac{\partial G_{i,m-1}}{\partial x_{m-1}}\delta x_{m-1} + \ldots + \frac{\partial G_{i,m-1}}{\partial \theta_m}\delta \theta_m, \quad i=1,2,3,4. \tag{2.58}$$

There are 4m-2 simultaneous linear equations for the 4m-2 unknown corrections. The corrections for r and L_r at the center are zero since these two quantities vanish identically. All the coefficients are readily calculated from the approximate model.

The above system of equations would be impossible to solve in general for a reasonable number of shells except for the coefficient matrix being non-zero only near the diagonal. Hence the system may be solved by a recursive procedure.

Equation (2.56) gives two equations in four unknowns. The first two of these may be expressed as a linear function of the other two:

$$\delta x_1 = C_{x1}\delta p_1 + D_{x1}\delta \theta_1 + E_{x1}, \tag{2.59a}$$

$$\delta \ell_1 = C_{\ell 1}\delta p_1 + D_{\ell 1}\delta \theta_1 + E_{\ell 1}. \tag{2.59b}$$

For j=1 equation (2.57) gives four equations in the eight unknown corrections δx_1, $\delta \ell_1$, δp_1, $\delta \theta_1$, δx_2, $\delta \ell_2$, δp_2, and $\delta \theta_2$. The first two of these may be eliminated by use of equations (2.59), thus leaving four equations in the six unknowns. Solving for four of these in terms of the last two, one may write:

$$\delta p_1 = C_{p2}\delta p_2 + D_{p2}\delta\theta_2 + E_{p2}, \tag{2.60a}$$

$$\delta\theta_1 = C_{\theta 2}\delta p_2 + D_{\theta 2}\delta\theta_2 + E_{\theta 2}, \tag{2.60b}$$

$$\delta x_2 = C_{x2}\delta p_2 + D_{x2}\delta\theta_2 + E_{x2}, \tag{2.60c}$$

$$\delta \ell_2 = C_{\ell 2}\delta p_2 + D_{\ell 2}\delta\theta_2 + E_{\ell 2}. \tag{2.60d}$$

Equations (2.60c) and (2.60d) are the same as equations (2.59) except that j=2 rather than j=1. Hence this process may be repeated and coefficients set up for every shell. In general

$$\delta p_j = C_{p,j+1}\,\delta p_{j+1} + D_{p,j+1}\,\delta\theta_{j+1} + E_{p,j+1}, \tag{2.61a}$$

$$\delta\theta_j = C_{\theta,j+1}\,\delta p_{j+1} + D_{\theta,j+1}\,\delta\theta_{j+1} + E_{\theta,j+1}, \tag{2.61b}$$

$$\delta x_{j+1} = C_{x,j+1}\,\delta p_{j+1} + D_{x,j+1}\,\delta\theta_{j+1} + E_{x,j+1}, \tag{2.61c}$$

$$\delta \ell_{j+1} = C_{\ell,j+1}\,\delta p_{j+1} + D_{\ell,j+1}\,\delta\theta_{j+1} + E_{\ell,j+1}. \tag{2.61d}$$

For j=m-1, equation (2.58) must be used which is four equations in the six unknowns δx_{m-1}, $\delta \ell_{m-1}$, δp_{m-1}, $\delta\theta_{m-1}$, δp_m, and $\delta\theta_m$. The first two are eliminated by equations (2.61c) and (2.61d). This leaves four equations in four unknowns which may be directly evaluated. Then knowing δp_{m-1} and $\delta\theta_{m-1}$ and using equations (2.61) the corrections for the next shell out are obtained. This process is continued until the surface is reached and all the corrections are known.

The C, D, and E coefficients are obtained from equations (2.56) through (2.58). For the outer boundary differentiate equations (2.47) and (2.48) and substitute into equation (2.56). Then the coefficients in equations (2.59) become:

$$C_{x1} = \alpha_1, \qquad D_{x1} = \beta_1, \qquad E_{x1} = R_1$$

$$C_{\ell 1} = \alpha_2 \ell_1/5, \qquad D_{\ell 1} = \beta_2 \ell_1/5, \qquad E_{\ell 1} = R_2 \ell_1/5. \tag{2.62}$$

The G_{ij} equations are somewhat more involved. Replace the δx_j and $\delta \ell_j$ in equation (2.57) from equations (2.61c) and (2.61d). Then after collecting like terms for δp_j and $\delta \theta_j$ equation (2.57) becomes

$$\begin{aligned} G_{ij} &+ \left(\frac{\partial G_{ij}}{\partial x_j} C_{xj} + \frac{\partial G_{ij}}{\partial \ell_j} C_{\ell j} + \frac{\partial G_{ij}}{\partial p_j}\right) \delta p_j \\ &+ \left(\frac{\partial G_{ij}}{\partial x_j} D_{xj} + \frac{\partial G_{ij}}{\partial \ell_j} D_{\ell j} + \frac{\partial G_{ij}}{\partial \theta_j}\right) \delta \theta_j + \frac{\partial G_{ij}}{\partial x_j} E_{xj} + \frac{\partial G_{ij}}{\partial \ell_j} E_{\ell j} \\ &+ \frac{\partial G_{ij}}{\partial x_{j+1}} \delta x_{j+1} + \frac{\partial G_{ij}}{\partial \ell_{j+1}} \delta \ell_{j+1} + \frac{\partial G_{ij}}{\partial p_{j+1}} \delta p_{j+1} + \frac{\partial G_{ij}}{\partial \theta_{j+1}} \delta \theta_{j+1} = 0. \end{aligned} \tag{2.63}$$

This equation has the form

$$a_i \delta p_j + b_i \delta \theta_j + c_i \delta x_{j+1} + d_i \delta \ell_{j+1} = e_i \tag{2.64}$$

where

$$a_i = \frac{\partial G_{ij}}{\partial p_j} + \frac{\partial G_{ij}}{\partial x_j} C_{xj} + \frac{\partial G_{ij}}{\partial \ell_j} C_{\ell j}, \tag{2.65a}$$

$$b_i = \frac{\partial G_{ij}}{\partial \theta_j} + \frac{\partial G_{ij}}{\partial x_j} D_{xj} + \frac{\partial G_{ij}}{\partial \ell_j} D_{\ell j}, \tag{2.65b}$$

$$c_i = \frac{\partial G_{ij}}{\partial x_{j+1}}, \tag{2.65c}$$

$$d_i = \frac{\partial G_{ij}}{\partial \ell_{j+1}}, \tag{2.65d}$$

$$e_i = -\frac{\partial G_{ij}}{\partial p_{j+1}} \delta p_{j+1} - \frac{\partial G_{ij}}{\partial \theta_{j+1}} \delta \theta_{j+1} + \Gamma_{ij} \tag{2.65e}$$

with Γ_{ij} defined as

$$\Gamma_{ij} = - G_{ij} - \frac{\partial G_{ij}}{\partial x_j} E_{xj} - \frac{\partial G_{ij}}{\partial \ell_j} E_{\ell j}. \tag{2.65f}$$

The system of four equations given by equation (2.64) may be solved by Cramer's Rule. The solutions will then express δp_j, $\delta \theta_j$, δx_{j+1}, and $\delta \ell_{j+1}$ in terms of a linear combination of δp_{j+1} and $\delta \theta_{j+1}$, which is just the form of equations (2.61).

From equations (2.35) through (2.37) note that for all j

$$c_1 = \frac{\partial G_{1j}}{\partial x_{j+1}} = 0, \quad d_2 = \frac{\partial G_{ij}}{\partial \ell_{j+1}} = 0, \text{ and } \quad d_3 = \frac{\partial G_{ij}}{\partial \ell_{j+1}} = 0. \tag{2.66}$$

Thus the determinant of the coefficients becomes

$$\Delta = \begin{vmatrix} a_1 & b_1 & 0 & d_1 \\ a_2 & b_2 & c_2 & 0 \\ a_3 & b_3 & c_3 & 0 \\ a_4 & b_4 & c_4 & d_4 \end{vmatrix}. \tag{2.67}$$

To solve for δp_j replace the "a" column by e_i's. The solution is then the quotient of this new determinant and equation (2.67). Since the last column contains two zero elements, it is convenient to expand about this column. Then

$$\delta p_j = \frac{1}{\Delta} \{-d_1[e_2(b_3c_4-b_4c_3) - e_3(b_2c_4-b_4c_2) + e_4(b_2c_3-b_3c_2)]$$

$$+d_4[e_1(b_2c_3-b_3c_2) - e_2b_1c_3 + e_3b_1c_2]\} \tag{2.68}$$

But e_i contains linear terms in δp_{j+1} and $\delta \theta_{j+1}$ and a constant term Γ_{ij}. All other terms in equation (2.68) are constant terms. Thus the solution will separate into the C, D, and E coefficients. It is sufficient to substitute for e_i the appropriate factor from equations (2.65e)

and (2.65f). Thus for the $C_{p,j+1}$ replace e_i in equation (2.68) by the coefficient of δp_{j+1} in equation (2.65e). For $D_{p,j+1}$ replace e_i by the coefficient of $\delta\theta_{j+1}$ and for $E_{p,j+1}$ replace e_i by Γ_{ij}. This process may be repeated for $\delta\theta_j$, δx_{j+1}, and $\delta\ell_{j+1}$, thus obtaining all twelve of the C, D, and E coefficients.

For the C coefficients one then obtains:

$$C_{p,j+1} = \frac{1}{\Delta}\{-d_1[g_2(b_3c_4-b_4c_3) - g_3(b_2c_4-b_4c_2) + g_4(b_2c_3-b_3c_2)] + d_4[g_1(b_2c_3-b_3c_2) - g_2b_1c_3 + g_3b_1c_2]\}, \tag{2.69a}$$

$$C_{\theta,j+1} = \frac{1}{\Delta}\{-d_1[g_2(a_4c_3-a_3c_4) - g_3(a_4c_2-a_2c_4) + g_4(a_3c_2-a_2c_3)] + d_4[g_1(a_3c_2-a_2c_3) + g_2a_1c_3 - g_3a_1c_2]\}, \tag{2.69b}$$

$$C_{x,j+1} = \frac{1}{\Delta}\{-d_1[g_2(a_3b_4-a_4b_3) - g_3(a_2b_4-a_4b_2) + g_4(a_2b_3-a_3b_2)] + d_4[g_1(a_2b_3-a_3b_2) - g_2(a_1b_3-a_3b_1) + g_3(a_1b_2-a_2b_1)]\}, \tag{2.69c}$$

$$C_{\ell,j+1} = \frac{1}{\Delta}\{g_1\Delta_1 + g_2\Delta_2 + g_3\Delta_3 + g_4\Delta_4\} \tag{2.69d}$$

where Δ_i is the cofactor of d_i in equation (2.67) and

$$g_i = -\frac{\partial G_{ij}}{\partial p_{j+1}}. \tag{2.70}$$

The expressions for the D and the E coefficients are similar. For the D coefficients

$$g_i = -\frac{\partial G_{ij}}{\partial \theta_{j+1}}. \tag{2.71}$$

The fact that $\partial G_{2j}/\partial\theta_{j+1} = 0$ for all j means that every term containing g_2 in equations (2.69) vanishes, thus simplifying the expressions. For the E coefficients

$$g_i = \Gamma_{ij}. \tag{2.72}$$

The last shell for which equations (2.69) are to be applied is for j=m-2. For j=m-1 equation (2.58) must be used. Then equation (2.64) becomes

$$a_i \delta p_{m-1} + b_i \delta\theta_{m-1} + \frac{\partial G_{i,m-1}}{\partial p_m} \delta p_m + \frac{\partial G_{i,m-1}}{\partial \theta_m} \delta\theta_m = \Gamma_{i,m-1}. \qquad (2.73)$$

But this is four equations in only four unknowns and hence may be readily solved.

When all the corrections have been obtained the approximate model can be improved. Before the corrections are applied, they are examined and multiplied by an appropriate factor to limit the size of the largest correction actually applied. When the computed corrections are small, the full correction is applied. This helps prevent overshoot and increases the likelihood of convergence. Iteration is continued until all the corrections are of the order of 10^{-3} or 10^{-4} of the variables. The model is then considered converged.

II-6. Core boundary conditions

Much computer time is spent in calculating portions of the star that are relatively uninteresting for the investigation of core helium burning. Also the outer portions of the star may be changing relatively rapidly and hence short time steps must be taken even though the core of the star is almost static. These problems can be overcome by evolving just the core of the star.

The difference equations (2.52) link only the variables between two adjacent shells. Hence if all the variables were specified at a given shell, the portion of the star exterior to the shell would be decoupled from the interior portion. For the core helium burning one is interested

in varying the reaction rate parameters for the helium burning in the core. If one could specify the correct structure variables at some point just outside the core, then there would be no need to compute the envelope.

As discussed in chapter I, due to the extreme temperature dependence of the energy generation rate, the star will adjust itself to moderate changes in the reaction rate parameters by a very small change in the temperature. Hence, there will be little difference in the structure variables outside the core for two stars differing in the reaction rate parameters. The values of the structure variables at a specified point obtained from one evolutionary sequence may then be applied as an outer boundary condition for the core evolutions.

The outer boundary of the core will no longer be a fitting point as described in section II-3. Divide the core up into concentric shells as was done for the entire star in section II-4, with j=1 as the outer boundary. Equations (2.35) through (2.38b) and (2.43) through (2.46b) can then be applied. These give 4m-4 equations, and there still are 4m-4 equations after differentiating and writing in the form of equations (2.52) and (2.53). But there are 4m structure variables which yield 4m-2 unknown corrections,(since the corrections for r and L_r identically vanish at the center) if corrections are sought for all variables. At the outer boundary there are four structure variables. If all four of these are fixed, 4m-6 unknown corrections are left. And with 4m-4 equations the problem is overspecified. The core is unstable in time, and the structure variables near the outer boundary become quite unrealistic after several time steps are taken.

The correct application of the outer boundary conditions is to

specify two of the structure variables and allow corrections to be applied to the other two. This leads to 4m-4 equations in 4m-4 unknown corrections.

From equation (2.59) it is trivial to set the C, D, and E coefficients to zero. Then δx_1 and $\delta \ell_1$ would vanish and x_1 and ℓ_1 would be fixed as the outer boundary conditions. However, x and ℓ are also fixed at the center of the core. This type of outer boundary condition would specify x and ℓ at two points and would give no specification on p or θ. Hence it is desirable to use p and θ as outer boundary conditions.

New expressions for the C, D, and E coefficients must now be derived. For j=1 differentiate equation (2.52) but allow variations only in x_1, ℓ_1, x_2, ℓ_2, p_2, and θ_2. Then equation (2.57) becomes

$$-G_{i1} = \frac{\partial G_{i1}}{\partial x_1}\delta x_1 + \frac{\partial G_{i1}}{\partial \ell_1}\delta \ell_1 + \frac{\partial G_{i1}}{\partial x_2}\delta x_2 + \frac{\partial G_{i1}}{\partial \ell_2}\delta \ell_2 + \frac{\partial G_{i1}}{\partial p_2}\delta p_2 + \frac{\partial G_{i1}}{\partial \theta_2}\delta \theta_2. \tag{2.74}$$

This equation can be written as

$$a_i \delta x_1 + b_i \delta \ell_1 + c_i \delta x_2 + d_i \delta \ell_2 = e_i \tag{2.75}$$

where

$$a_i = \frac{\partial G_{i1}}{\partial x_1}, \tag{2.76a}$$

$$b_i = \frac{\partial G_{i1}}{\partial \ell_1}, \tag{2.76b}$$

$$c_i = \frac{\partial G_{i1}}{\partial x_2}, \tag{2.76c}$$

$$d_i = \frac{\partial G_{i1}}{\partial \ell_2}, \tag{2.76d}$$

$$e_i = - \frac{\partial G_{i1}}{\partial p_2} \delta p_2 - \frac{\partial G_{i1}}{\partial \theta_2} \delta \theta_2 - G_{i1}. \tag{2.76e}$$

Equations (2.75) can be solved for δx_1, $\delta \ell_1$, δx_2, and $\delta \ell_2$ in terms of δp_2 and $\delta \theta_2$. Thus

$$\delta x_1 = C_{x1} \delta p_2 + D_{x1} \delta \theta_2 + E_{x1}, \tag{2.77a}$$

$$\delta \ell_1 = C_{\ell 1} \delta p_2 + D_{\ell 1} \delta \theta_2 + E_{\ell 1}, \tag{2.77b}$$

$$\delta x_2 = C_{x2} \delta p_2 + D_{x2} \delta \theta_2 + E_{x2}, \tag{2.77c}$$

$$\delta \ell_2 = C_{\ell 2} \delta p_2 + D_{\ell 2} \delta \theta_2 + E_{\ell 2}. \tag{2.77d}$$

The last two equations are the same as equations (2.60c) and (2.60d), and the equations for these corrections are thus "matched" to the previous method of solution. The only modification is then to replace equations (2.59), (2.60a), and (2.60b) by equations (2.77a) and (2.77b).

The C, D, and E coefficients may be found by a similar technique to that previously used. First note that

$$\begin{aligned} a_1 &= \frac{\partial G_{11}}{\partial x_1} = 0, \quad b_2 = \frac{\partial G_{21}}{\partial \ell_1} = 0, \quad b_3 = \frac{\partial G_{31}}{\partial \ell_1} = 0, \\ c_1 &= \frac{\partial G_{11}}{\partial x_2} = 0, \quad d_2 = \frac{\partial G_{21}}{\partial \ell_2} = 0, \quad d_3 = \frac{\partial G_{31}}{\partial \ell_2} = 0. \end{aligned} \tag{2.78}$$

Thus the determinant of the coefficients becomes

$$\Delta = \begin{vmatrix} 0 & b_1 & 0 & d_1 \\ a_2 & 0 & c_2 & 0 \\ a_3 & 0 & c_3 & 0 \\ a_4 & b_4 & c_4 & d_4 \end{vmatrix}. \tag{2.79}$$

The correction δx_1 is obtained by replacing a_i by e_i and dividing the new determinant by Δ. The coefficient C_{x1} is obtained by using only

the coefficient of δp_2 from equation (2.76e). Again, it is convenient to expand about the last column.

The C coefficients are then given by

$$C_{x1} = \frac{1}{\Delta} \{(b_4 d_1 - b_1 d_4)(g_2 c_3 - g_3 c_2)\}, \tag{2.80a}$$

$$C_{\ell 1} = \frac{1}{\Delta} \{-d_1[g_2(a_4 c_3 - a_3 c_4) - g_3(a_2 c_4 - a_4 c_2) + g_4(a_3 c_2 - a_2 c_3)] + d_4[g_1(a_3 c_2 - a_2 c_3)]\}, \tag{2.80b}$$

$$C_{x2} = \frac{1}{\Delta} \{(b_1 d_4 - b_4 d_1)(g_2 a_3 - g_3 a_2)\}, \tag{2.80c}$$

$$C_{\ell 2} = \frac{1}{\Delta} \{-b_1[g_2(a_3 c_4 - a_4 c_3) - g_3(a_2 c_4 - a_4 c_2) + g_4(a_2 c_3 - a_3 c_2)] + b_4[g_1(a_2 c_3 - a_3 c_2)]\}, \tag{2.80d}$$

where

$$g_i = - \frac{\partial G_{i1}}{\partial p_2} . \tag{2.81}$$

For the D equations

$$g_i = - \frac{\partial G_{i1}}{\partial \theta_2} . \tag{2.82}$$

And since $\partial G_{21}/\partial \theta_2 = 0$ every term containing g_2 will vanish. For the E coefficients

$$g_i = - G_{i1}. \tag{2.83}$$

The structure equations of the star have now been solved. It is only necessary to specify the auxiliary variables, the composition parameters, and the outer boundary conditions and the problem is then complete. It should be noted that the above procedure for the core boundary conditions is only valid if the outer boundary is radiative. If it is convective, then the determinant of the coefficients becomes singular. It is desirable from other considerations that the outer

boundary of the core be radiative. This prevents an unknown amount of material being mixed down into the core from above. There is no way of knowing how far out the convective region extends and what the composition is outside of the core.

CHAPTER III

THERMONUCLEAR REACTIONS

III-1. Cross-sections

The basis of stellar evolution is the release of energy by the thermonuclear reactions. This release changes the composition in the star which in turn changes the structure of the star. The rate of energy released, ε (in ergs/gram/sec), depends on the energy available from each reaction, Q, and the reaction cross-section. The theory of the thermonuclear reaction rates is given in detail by Clayton (1968) and is summarized by Reeves (1965) and Fowler, Caughlan, and Zimmerman (1967), hereafter referred to as FCZ.

Consider a reaction of the following type:

$$a + X \rightarrow Y + b.$$

Here a nucleus of type a interacts with a nucleus of type X producing a nucleus of type Y and a nucleus of type b. Particle b may also be a photon or other such particle. This reaction is written as

$$X(a,b)Y.$$

The cross-section for this reaction is defined to be

$$\sigma(\text{cm}^2) = \frac{\text{number of reactions/nucleus X/unit time}}{\text{number of incident particles/cm}^2\text{/unit time}} . \quad (3.1)$$

Now suppose that the target nuclei are in the form of a gas with N_X particles per unit volume. The reaction rate per unit volume will be given by the product of σ, N_X, and the flux of particles of type a.

If the flux of type a particles is due to a uniform translation with velocity v of a gas of type a particles with a number density N_a, then the flux is given by vN_a, so the reaction rate is

$$r = \sigma(v)v\ N_a N_X \tag{3.2}$$

If the velocity of the particles is due to a state of thermodynamic equilibrium, as is found in the interior of stars, there is a Maxwellian distribution of relative velocities, $\Phi(v)$, which may be taken to be normalized. Then the total reaction rate per unit volume is

$$r_{aX} = N_a N_X \int_0^\infty v\sigma(v)\Phi(v)\ dv = N_a N_X\ \langle\sigma v\rangle_{aX}. \tag{3.3}$$

Here $\langle\sigma v\rangle$ represents the expectation value of σv over the distribution of velocities. This is also denoted as

$$\lambda_{aX} = \langle\sigma v\rangle_{aX}. \tag{3.4}$$

If particle a is identical to particle X, then a factor of ½ must be introduced to avoid counting each pair twice. This can be written formally as

$$r_{aX} = \frac{N_a N_X \lambda_{aX}}{1+\delta_{aX}} \tag{3.5}$$

where δ_{aX} is the Kronecker delta, defined to be unity if a is identical to X and zero otherwise.

It is useful to define several other related quantities. The lifetime of a species X against reactions with species a is

$$\tau_a(X) = \frac{N_X}{r_{aX}} = \frac{1}{N_a \lambda_{aX}}, \tag{3.6}$$

or

$$\frac{1}{\tau_a(X)} = - \frac{1}{N_X} \left(\frac{\partial N_X}{\partial t}\right)_a \tag{3.7}$$

where the partial derivative indicates the rate of change of N_X due to interactions with particles of type a.

The number density can be related to the fractional abundance by mass of the nuclear species, X_i, by

$$N_i = \rho N_o \frac{X_i}{A_i} \tag{3.8}$$

where ρ is the mass density, N_o is Avogadro's number, and A_i is the atomic mass of species i.

The energy generation rate per unit mass is given by

$$\epsilon_{aX} = \frac{r_{aX} Q_{aX}}{\rho} \tag{3.9}$$

where Q_{aX} is the energy released per reaction.

Introducing explicitly the form of the Maxwellian distribution equation (3.3) becomes

$$\lambda_{aX} = 4\pi \left(\frac{\mu}{2\pi kT}\right)^{3/2} \int_0^\infty v^3 \sigma(v)\ e^{-\mu v^2/2kT}\ dv \tag{3.10}$$

where μ is the reduced mass of the interacting nuclei, T is the temperature in °K, and k is Boltzmann's constant. This form of the equation is not the most useful. It is much more convenient to express λ_{aX} as an integral over the energy. Then equation (3.10) becomes

$$\lambda_{aX} = \left(\frac{8}{\mu\pi}\right)^{\frac{1}{2}} (kT)^{-3/2} \int_0^\infty \sigma(E)\ E\ e^{-E/kT}\ dE. \tag{3.11}$$

The entire problem of obtaining the reaction rates then reduces to determining $\sigma(E)$ and evaluating equation (3.11).

III-2. Nonresonant cross-sections

At low energy the nuclear reactions can proceed only by the interacting nuclei penetrating the repulsive coulomb barrier between them. Gamow (1928) first derived the form of the barrier penetration. The result is that the cross-section for low energy may be written as (Clayton 1968)

$$\sigma(E) = \frac{S(E)}{E} \; e^{-(E_g/E)^{\frac{1}{2}}} \tag{3.12}$$

where E_g is the Gamow energy defined to be

$$E_g = (2\pi\alpha Z_a Z_\chi)^2 \frac{\mu c^2}{2} \tag{3.13}$$

with α the fine structure constant, Z_a and Z_χ are the charges on the nuclei, and c is the speed of light. It is useful to define a quantity A such that

$$A = \frac{A_a A_\chi}{A_a + A_\chi} = \frac{\mu}{m_{amu}} \tag{3.14}$$

where A_i is the atomic mass of the nuclei and m_{amu} is the mass of one atomic mass unit. Thus A is the reduced atomic mass for the interacting nuclei. The Gamow energy can then be written numerically as

$$E_g^{\frac{1}{2}} = 0.98948 \; Z_a Z_\chi \; A^{\frac{1}{2}} \quad (\text{MeV})^{\frac{1}{2}}. \tag{3.15}$$

Substituting equation (3.12) into equation (3.11) gives

$$\lambda = \left(\frac{8}{\mu\pi}\right)^{\frac{1}{2}} (kT)^{-3/2} \int_0^\infty S(E) \; e^{-E/kT} \; e^{-(E_g/E)^{\frac{1}{2}}} \; dE. \tag{3.16}$$

For small values of E the second exponential factor goes to zero, and for large values of E the first exponential factor goes to zero. The product of the two form a peak, the Gamow peak, and almost all of the contribution to the integral will come from this region. Physically this means that almost all of the reactions in the interior of a star come from the few particles moving in the high energy tail of the Maxwellian velocity distribution. The energy of the Gamow peak is usually quite small by nuclear physics standards but is larger than kT, the thermal energy.

The factor S(E) in equation (3.12) is the astrophysical S factor. It contains the energy dependence of the penetration not included explicitly in equation (3.12) plus any intrinsic nuclear force factors. Whereas σ is a rapidly varying function at low energies, S is a slowly varying function of E except near a nuclear resonance. Thus one may be more confident in extrapolating S over a large energy than in extrapolating σ.

Expanding S(E) in a Maclaurin series in E and keeping only the first three terms, one obtains

$$S(E) = S(0)\left[1 + \frac{S'(0)}{S(0)} E + \tfrac{1}{2} \frac{S''(0)}{S(0)} E^2\right]. \qquad (3.17)$$

The primes represent differentiating with respect to E.

Substituting equation (3.17) into (3.16) yields after some algebra (Caughlan and Fowler 1962, Bahcall 1966)

$$\lambda_{aX} = \left[1.3006\times10^{-8} \left(Z_a Z_X/A\right)^{1/3} S_{eff}\right] T^{-2/3} e^{-\tau}. \qquad (3.18)$$

This result involves various approximations for the integral that use the fact that the major contribution comes from only a small region.

The quantity S_{eff} is

$$S_{eff} = S(0)\ [1 + 9.807\times10^{-5} W^{1/3}\ T^{1/3} + 1.22\times10^{-7}\ \frac{S'(0)}{S(0)}\ W^{1/3}\ T^{2/3}$$

$$+ 8.378\times10^{-11}\ \frac{S'(0)}{S(0)}\ T + 7.447\times10^{-15}\ \frac{S''(0)}{S(0)}\ W^{2/3}\ T^{4/3}$$

$$+ 1.300\times10^{-17}\ \frac{S''(0)}{S(0)}\ W^{1/3}\ T^{5/3}] \qquad (3.19)$$

where

$$W = Z_a^2\ Z_X^2\ A, \qquad (3.20)$$

$$\tau = 4.2487\times10^{3}\ W^{1/3}\ T^{-1/3}. \qquad (3.21)$$

The maximum of the Gamow peak occurs at an energy E_o given by

$$E_o = [\pi\alpha Z_a Z_X kT\ (\mu c^2/2)^{\frac{1}{2}}]^{2/3}. \qquad (3.22)$$

It has a width, between the 1/e points of

$$\Delta E_o = 4(E_o kT/3)^{\frac{1}{2}}. \qquad (3.23)$$

The quantity τ is given in terms of E_o by

$$\tau = 3E_o/kT \qquad (3.24)$$

So far only the coulomb barrier penetration has been considered explicitly. The remaining contribution has been approximated by the first three terms of a Maclaurin series. For lack of anything better these three terms, S(0), S'(0)/S(0), and S''(0)/S(0), could be measured in the laboratory. Equation (3.18) and (3.19) would then give the reaction rate.

III-3. Nuclear reaction models

If a model of the nuclear reaction can be established, then either $\sigma(E)$ or $S(E)$ may be readily derived from that model. Such a model will explicitly include the "nuclear physics" of the interaction and, hopefully, be more accurate than the preceeding treatment.

The properties of nuclear matter that are relevant to nuclear burning under astrophysical conditions are given by Clayton (1968). The nucleus is somewhat similar to the atomic structure of an atom with a set of discrete eigenstates characterized by discrete energies and various quantum numbers characteristic of the symmetries of the states. Several different models of the nucleus have been made; however, the present understanding of nuclear forces is sufficiently weak that many of the useful properties are known only through laboratory measurements.

An important class of reactions consists of those reactions that proceed through an allowed state of an intermediate compound nucleus. Schematically

$$a + X \rightarrow W \rightarrow Y + b$$

where W is the compound nucleus. The particles a + X are designated as the incident channel, and Y + b is the exit channel. For elastic collisions these are identical. In general there may be more than one exit channel, with the number of exit channels increasing as the energy of the incident particles is increased.

For this reaction to occur angular momentum must be conserved at all stages. Thus

$$\vec{J}_n = \vec{J}_a + \vec{J}_X + \vec{L} \tag{3.25}$$

where $\vec{J}_n$ is the angular momentum of the state with energy E_n in the

compound nucleus W, $\vec{J}_a$ and $\vec{J}_X$ are the spins of particles a and X, and $\vec{L}$ is the orbital angular momentum of particle a relative to X. A similar relation must also hold for the exit channel.

In addition parity must also be conserved as

$$\pi_n(W) = \pi(a)\ \pi(X)\ (-1)^{\ell} \tag{3.26}$$

where $\pi_n(W)$ is the parity of the E_n state in the compound nucleus W, $\pi(a)$ and $\pi(X)$ are the parities of the particles a and X, and ℓ is the relative angular momentum quantum number of particle a relative to X. These quantities can be determined by laboratory measurements.

Any unbound state in the compound nucleus will have a finite lifetime, τ, and by the uncertainty principle a spread in energy, Γ, referred to as the width of the state. The relation between the lifetime and the width is

$$\Gamma = \frac{h}{2\pi\tau} \tag{3.27}$$

where h is Planck's constant. If several different exit channels are available, then each will have its own partial width. The sum of all the partial widths is the total width of the state.

One formal method to handle the nuclear reactions that proceed through a compound nucleus is the R-matrix theory first derived by Wigner and Eisenbud (1947) and Wigner (1949). An excellent review of this theory is given by Lane and Thomas (1958) from which the presentation here is taken.

The R matrix provides a way of describing the interaction of a pair of particles in the incident channel, denoted by the subscript c, and an exit channel, c'. The total system is separated into two regions by a surface of radius a_c, the channel radius, beyond which all forces are

purely radial. Presumably any choice of a_c greater than a certain minimum would give the same observable results. The elements of the R matrix are dependent on a_c but the cross-sections are not. A choice for a_c is made by determining the sum of the radii of the interacting nuclei using a simple empirical formula. In addition to depending on a_c, the elements of the R matrix, $R_{cc'}$, also depend on E, the energy of the interacting particles, and a boundary condition parameter B_c.

The theory is formally derived by splitting the total wavefunction for the system into an exterior portion and an interior portion. These are then matched at the boundary, $r=a_c$, by a prescription specified by B_c. The external wavefunctions may be expressed in terms of the regular and the irregular coulomb wavefunctions, F_c and G_c. Three independent quantities are needed to specify the external wavefunctions at the boundary. These are taken to be: S_c, the shift factor; P_c, the penetration factor; and ϕ_c, the hard-sphere scattering phase shift.

The form of any element of the R matrix is given by (Lane and Thomas 1958)

$$R_{cc'} = \sum_{\lambda} \frac{\gamma_{\lambda c}\, \gamma_{\lambda c'}}{E_\lambda - E} \tag{3.28}$$

where λ labels the complete set of states. The $\gamma_{\lambda c}$'s are the reduced width amplitudes. The E_λ's are the energy eigenvalues of the states. Both the reduced width amplitudes and the energy eigenvalues are energy independent quantities depending on a_c and B_c. The squared quantities $\gamma_{\lambda c}^2$ are referred to as the reduced level widths.

The observed cross-sections should be independent of B_c, and if the summation in equation (3.28) is over a complete set of states, then the cross-section is independent of a_c and B_c. However, in practice

only the first few terms of equation (3.28) are used. For this finite-level approximation there is a specific value of B_c that will give the same values of the parameters E_λ and $\gamma_{\lambda c}^2$ as would be obtained from the infinite-level fit. For a given E_λ this value of B_c is just the value of the shift factor evaluated at that energy (Barker, et al. 1968). If one level dominates or if one is interested only in a limited energy range, then a best value of B can be determined.

The parameters in equation (3.28) can be determined by fitting the cross-sections or phase shifts as predicted by the theory to observed quantities. The problem then can be reversed and new cross-sections can be determined from the parameters. One can extrapolate with some confidence to regions that cannot be measured directly.

For a single channel process, where the exit channel is identical to the incident channel, the R matrix becomes a single element, the R function. For many cases the complete characterization of the channel inherent in the subscript c is reduced to specification of the relative orbital angular momentum quantum number ℓ. Then

$$R_\ell = \sum_\lambda \frac{\gamma_{\lambda\ell}^2}{E_{\lambda\ell} - E} . \tag{3.29}$$

The phase shift for such an interaction is given by

$$\delta_\ell = \arctan \left[\frac{P_\ell(E)}{R_\ell(E)^{-1} - S_\ell(E) + B_c}\right] + \omega_\ell - \phi_\ell \tag{3.30}$$

where ω_ℓ is the contribution from the coulomb field.

For reactions of interest to nuclear burning a two channel process is needed. The problem may be further specified by assuming a photon in the exit channel. This must be handled somewhat outside the assumptions of the R-matrix theory. In this case the cross-section may be expressed

as (Barker 1970)

$$\sigma_{c\gamma} = \frac{3\pi}{k_c^2} \left| \frac{2P_c^{\frac{1}{2}} P_\gamma^{\frac{1}{2}} R_{c\gamma}}{(1 - R_{cc}L_c)(1 - R_{\gamma\gamma}L_\gamma) - L_c R_{c\gamma}^2 L_\gamma} \right|^2 \qquad (3.31)$$

where k_c is the wave number of the interacting particles and L_c is defined to be

$$L_c = S_c + iP_c. \qquad (3.32)$$

The subscript γ refers to the photon exit channel.

If certain of the reduced width amplitudes are small, the gamma widths, then equation (3.31) can be simplified, and one obtains

$$\sigma_{c\gamma} = \frac{3\pi}{k_c^2} 4P_c P_\gamma \left| \frac{R_{c\gamma}}{1 - R_{cc}(S_c - B_c + iP_c)} \right|^2 \qquad (3.33)$$

A related quantity to the reduced level width is the dimensionless reduced width (Burbidge, et al. 1957). In terms of the reduced level width the dimensionless reduced width is

$$\theta_\lambda^2 = \frac{2}{3} \frac{4\pi^2}{h^2} \mu a_c^2 \gamma_\lambda^2 . \qquad (3.34)$$

An alternate method of deriving cross-sections which is appropriate for the $^{12}C(\alpha,\gamma)^{16}O$ reaction is given by Burbidge, et al.(1957). The expression for S_{eff} is given as (FCZ)

$$S_{eff} = 2.67\times10^6 \frac{\theta_\alpha^2 \Gamma_\gamma}{(E_o + |E_r|)^2} \quad \text{MeV-barn} \qquad (3.35)$$

where θ_α^2 is the dimensionless reduced alpha-particle width and Γ_γ is the photon width of the appropriate state in ^{16}O. This is derived taking into account only one state in the compound nucleus, whereas with R-matrix

theory the effects of several levels may be included, and more importantly the effects of interference between states of like angular momentum and parity can be taken into account.

III-4. Resonant cross-sections

For many nuclear reactions a single level dominates the cross-section. The formalism of the R-matrix theory can then be used to derive the form of the cross-section. The result is the Breit-Wigner single-level formula originally derived by perturbation considerations. This is expressed as (Clayton 1968)

$$\sigma(E) = \frac{h^2}{8\pi\mu E} \frac{\omega_r \Gamma_1 \Gamma_2}{(E-E_r)^2 + \Gamma^2/4} \tag{3.36}$$

where the statistical factor ω_r is given by

$$\omega_r = \frac{(2J_r + 1)(1 + \delta_{aX})}{(2J_a + 1)(2J_X + 1)} , \tag{3.37}$$

Γ_1 is the partial width for decay back into the incident channel, Γ_2 is the partial width for decay into the exit channel, and Γ is the total width of the state, which is just the sum of the two partial widths. The energy E_r is the resonance energy for the state with angular momentum J_r in the compound nucleus.

Equation (3.36) may be evaluated by assuming that the resonance is sharp; that is, $\Gamma << \Delta E_o$. In this approximation the reaction rate becomes (FCZ)

$$\lambda_{aX} = \left(\frac{h^2}{2\pi\mu kT}\right)^{3/2} \frac{2\pi}{h} (\omega\gamma)_r \, e^{-E_r/kT} \tag{3.38}$$

where

$$(\omega\gamma)_r = \frac{\omega_r \Gamma_1 \Gamma_2}{\Gamma} . \tag{3.39}$$

Numerically this reduces to

$$\lambda_{aX} = 8.0859\ A^{-3/2}\ (\omega\gamma)_r\ T^{-3/2}\ e^{-1.1605\times10^{10}\ E_r/T}. \qquad (3.40)$$

If the energy of the resonant state is high, it is likely that it will decay back into the incident channel. If this decay mode dominates, then $\Gamma_1 >> \Gamma_2$ and $(\omega\gamma)_r \simeq \omega_r$. Under these conditions, the number density of the nuclei existing in the resonant state, N*, is (Clayton 1968)

$$N^* = \frac{N_a N_X\ \omega_r}{(1 + \delta_{aX})} \frac{h^3}{(2\pi\mu kT)^{3/2}} e^{-E_r/kT}, \qquad (3.41)$$

or evaluating the constants

$$N^* = 5.2604\times10^{-21} \frac{N_a N_X\ \omega_r}{(1 + \delta_{aX})} (AT)^{-3/2}\ e^{-1.1605\times10^{10}\ E_r/T}. \qquad (3.42)$$

The contribution made by a wing of a resonance to a reaction can now be simply derived. Equation (3.12) can be solved for S(E) and equation (3.36) substituted for $\sigma(E)$. Neglecting variations in the penetration factor other than the Gamow term, the astrophysical S factor becomes

$$S(0) = S_r \frac{\Gamma^2/4}{E_r^{\,2} + \Gamma^2/4} \qquad (3.43)$$

where

$$S_r = \sigma_r\ E_r\ e^{-(E_g/E)^{1/2}} \qquad (3.44)$$

with σ_r the cross-section as measured at resonance.

Equation (3.43) is in reality a non-resonant reaction rate, but the form of the astrophysical S factor is now known, whereas in section

III-2 it was assumed only to be a slowly varying function of the interaction energy.

III-5. Electron screening

The reaction rates as given in the preceeding sections are modified by the presence of a dense electron cloud. The net negative charge surrounding each nucleus reduces the coulomb repulsion, hence increasing the reaction rates. The theory of electron screening used here follows Salpeter (1954).

When two nuclei of charge Z_1 and Z_2 interact the shielding charge density introduces a perturbing potential. The total coulomb interaction energy is

$$U_{tot}(r_{12}) = \frac{Z_1 Z_2 e^2}{r_{12}} + U_s(r_{12}) \tag{3.45}$$

where $U_s(r_{12})$ is the screening term.

This term will be essentially constant near the nucleus and the potential can be replaced by U_o, the screening potential at the origin. The effect of the screening in this case is to multiply the reaction rate by the factor

$$f = e^{-U_o/kT} . \tag{3.46}$$

When the coulomb interaction energy between the nuclei is small compared to the thermal energy kT, the screening is said to be "weak". When the coulomb energy is large relative to kT, the screening is "strong". These limits are not extremely difficult to handle. The intermediate case is generally more of a problem to express analytically, but it may be adequately handled by an interpolation scheme.

Let the two reacting nuclei have charge Z_1 and Z_2. For convenience take $Z_1 > Z_2$. The weak-screening factor between the nuclei as given by Salpeter (1954) is

$$\ln f_w = 0.188\ Z_1 Z_2\ \zeta \left(\frac{\rho}{T_6^3}\right)^{\frac{1}{2}} \tag{3.47}$$

where T_6 is defined by the more general formula

$$T_n = 10^{-n}\ T, \tag{3.48}$$

and ζ is

$$\zeta = \left[\sum_i \frac{X_i Z_i^2}{A_i} + \left(\frac{\partial \ln \rho}{\partial \psi}\right)_T \frac{1}{\mu_e}\right]^{\frac{1}{2}} \tag{3.49}$$

where μ_e is the electron molecular weight and ψ is the degeneracy parameter. These quantities will be discussed in detail in a subsequent chapter. For low degeneracy the derivative is unity, while for extreme degeneracy it approaches zero.

For the case of strong-screening the screening factor is

$$\ln f_s = 0.205\ [(Z_1+Z_2)^{5/3} - Z_1^{5/3} - Z_2^{5/3}] \left(\frac{\rho}{\mu_e}\right)^{1/3} T_6^{-1} \tag{3.50}$$

with the restrictions that

$$Z_1 << \rho^{1/3} \quad \text{and} \quad 0.23\ Z_1^{2/3} Z_2 \left(\frac{\rho}{\mu_e}\right)^{1/3} T_6^{-1} >> 1. \tag{3.51}$$

The intermediate screening can be computed approximately by a simple interpolation formula from Thomas (1967) and modified by Straka (1971). The screening factor for all possible cases then becomes

$$\ln f = \begin{cases} \ln f_w & \ln f_w \leq 0.1, \quad (3.52a) \\ \ln f_s & \ln f_s \geq 10, \quad (3.52b) \\ \dfrac{(10 - \ln f_s)^2 \ln f_w + (\ln f_w - 0.1) \ln f_s}{(\ln f_w - 0.1) + (10 - \ln f_s)^2} & \text{elsewhere.} \quad (3.52c) \end{cases}$$

Hydrogen burning generally takes place in regions of low degeneracy and hence weak screening. Only equation (3.47) is used and with the derivative set to unity. The helium burning reactions occur under conditions of weak to intermediate degeneracy in the upper main sequence stars, so equation (3.52) must be used.

CHAPTER IV

NUCLEAR BURNING

IV-1. Hydrogen burning reactions

The first major nuclear burning phase is the core hydrogen burning. The hydrogen burning reactions involve several competing processes. These are generally separated into the proton-proton chains and the CNO (for carbon, nitrogen, and oxygen) cycle. The pp chains have a smaller temperature dependence and are dominant at lower temperatures then the CNO cycle. In the upper main sequence stars the CNO cycle supplies almost all of the nuclear energy, and in the process forces a large convective core on the star, which has a large influence on the evolution of the star just off the main sequence.

Both hydrogen burning processes ultimately involve the fusing of four hydrogen nuclei into one helium nucleus. A detailed discussion of these processes may be found in Clayton (1968).

The pp chains begin with the reactions

$$^{1}H(p, \beta^{+}\nu)^{2}H(p,\gamma)^{3}He.$$

The second of the two above reactions is much faster than the first, so the overall reaction rate is determined by the rate of the first.

The next reaction depends on the temperature region, thus

$$^{3}He(^{3}He,2p)^{4}He \qquad T > 8\times10^{6}\ ^{\circ}K, \qquad PPI$$

$$^{3}He(\alpha,\gamma)^{7}Be \qquad T > 13\times10^{6}\ ^{\circ}K.$$

This last reaction requires the presence of ^{4}He, but this condition is almost always met. The ^{7}Be may react in two ways that complete the chains:

$$^{7}Be(e^{-},\nu)^{7}Li(p,\alpha)^{4}He, \qquad \text{PPII}$$

$$^{7}Be(p,\gamma)^{8}Be(\beta^{+}\nu)^{8}Be^{*}(\alpha)^{4}He. \qquad \text{PPIII}$$

The net result for these three chains is the production of one helium nucleus from four hydrogen nuclei, but the energy released from each chain will be different due to different neutrino losses. The neutrinos will carry the energy out through the star without any further interactions with the material of the star. There is a spectrum of energy available to each neutrino produced, but an average neutrino energy may be used for each reaction.

The PPI chain takes two proton-proton reactions whereas the PPII and the PPIII chains require only one. As this reaction is generally the slowest of all the reactions involved in these chains, the rate of energy generation is greater in the last two chains. Hence the actual energy generated will be a function not only of the temperature but also of the abundances of ^{3}He and ^{4}He. For the present work it will suffice to assume equilibrium abundances for all the intermediate nuclei and use a combined formula for the energy generation rate.

The reaction rates are adopted from Hofmeister, Kippenhahn, and Weigert (1964) which were based on the results of Fowler (1960) and Caughlan and Fowler (1962). These have been revised somewhat (Bahcall and May 1968), but the previous rates will be used since further

revisions are likely and the proton-proton chains are relatively unimportant in the upper main sequence stars.

For the pp chains the energy generation rate is given by

$$\varepsilon_{pp} = 2.23\times10^{6}\ \rho\ X^{2}\ T_{6}^{-2/3}\ f_{pp}\ \Phi\ e^{-33.804/T_{6}^{1/3}} \tag{4.1}$$

where f_{pp} is the screening factor, and T_6 is defined by equation (3.48). The factor Φ accounts for the different energy released by the three chains. It is calculated by

$$\Phi = 1 + (0.957 + 0.5\alpha_2)\ \phi^{-1}, \tag{4.2}$$

with

$$\phi^{-1} = -\alpha_1 + \alpha_1(1 + 2\alpha_1^{-1})^{\frac{1}{2}} \tag{4.3}$$

where α_1 is a measure of the fraction of reactions following PPII and PPIII and α_2 gives the fraction following PPIII. These are given by

$$\alpha_1 = 5\times10^{16}\ (Y/X)^{2}\ e^{-100/T_{6}^{1/3}}, \tag{4.4}$$

$$\alpha_2 = [1 + \tau_p(7)/\tau_e(7)]^{-1}. \tag{4.5}$$

The ratio of the ^{7}Be lifetimes is given as

$$\tau_p(7)/\tau_e(7) = 5.44\times10^{-17}\ (1+X)/X\ T_{6}^{1/6}\ e^{102.4/T_{6}^{1/3}}. \tag{4.6}$$

The CNO cycle begins with the reactions

$$^{12}C(p,\gamma)^{13}N(\beta^{+}\nu)^{13}C(p,\gamma)^{14}N(p,\gamma)^{15}O(\beta^{+}\nu)^{15}N.$$

The last product may react in two ways:

$$^{15}N(p,\alpha)^{12}C,$$

$$^{15}N(p,\gamma)^{16}O(p,\gamma)^{17}F(\beta^{+}\nu)^{17}O(p,\alpha)^{14}N.$$

The first reaction completes the cycle producing one ^{4}He nucleus and the original ^{12}C, but the second reaction does not complete the cycle but rather enters midway into the main cycle.

The $^{14}N(p,\gamma)^{15}O$ is the slowest reaction. After a sufficient time for equilibrium to occur, most of the CNO intermediate isotopes will be in the form of ^{14}N. For the present work it is assumed that all the initial ^{12}C and ^{16}O has been converted to ^{14}N. This gives a small error in the initial ^{14}N abundance, but it will have a negligible effect on the evolution of the star and on the helium burning.

The reaction rates used are those given by Hofmeister, Kippenhahn, and Weigert (1964). They agree well with those given by FCZ. The energy generation rate for the CNO cycle is

$$\varepsilon_{CNO} = 8\times10^{27}\ \rho\ X\ X_N\ f_N\ T_6^{-2/3}\ e^{-152.28/T_6^{1/3}} \qquad (4.7)$$

where f_N is the electron screening factor for the $^{14}N(p,\gamma)^{15}O$ reaction. Numerically f_N is seven times the screening factor for the proton-proton chains. The abundance of ^{14}N is taken to be

$$X_N = 0.607\ Z_{met}. \qquad (4.8)$$

The total energy generation rate for the hydrogen burning reactions is computed according to:

$$\varepsilon = \begin{cases} 0 & T_6 < 5.4, \qquad (4.9a) \\ \varepsilon_{pp} & 5.4 < T_6 < 12, \qquad (4.9b) \\ \varepsilon_{pp} + \varepsilon_{CNO} & 12 < T_6 < 30, \qquad (4.9c) \\ \varepsilon_{CNO} & 30 < T_6. \qquad (4.9d) \end{cases}$$

The proton-proton chains do not go to completion below about 8×10^6 °K, but the entire chain was used rather than to truncate it abruptly and introduce convergence difficulties in the numerical solution. The energy generated from this temperature region is an extremely small fraction of the total energy generated and even integrated over a very long time will not affect the composition noticeably.

IV-2. Triple-alpha process

The triple-alpha process ignites at about 80×10^6 °K as compared to $10\text{-}30\times10^6$ °K for the hydrogen burning reactions. Hence it may be assumed that there is no hydrogen present when the helium burning reactions take place. This process takes place by two resonant reactions, with the temporary formation of ^{8}Be as the first stage. Schematically this is

$$^4\text{He}(\alpha)^8\text{Be}(\alpha)^{12}\text{C}(\gamma\gamma \text{ or } e^+e^-)^{12}\text{C}.$$

The ground state of ^{8}Be is unstable against decay back into two alpha particles by 92 keV (Benn, et al. 1966). The total width of the state is 2.5 eV (Clayton 1968) which corresponds to a lifetime of around 10^{-16} seconds. This time is much longer than the time required for two alpha particles to scatter past each other in a nonresonant way. It is also long enough for an occasional interaction with a third alpha particle to complete the second reaction in the triple-alpha process.

Most of the ^{8}Be will decay back into two alphas. As a result an equilibrium abundance will be built up. The number density of the ^{8}Be can be evaluated by equation (3.42). With the inclusion of the screening factor $f_{\alpha\alpha}$ this becomes

$$N^*_{Be} = 1.8598\times10^{-21}\, N_\alpha^{\,2}\, T^{-3/2}\, e^{-1.1605\times10^{10}\, E_r/T}\, f_{\alpha\alpha} \qquad (4.10)$$

where E_r = 0.092 MeV.

The second reaction in the triple-alpha process is also a resonant one. The combined mass of ^{8}Be and ^{4}He lies 0.270 MeV below a $J^\pi = 0^+$ state in ^{12}C. This is well within the Gamow peak for $T_8 = 1$.

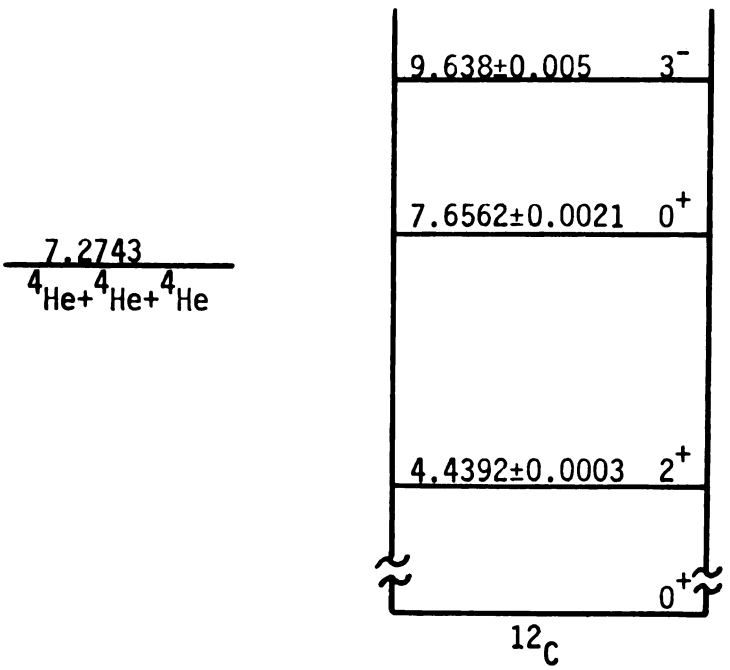

Figure 4-1. Energy level diagram for ^{12}C.

The energy level diagram for ^{12}C is shown in Figure 4-1. The energies are in MeV relative to the ground state. The spin and parity designations are in the form J^π. The data are taken from Ajzenberg-Selove and Lauritsen (1968) except for the energy of the second excited state which is from Austin, Trentelman, and Kashy (1971).

The 7.6562 MeV state in ^{12}C has three decay modes. The first and most dominant one is decay back into the incident channel. The second mode is a cascade of two gammas through the 4.44 MeV state, since a direct gamma transition to the ground state is forbidden. The third decay channel is a direct electron-positron pair emission to the ground

state, but this width is small. The equilibrium number density of the $^{12}C^*$ excited state can be calculated from equation (3.42). The necessary data for this reaction are summarized in Table 4-1.

Table 4-1. Beryllium-alpha reaction.

quantity	value	reference
A	8/3	Equation (3.14)
$J(^8Be)$	0	Lauritsen and Ajzenberg-Selove (1966)
E_x	7.6562±0.0021 MeV	Austin, Trentelman, and Kashy (1971)
J_r^π	0^+	Ajzenberg-Selove and Lauritsen (1968)
ω_r	1	Equation (3.37)
Γ	9.7±3.3 eV	Ajzenberg-Selove and Lauritsen (1968)
Γ_γ	2.8±1.0 meV	Ajzenberg-Selove and Lauritsen (1968)
Γ_π	64.±4. μeV	Ajzenberg-Selove and Lauritsen (1968)
χ	381.9±2.4 keV	Austin, Trentelman, and Kashy (1971)

With these data the equilibrium number density of $^{12}C^*$ is

$$N_C^* = 1.2080\times10^{-21}\, N_{Be}^*\, N_\alpha\, T^{-3/2}\, f_{Be\alpha}\, e^{-1.160\times10^{10}\, E_r'/T} \qquad (4.11)$$

where E_r' is the energy difference between the 7.66 MeV state in ^{12}C and the combined mass of ^8Be and ^4He.

Combining equation (4.11) with (4.10) one obtains

$$N_C^* = 2.2467\times10^{-42}\, N_\alpha^2\, T^{-3}\, f_{\alpha\alpha}\, f_{Be\alpha}\, e^{-1.1605\times10^{10}\, \chi/T} \qquad (4.12)$$

where χ is the sum of the resonant energies of the two reactions and is included in Table 4-1. The value given here disagrees by 11.9 keV with the value given by FCZ.

Since $^{12}C^*$ is in equilibrium the net reaction rate, which is the net production rate, must equal the destruction rate through the gamma transition. The contribution to the destruction rate via the electron-positron channel may be neglected since it is extremely small. Thus

$$r_{3\alpha} = \frac{N_C^*}{\tau_\alpha(12)} = \frac{2\pi N_C^* \Gamma_\gamma}{h}. \tag{4.13}$$

The energy generation rate then becomes

$$\varepsilon_{3\alpha} = 1.3572\times10^{11}\ \Gamma_\gamma(\text{meV})\ \rho^2\ Y^3\ T_8^{-3}\ f_{3\alpha}\ e^{-0.11605\ \chi(\text{keV})/T_8} \tag{4.14}$$

where $f_{3\alpha}$ is the combined screening factors for both reactions.

The uncertainty in equation (4.14) is mainly contained in the uncertainties in Γ_γ and χ. Define two numerical constants as

$$C_{3\alpha} = 1.3572\times10^{11}\ \Gamma_\gamma(\text{meV}), \tag{4.15}$$

$$E_{3\alpha} = 0.11605\ \chi(\text{keV}), \tag{4.16}$$

so that

$$\varepsilon_{3\alpha} = C_{3\alpha}\ \rho^2\ Y^3\ T_8^{-3}\ f_{3\alpha}\ e^{-E_{3\alpha}/T_8}. \tag{4.17}$$

The values of these constants used in the present work are given in Table 4-2. It was decided to use limits somewhat greater than those given in Table 4-1 since interpolation seems to be a safer procedure than extrapolation. The above quoted values of the errors are only those that were foreseen and understood by the experimentalist, and there may be other unrecognized errors. These three cases then represent the "extreme" values of the energy generation rate as well as the "best" value. Note that the extreme minimum value is obtained by using

the minimum value of $C_{3\alpha}$ and the maximum value of $E_{3\alpha}$. A similar procedure is used to obtain the maximum value of the energy generation rate.

Table 4-2. Triple-alpha reaction rate parameters.

case	Γ_γ(meV)	$C_{3\alpha}(10^{11})$	χ(keV)	$E_{3\alpha}$
minimum	1.8	2.443	384.8	44.66
mean	2.9	3.936	381.9	44.32
maximum	4.0	5.429	379.0	43.98

At 9.638 MeV there is another state in ^{12}C, and with $J^\pi = 3^-$ it can interact with an ℓ=3 capture, but because of the high E_r it becomes important only for $T > 4\times10^9$ °K (FCZ) and can be neglected for the present investigation.

There is also the remote possibility of ^{12}C being produced by a three-body reaction (Austin 1970). This could only occur if the amplitudes interfered to greatly change this process. At the present there is no way to calculate what the reaction rate should be or even to suspect that it may make any contribution at all.

IV-3. Carbon-alpha reaction

As soon as some carbon is produced by the triple-alpha process an additional reaction can take place and produce ^{16}O with an alpha capture by the carbon. Schematically this is

$$^{12}C(\alpha)^{16}O^*(\gamma)^{16}O.$$

The situation is somewhat more complicated than the corresponding

beryllium-alpha capture. The combined mass of ^{12}C and ^{4}He lies just above a resonant state in ^{16}O. The energy level diagram is given in Figure 4-2. The notation is the same as for Figure 4-1. The data are taken from Ajzenberg-Selove and Lauritsen (1959).

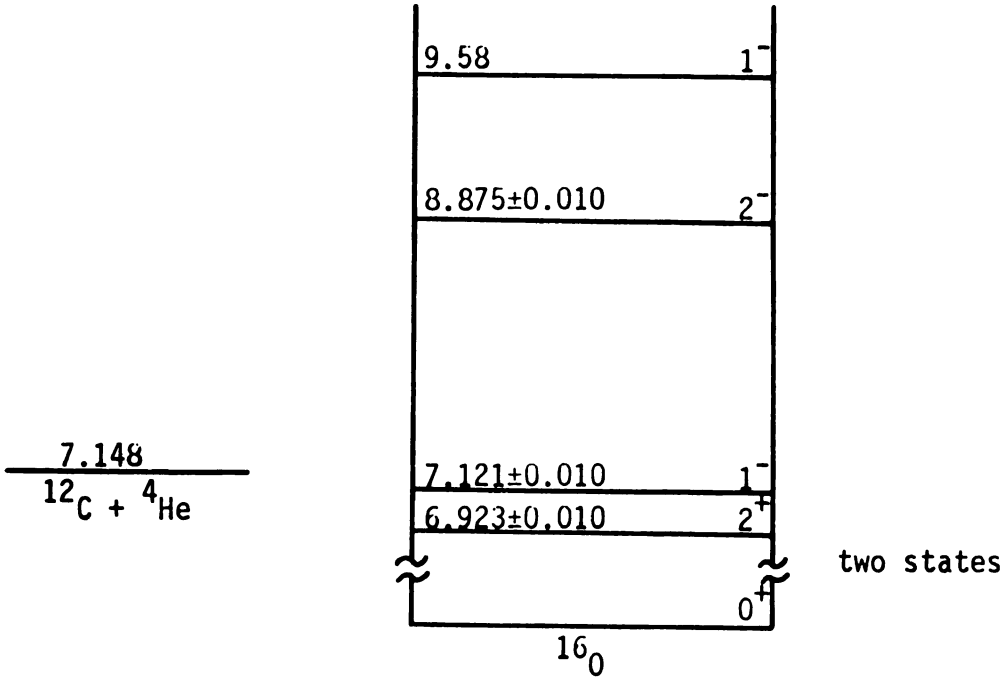

Figure 4-2. Energy level diagram for ^{16}O.

The cross-section can be calculated by assuming that the reaction is a nonresonant reaction proceeding through the high energy tail of the 7.12 MeV state with no other state contributing. The result of such a calculation is given in equation (3.35). This can be reduced to

$$S_{eff} = 2.0724\times10^{11} \frac{\theta_{\alpha}^{2}}{T^{4/3}\,(1+5.\times10^{4}\,T^{-2/3}\,)^{2}} \qquad (4.18)$$

where Γ_{γ} has been set to 66. meV as given by Swann and Metzger (1957). The largest uncertainty in this equation is the dimensionless reduced alpha width. Unfortunately there is no way to measure this quantity directly, but it must be calculated by a theoretical model. Various

attempts have been made to derive values for this quantity. Stephenson (1966) found $\theta_\alpha^2=0.085\pm0.04$ by using a very specific model for the ^{16}O nucleus. From stripping reactions Loebenstein, et al. (1967) estimated $0.06\leq\theta_\alpha^2\leq0.14$.

The formulation leading to equation (4.18) also neglects the other states in ^{16}O. The next higher state at 8.88 MeV cannot contribute since it has the wrong parity for its angular momentum state. Both ^{12}C and ^4He have 0^+ ground states. The conservation of angular momentum may be satisfied by an $\ell=2$ capture, but then equation (3.26), the conservation of parity, would be violated. Hence, this state is invisible to the $^{12}C(\alpha,\gamma)^{16}O$ reaction.

The next state is at 9.58 MeV and with an E_r of 2.43 MeV would contribute very little to the reaction except for $T>5\times10^8$ °K (Reeves 1965). However, it has $J^\pi=1^-$, which is the same as the 7.12 MeV state. There may be interference effects between the states that could drastically affect the cross-section in the energy range between them.

The R-matrix theory of section III-3 provides a way of including the effects of the other 1^- states. Barker (1971) developed a four-level formula for the ^{16}O nucleus. Further calculations were done using his formulation in the course of the present investigation. The basic scheme is to fit the $^{12}C+\alpha$ elastic scattering phase shifts to equation (3.30) with $\ell=1$ to get estimates for the energy eigenvalues and the reduced level widths. Then using these values obtain the $^{12}C+\alpha$ capture cross-sections by the use of equation (3.33), and then select the values of the parameters that compare most favorably with the observed cross-sections.

The first three levels in Barker's formulation are the 7.12, 9.59,

and 12.44 MeV states, and the fourth level is a background representing all the other 1^- states. The energy of this state is fixed at 10 MeV above the $^{12}C+\alpha$ threshold. The energy of the lowest level is also fixed at 7.116 MeV, which is 0.046 MeV below the threshold.

The channel radius a is chosen to be 6 fm, and the boundary condition parameter B is set equal to the shift factor at the energy of the first level, which for a=6 fm is -3.8882.

The elastic scattering phase shifts are fit over an energy range of 2.5 - 7.5 MeV. The data are taken from Jones, et al. (1962) with errors assigned as ±5°, Clark, et al. (1968) with errors as given, and Morris, et al. (1968) with errors of ±4°. There are a total of 54 data points (Barker 1970).

The data of N points are fitted by a least squares procedure such that χ^2 is minimized, where χ^2 is given by

$$\chi^2 = \sum_{i=1}^{N} \left[\frac{\delta_{obs}(i) - \delta_{cal}(i)}{\zeta(i)} \right]^2 \qquad (4.19)$$

where δ_{obs} are the experimental data, each with an error of ζ, and δ_{cal} is obtained from equation (3.30) evaluated at the energy of the observed phase shift.

The results are tabulated in Table 4-3. The quantity N_f is the number of degrees of freedom, which is the number of data points minus the number of free parameters in the fit. The best fits are for $\gamma_{1\alpha}^2=0$, but acceptable fits are obtained for $\gamma_{1\alpha}^2 \leq 0.1$.

The fits were repeated for different channel radii and different values of the background level (Barker 1970, 1971). For small changes in the channel radius (a = 5.0-7.0 fm) and for large changes in the

background level (E_4 = 10.-100. MeV) there was little difference in the quantity χ^2/N_f.

Table 4-3. Carbon-alpha elastic phase shift fits.

a = 6.0 fm, B = -3.8882, E_1 = -0.046 MeV, N_f = 49

$\gamma_{1\alpha}^2$ (MeV)	E_2 (MeV)	$\gamma_{2\alpha}^2$ (MeV)	E_3 (MeV)	$\gamma_{3\alpha}^2$ (MeV)	E_4 (MeV)	$\gamma_{4\alpha}^2$ (MeV)	χ^2/N_f
0.000	3.0419	0.1889	5.3327	0.0112	10.0	0.6928	0.858
0.005	3.0493	0.1898	5.3328	0.0112	10.0	0.7005	0.968
0.010	3.0500	0.1906	5.3327	0.0111	10.0	0.7096	0.990
0.020	3.0520	0.1924	5.3330	0.0112	10.0	0.7244	0.941
0.040	3.0533	0.1960	5.3330	0.0112	10.0	0.7551	1.034
0.060	3.0555	0.1996	5.3333	0.0112	10.0	0.7859	1.138
0.100	3.0597	0.2068	5.3338	0.0112	10.0	0.8466	1.378
0.200	3.0693	0.2253	5.3355	0.0115	10.0	0.9955	2.340
0.400	3.0863	0.2638	5.3396	0.0122	10.0	1.2874	4.620

The range of acceptable values of the channel radius and the dimensionless reduced alpha width for the first state can be further limited by fitting the spectrum of delayed α particles following ^{16}N β-decay (Barker 1971). The fits limit the channel radius to 6.5±1 fm. For each value of the channel radius the corresponding θ_α^2 is fairly well determined. For a = 6 fm, θ_α^2 = 0.062 (Barker 1971), and from equation (3.34) the reduced level width becomes $\gamma_{1\alpha}^2$ = 0.035.

Once the values of the energy eigenvalues and the reduced level widths are determined then the two-channel many-level R-matrix formula of equation (3.33) may be used to evaluate the cross-section of the $^{12}C+\alpha$ capture reaction.

The remaining parameters to be determined are the gamma reduced width amplitudes, $\gamma_{\lambda\gamma}$. Assume that only the first two are not negligible.

Then $\gamma_{1\gamma}^2$ is determined from the measured lifetime of that state, and $\gamma_{2\gamma}^2$ is chosen to fit the measured cross-section at the 9.59 MeV peak. There then remains the sign of $\gamma_{1\gamma}/\gamma_{2\gamma}$ to be determined. If this is positive, there will be destructive interference in the energy range between the states.

The cross-section at the 9.59 MeV peak (E_α=3.2 MeV) is taken to be 42nb (Jaszczak and Macklin 1971). The gamma width of the 7.12 MeV state is 57meV, which is a weighted mean of the widths given by Swann and Metzger (1957), Evers, et al. (1968), and Swann (1970).

The cross-sections have been measured down to about 1.6 MeV (Jaszczak, et al. 1970), but the Gamow peak for this reaction is approximately at 0.4 MeV, so a relatively long extrapolation must be made. Figure 4-3 shows how the calculated cross-sections compares with the measured values from Jaszczak and Macklin (1971).

The behavior of the calculated cross-sections would indicate that the sign of $\gamma_{1\gamma}/\gamma_{2\gamma}$ should be taken as negative and large values of $\gamma_{1\alpha}^2$ are needed to best fit the measured points. However, the elastic phase shift fits gave best fits for small values, and the delayed α spectrum from ^{16}N β-decay indicated an intermediate value. The only solution to the dilemma for the present investigation is to compute several different evolutionary sequences with different values of the carbon-alpha reaction rate parameters.

A recent three-level R-matrix calculation by Weisser, et al. (1971) indicates that if more precise experimental data were available, such an analysis could yield a good value for the carbon-alpha cross-section in the astrophysical region of interest. There is also the possibility of reactions involving the 2^+ states in ^{16}O. However, with more precise

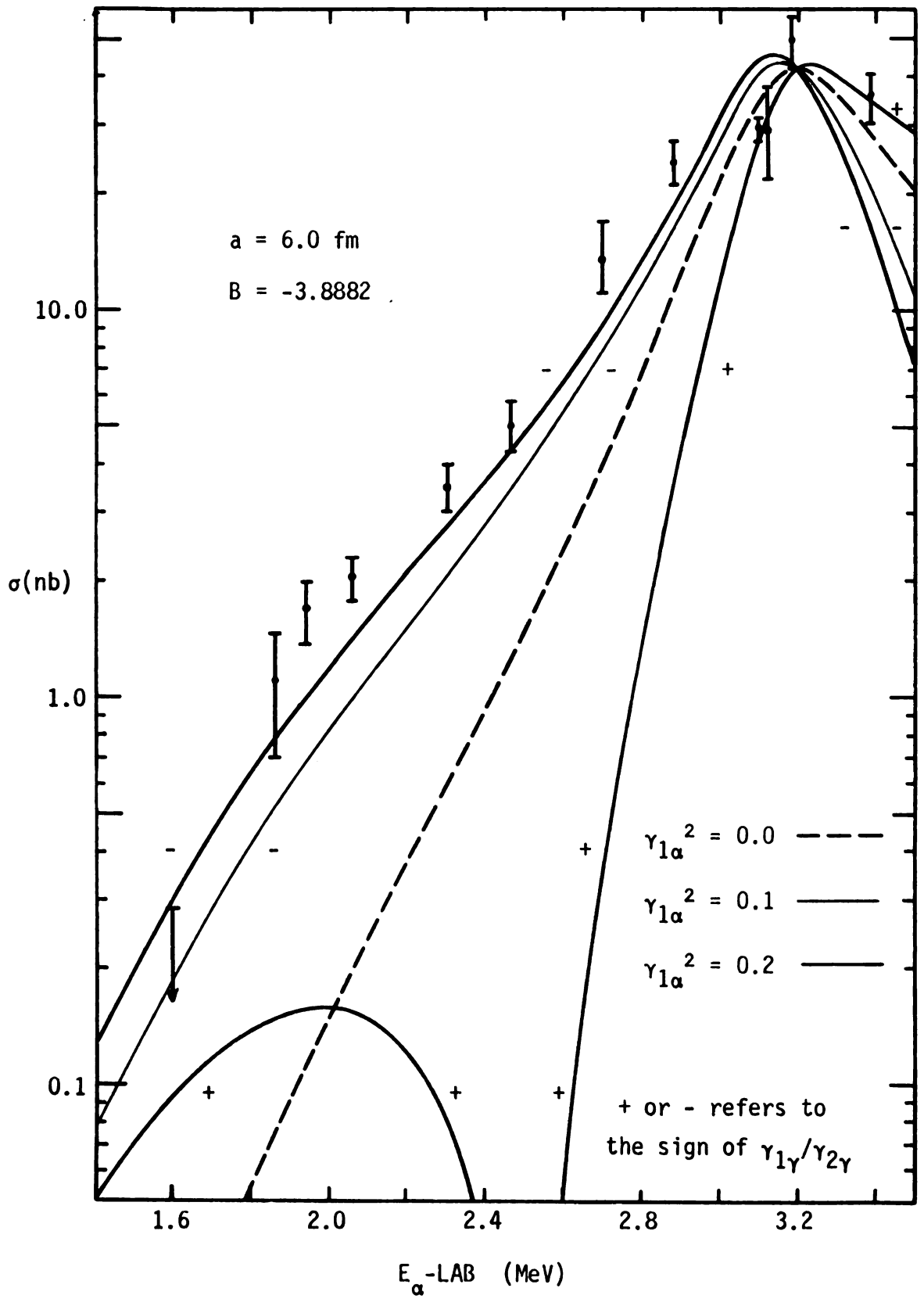

Figure 4-3. Carbon-alpha capture cross-section.

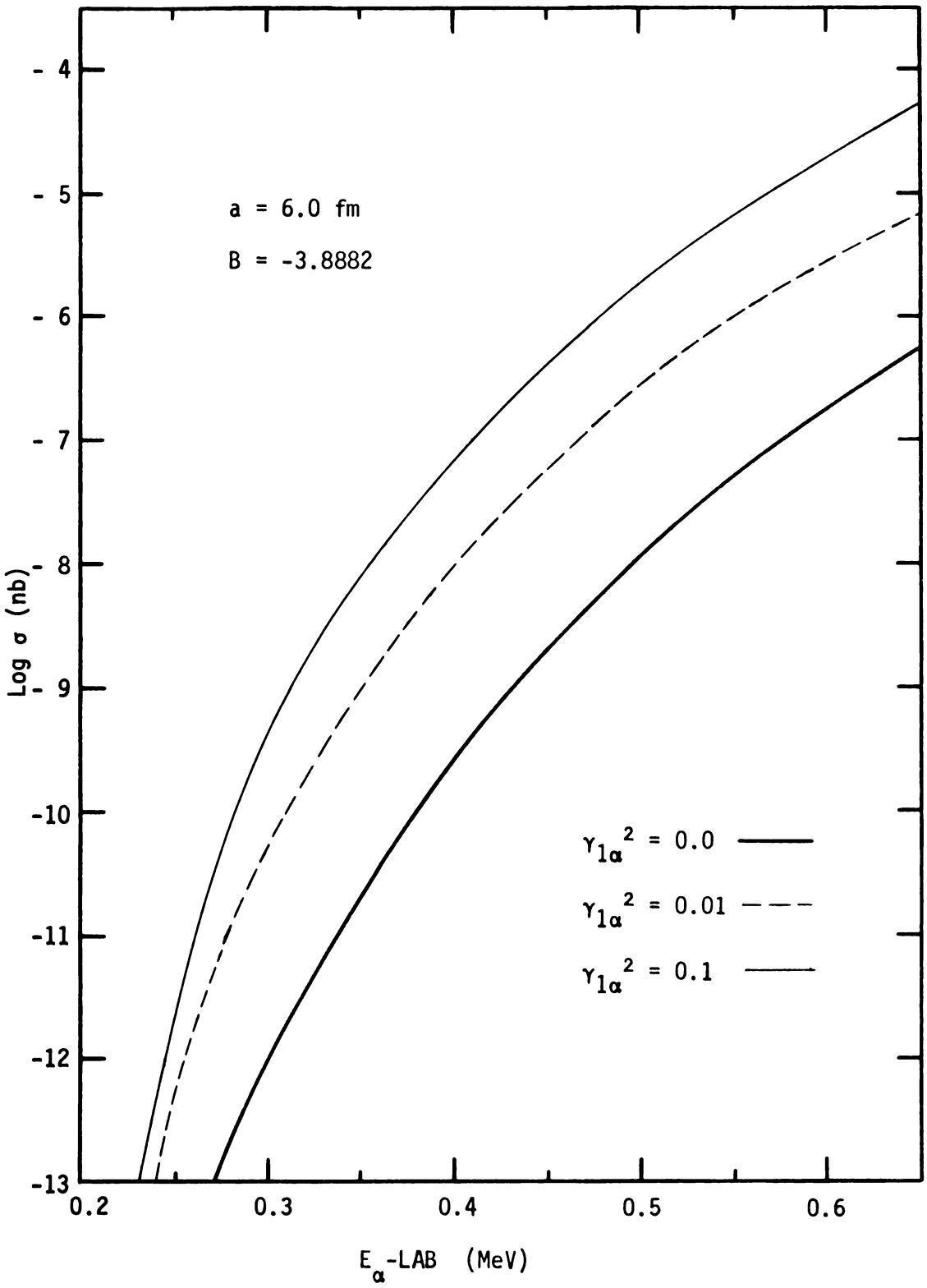

Figure 4-4. Low energy behavior of the cross-section.

data even the effect of these reactions could be taken into account.

The behavior of the carbon-alpha capture cross-section at astrophysical energies is given in Figure 4-4. The Gamow peak occurs at approximately 0.4 MeV. For all the curves the sign of $\gamma_{1\gamma}/\gamma_{2\gamma}$ is taken to be negative. Even for a very small value of $\gamma_{1\alpha}{}^2$ the cross-section is significantly larger than for $\gamma_{1\alpha}{}^2 = 0$, which gives the contribution from the other states alone. Thus one would expect that the parameterization of FCZ, equation (4.18), should reasonably fit the cross-sections.

From the R-matrix calculations the cross-sections are obtained numerically as functions of the energy. To obtain the reaction rates the cross-sections must be integrated over the Maxwellian distribution. The integral of equation (3.11) can be evaluated numerically using Simpson's rule for several different values of the temperature. The range of the energy of the cross-section is taken to be 0.060 - 1.860 MeV with values of the cross-section given at intervals of 0.004 MeV. Decreasing the size of the intervals has no effect on the reaction rates, and at both the lower end and the upper end of the energy range the contribution to the integral is completely negligible. Temperatures are considered over a range of $T_8 = 0.8\text{-}5.0$, with intervals of 0.05. This covers the entire temperature range in which helium burning reactions are expected to take place.

Using equations (4.18) and (3.18) the FCZ parameterization for the reaction rate becomes

$$\lambda_{C\alpha} = \frac{R\times 10^{-15}}{T_9{}^2\ (1 + 0.05T_9{}^{-2/3})^2}\ e^{-S/T_9{}^{1/3}} \qquad (4.20)$$

where R and S are parameters to be adjusted to minimize

$$\chi^2 = \sum_i \left[\frac{\lambda_i - \lambda_{C\alpha}(T_i)}{\zeta_i} \right]^2 \qquad (4.21)$$

where λ_i are evaluated from the integrations of equation (3.11) at a temperature T_i. The weights, ζ_i, are arbitrary, but since the values of λ_i vary over several orders of magnitude a more reasonable fit can be obtained if the weights are assigned a constant fraction of the rates themselves. This makes the absolute value of χ^2 arbitrary, but the relative values can be used as a measure of the goodness of the fit.

Table 4-4. Fits to the FCZ parameterization.

γ_α^2 (MeV)	R	S	χ^2
0.005	0.21021	32.5745	80 120.
0.010	0.26731	32.4054	39 907.
0.020	0.40048	32.3020	15 927.
0.040	0.61730	32.2067	4 231.
0.060	0.81361	32.1605	1 212.
0.100	1.17690	32.1139	9.

The results of the fits are given in Table 4-4. The number of points in the fits is 85, and two parameters are varied. The weights ζ_i are set to 10^{-3} of the rates. As expected the largest values of $\gamma_{1\alpha}^2$ give the best fits. Reasonable fits are obtained by allowing both parameters to vary. If S is fixed at the FCZ value of 32.12, the values of χ^2 obtained are at least 20 times larger than those given above. No significant improvement is found if the coefficient of $T_9^{-2/3}$ in equation (4.20) is also allowed to vary. The largest percentage residuals are found at either the extreme low end or the extreme high end of the temperature range. Near the middle of the range equation (4-20) gives fits that are within 4 percent for the smallest value of $\gamma_{1\alpha}^2$ and

within 0.04 percent for the largest.

Once the functional form of the reaction rate is chosen the energy generation rate may be written down. Thus for $Q_{C\alpha} = 7.1613$ MeV

$$\varepsilon_{C\alpha} = 8.6685\times10^{43} \frac{R\ \rho Y\ X_C\ f_{C\alpha}}{T^2\ (1 + 5.\times10^4\ T^{-2/3})^2} e^{-S\times10^3/T^{1/3}} . \qquad (4.22)$$

As with the triple-alpha reaction define two quantities

$$C_{C\alpha} = 8.6685\times10^{43}\ R, \qquad (4.23)$$

$$E_C = S\times10^3 \qquad (4.24)$$

such that the energy generation rate becomes

$$\varepsilon_{C\alpha} = C_{C\alpha} \frac{\rho\ Y\ X_C\ f_{C\alpha}}{T^2\ (1 + 5.\times10^4\ T^{-2/3})^2} e^{-E_{C\alpha}/T^{1/3}} . \qquad (4.25)$$

The values of these constants used in the present work are given in Table 4-5.

Table 4-5. Carbon-alpha reaction rate parameters.

$\gamma_{1\alpha}{}^2$(MeV)	$\theta_\alpha{}^2$	$C_{C\alpha}(10^{44})$	$E_{C\alpha}(10^4)$
0.005	0.0086	0.18222	3.2574
0.010	0.0173	0.23172	3.2405
0.020	0.0346	0.34716	3.2302
0.040	0.0692	0.53511	3.2207
0.060	0.1040	0.70528	3.2160
0.100	0.1730	1.02019	3.2114

IV-4. Oxygen-alpha reaction

The oxygen that is produced in the carbon-alpha reaction can undergo an additional alpha capture via several different levels in ^{20}Ne. Schematically this is

$$^{16}O(\alpha)^{20}Ne^{*}(\gamma)^{20}Ne \ .$$

The energy level diagram is given in Figure 4-5. The data are taken from Clayton (1968). The notation is the same as for Figure 4-1.

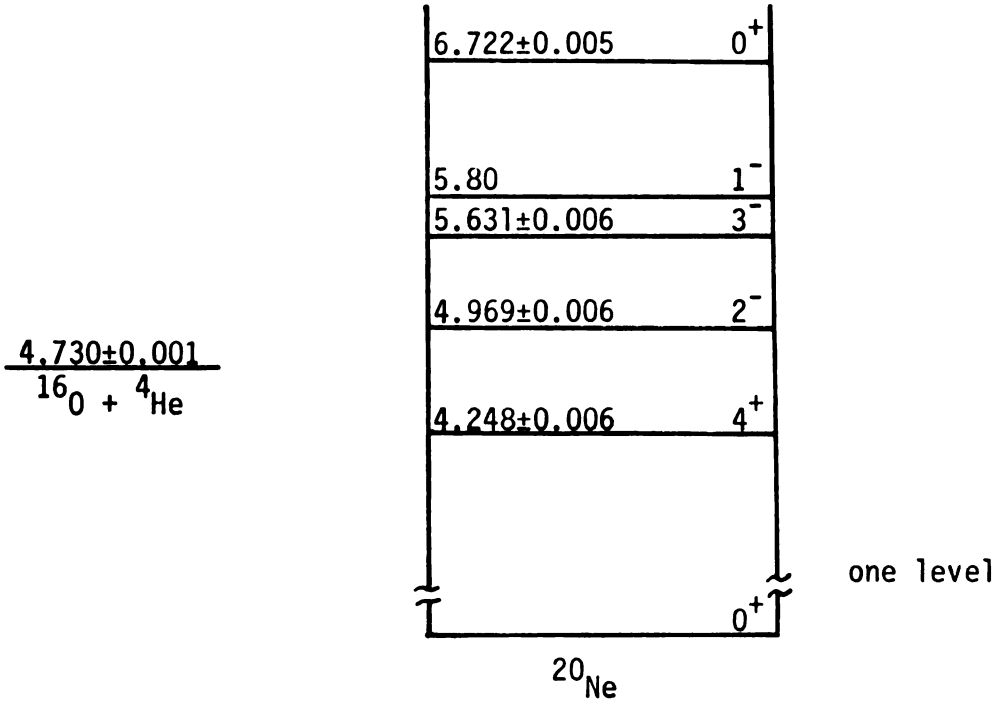

Figure 4-5. Energy level diagram for ^{20}Ne.

For T_8=1 the center of the Gamow peak is at 4.976 MeV, E_o=0.246 MeV, hence the 4.97 MeV level would be the dominant resonance if it were allowed to do so by the nuclear quantum numbers. This level is 2^- and there is no reaction of ^{16}O and ^{4}He that can give this combination.

The next available states are at 5.63, 5.80, and 6.72 MeV. These all have the correct combination of angular momentum and parity to be formed by the oxygen-alpha reaction.

For T_8=1 the reaction will proceed through the tails of the higher lying resonances. The width of the 5.63 MeV state is so much smaller than the widths of the two higher states that the nonresonant reaction rate is largely due to these two states. FCZ provides the data to evaluate this rate for the temperature range T_8<2. These are tabulated in Table 4-6.

Table 4-6. Oxygen-alpha reaction.

quantity	value	reference
Q	4.730 MeV	FCZ
A	3.2	Equation (3.14)
W	819.2	Equation (3.20)
S(0)	0.100 MeV-barns	FCZ
S'(0)/S(0)	0.0	FCZ
S"(0)/S(0)	0.0	FCZ
τ	$3.976\times10^4/T^{1/3}$	Equation (3.21)
E_x	5.622 MeV	Clayton (1968)
J_r^π	3^-	Clayton (1968)
$(\omega\gamma)_r$	1.12 meV	FCZ
E_r	0.901 MeV	Clayton (1968)

Equation (3.19) then becomes

$$S_{eff} = S(0)\left(1 + 1.05\times10^{-5}\ T^{1/3}\right) . \qquad (4.26)$$

For $1\times10^8<T<3\times10^8$ the temperature correction to S(0) varies only from 1.0048 to 1.0064; hence, it suffices to replace this factor by the

constant 1.005. Then S_{eff} becomes

$$S_{eff} = 0.1005 \ . \tag{4.27}$$

Any error introduced here will be negligible compared to the uncertainty in the total expression.

From equation (3.18) the energy generation rate can be written as

$$\varepsilon_{nr} = 9.597\times10^{31}\ \rho X_O\ Y\ T^{-2/3}\ f_{O\alpha}\ e^{-3.976\times10^4/T^{1/3}} \tag{4.28}$$

with an uncertainty of a factor of three (FCZ). This uncertainty will have a large effect on the abundance of neon and the heavier elements, but because the energy generation rate is very small compared to the carbon-alpha, very little neon will be produced. There will be little effect on the relative abundances of carbon and oxygen.

As the temperature increases the resonant reaction through the 5.63 MeV state becomes increasingly important even though the total width of the state is small. It becomes dominant for $T_8>2.5$. The resonant rate from this level can be evaluated by equation (3.40) and the data from Table 4-6. Then the energy generation rate becomes

$$\varepsilon_{res} = 6.7935\times10^{31}\ \rho X_O\ Y\ T^{-3/2}\ f_{O\alpha}\ e^{-1.0456\times10^{10}/T} \tag{4.29}$$

with an uncertainty of 30 percent.

The total energy generation rate for the oxygen-alpha reaction is then given by the sum of the nonresonant and the resonant contributions as

$$\varepsilon_{O\alpha} = \varepsilon_{nr} + \varepsilon_{res} \ . \tag{4.30}$$

IV-5. Neon-alpha reaction

Neon can undergo an additional alpha capture to become magnesium. This is the last reaction to be considered in the present work. This reaction can be written as

$$^{20}Ne(\alpha)^{24}Mg^{*}(\gamma)^{24}Mg \ .$$

The combined mass of ^{20}Ne and ^{4}He lies at an energy of 9.317 MeV in the ^{24}Mg nucleus. This is a region that is thick with available states. The energy level diagram is given in Figure 4-6. The data are taken from Endt and Van der Leun (1967).

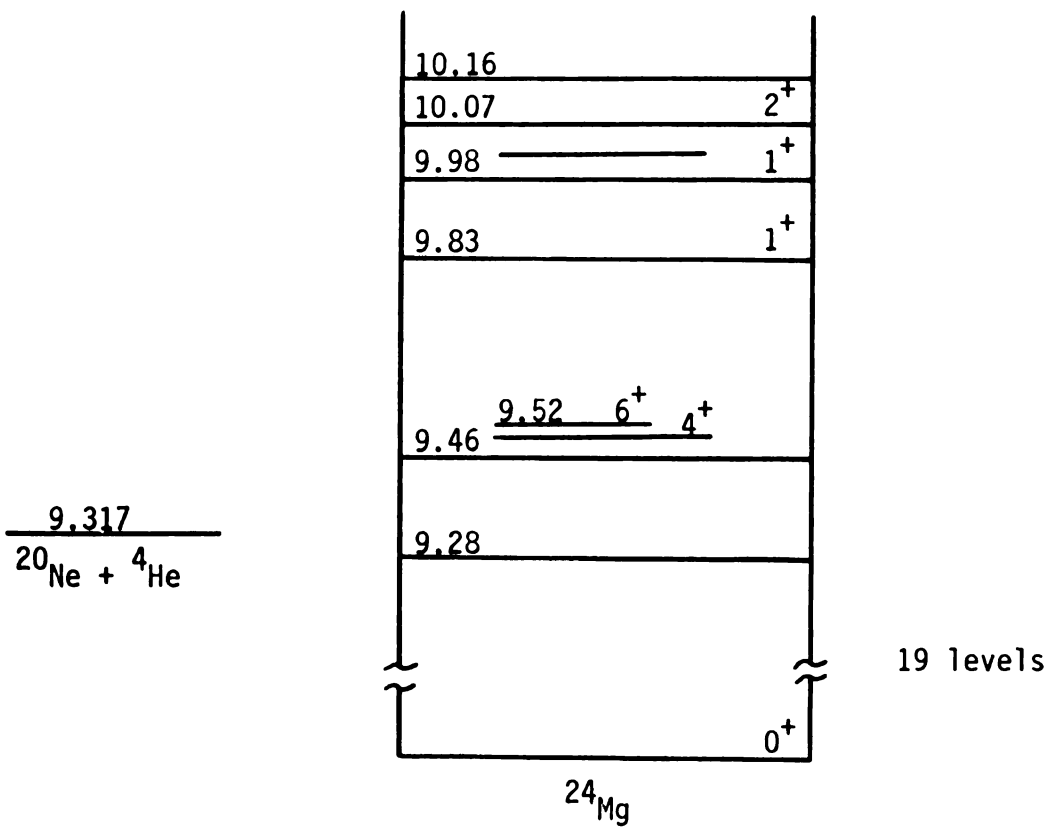

Figure 4-6. Energy level diagram for ^{24}Mg.

The reaction rate will be a sum of many resonant reaction rates. An upper limit for the reaction rate may be obtained from an optical model calculation of the ^{24}Mg nucleus. The calculation depends on there being several resonances within the Gamow peak for any temperature. Reeves (1966) provides a formula from which the reaction rate can be obtained. This is

$$\log \left(\frac{N_\alpha \lambda}{\rho Y}\right) = M - \frac{2}{3} \log T_8 - N T_8^{-1/3} - P T_8^{2/3}. \qquad (4.31)$$

The parameters as given by Reeves are: M = 19.7, N = 43.75, and P = 0.09. The energy released per reaction is 9.317 MeV. After exponentiating to base 10 and rearranging, the energy generation rate becomes

$$\varepsilon_{N\alpha} = 5.316\times10^{42} \rho X_{Ne} Y f_{Ne\alpha} T^{-2/3} e^{-4.676\times10^4/T^{1/3}} e^{-9.619\times10^{-7}T^{2/3}}. \qquad (4.32)$$

CHAPTER V

EQUATION OF STATE

V-1. Introduction

The solution of the structure equations requires the values of the auxiliary variables and their derivatives with respect to temperature and pressure. Several of these are expressed as functions of the density and the temperature (See equations (2.6) through (2.9)). To obtain the density and its partial derivatives with respect to pressure and temperature requires the use of the equation of state. The discussion presented here adheres closely to that of Zimmermann (1970).

The total pressure, P, at a point in a star is the sum of the partial pressures due to the molecules, atoms, ions, electrons, and radiation. Thus

$$P = P_m + P_a + P_i + P_e + P_r. \tag{5.1}$$

For most cases of stellar evolution P_m, the molecular pressure may be neglected since no molecules are normally present. Each of the other terms has a varying contribution to the total pressure depending on the point in the star. Near the surface where ionization is not complete atom pressure is important. Under conditions of high density the electrons become degenerate and the contribution of P_e may dominate.

The total pressure may be expressed as the sum of the gas pressure and the radiation pressure:

$$P = P_g + P_r \tag{5.2}$$

where

$$P_g = P_a + P_i + P_e. \tag{5.3}$$

Define β as the ratio of the gas pressure to the total pressure so that

$$\beta = P_g/P = 1 - P_r/P. \tag{5.4}$$

The radiation pressure is given as

$$P_r = \frac{a}{3} T^4 \tag{5.5}$$

where a is the radiation density constant. Then the derivatives of β can be written as

$$\left(\frac{\partial \beta}{\partial p}\right)_T = 1 - \beta \qquad \text{and} \qquad \left(\frac{\partial \beta}{\partial \theta}\right)_P = 4(\beta - 1) \tag{5.6}$$

where p and θ are defined by equations (2.14) and (2.15) to be the natural logarithms of the pressure P and the temperature T, respectively. The subscript T indicates that the derivative is taken with temperature held constant, and similarly for the subscript P.

It is convenient to include the derivation of the adiabatic gradient ∇_a and its derivatives in the discussion of the equation of state. It may be expressed as

$$\nabla_a = - \frac{1}{C_p} \left(\frac{\partial \rho}{\partial \theta}\right)_P \frac{P}{T\rho^2}. \tag{5.7}$$

The specific heat at constant pressure is required for both the adiabatic gradient and the gravitational energy term, equation (2.10).

From its definition and the first law of thermodynamics one obtains

$$C_p = \left(\frac{\partial U}{\partial T}\right)_P - \frac{P}{\rho^2}\left(\frac{\partial \rho}{\partial T}\right)_P \tag{5.8}$$

where U is the internal energy per unit mass. Equations (5.7) and (5.8) are independent of the form of the equation of state. Thus, once the density, the internal energy, and their derivatives are known, the specific heat and the adiabatic gradient can be obtained.

For a mixture of elements with fractional abundance by mass X_i, nuclear charge Z_i, and atomic weight A_i, the mean atomic weight μ_n of the atoms and the ions is given by

$$\frac{1}{\mu_n} = \sum_i \frac{X_i}{A_i}. \tag{5.9}$$

The mean atomic weight of the electrons μ_e is

$$\frac{1}{\mu_e} = \sum_i \frac{X_i Z_i}{A_i}. \tag{5.10}$$

V-2. Completely ionized perfect gas

Throughout most of the interior of the star the material is completely ionized and the ions and electrons behave as ideal gases. Only near the surface where ionization may be occuring or near the center where the electrons may become degenerate does the material deviate from an ideal gas behavior.

The density for such a gas is given by

$$\rho = \frac{\mu}{R}\frac{P_g}{T} \tag{5.11}$$

where R is the gas constant for a gas of protons, and μ is the mean molecular weight. Since P_a is zero, P_g is just the sum of the ion

pressure and the electron pressure, and μ is a constant given by

$$\frac{1}{\mu} = \frac{1}{\mu_n} + \frac{1}{\mu_e} . \tag{5.12}$$

By equation (5.4) the density may also be written as

$$\rho = \frac{\mu}{R} \frac{\beta P}{T} . \tag{5.13}$$

The derivatives can then be obtained as

$$\left(\frac{\partial \rho}{\partial p}\right)_T = \frac{\rho}{\beta} \qquad \text{and} \qquad \left(\frac{\partial \rho}{\partial \theta}\right)_p = \frac{(3\beta - 4)}{\beta} \rho . \tag{5.14}$$

The internal energy per gram has a contribution from the kinetic energy of the gas, the radiation, and a constant ionization energy. It may be written as

$$U = \frac{3}{2} \frac{RT}{\mu} + \frac{aT^4}{\rho} + U_{ion} . \tag{5.15}$$

The derivative with respect to temperature is then given by

$$\left(\frac{\partial U}{\partial T}\right)_p = \frac{3}{2} \frac{\beta P}{\rho T} . \tag{5.16}$$

The specific heat at constant pressure becomes

$$C_p = \frac{P}{\rho T} \left[\left(\frac{3}{2}\beta - 4\right) \left(\frac{\partial \rho}{\partial \theta}\right)_p + 6(1 - \beta)\right]. \tag{5.17}$$

From equation (5.7) the adiabatic gradient can be evaluated. The derivatives of C_p and ∇_a can be derived by straightforward differentiation. The derivation is somewhat tedious, but the derivatives may be calculated exactly. For finding the corrections to the models the derivatives only need to be known approximately.

V-3. Ionization of hydrogen and helium

The surface of a star may be sufficiently cool that atomic helium and hydrogen are present. Not far into the interior of the star all of the material is completely ionized. In a region where hydrogen and helium are ionizing, the atoms, ions, and electrons behave as ideal gases. The density may still be written as equation (5.13), but now the mean molecular weight is no longer a constant. It is a complex function of the temperature and the pressure. The evaluation of μ given here comes from Baker and Kippenhahn (1962).

The ionizations of hydrogen and helium are almost always independent of each other, but it is convenient to consider them simultaneously. Let y_i denote the fraction of atoms ionized such that:

y_1 = the fraction of hydrogen atoms ionized,

y_2 = the fraction of helium atoms ionized once or twice,

y_3 = the fraction of helium atoms ionized twice.

The number of free electrons per atom, E, is then

$$E = \sum_{i=1}^{3} \nu_i y_i + E_Z \tag{5.18}$$

where ν_i denotes the abundance of each element by number, and E_Z is the contribution from the metals. For i=1 the element is hydrogen, and for i=2 and i=3 it is helium. In terms of the fractional abundance by mass these are expressed as

$$\nu_1 = X\,\mu_n, \qquad \nu_2 = \nu_3 = Y\,\mu_n/A_{He}. \tag{5.19}$$

The number of free electrons from the metals may be readily calculated by assuming that the metals are completely ionized, and that they

contribute A/2 electrons. Then

$$E_Z = Z\ \mu_n/2 \tag{5.20}$$

where Z is the fractional abundance by mass of the metals.

In terms of E and the gas pressure, the electron pressure is given by

$$P_e = P_g\ E. \tag{5.21}$$

The Saha equation gives the relative abundances of different stages of ionization as a function of the temperature and the electron pressure. But by equations (5.18) and (5.21) the number of free electrons, and hence the electron pressure, depends on the relative abundances of the elements in the different stages of ionization. Thus to obtain the y_i's it is necessary to do a Newton-Raphson iteration on the Saha equation and make corrections to the guessed electron pressure until equation (5.21) reproduces the given gas pressure.

The mean molecular weight is then taken to be

$$\mu = \frac{\mu_n}{1 + E}\ . \tag{5.22}$$

For the case of complete ionization, $y_i = 1$ for all i, E becomes μ_n/μ_e, and equation (5.22) reduces to equation (5.12).

The derivatives of μ become

$$\left(\frac{\partial\ \ln\ \mu}{\partial\ p}\right)_T = -\ \frac{1}{1+E}\ \left(\frac{\partial E}{\partial p}\right)_T, \tag{5.23a}$$

$$\left(\frac{\partial\ \ln\ \mu}{\partial\ \theta}\right)_P = -\ \frac{1}{1+E}\ \left(\frac{\partial E}{\partial \theta}\right)_P\ . \tag{5.23b}$$

The density may be expressed as equation (5.13), but its derivatives must also include the derivatives of μ. Thus

$$\left(\frac{\partial \rho}{\partial p}\right)_T = \rho\left[1 + \frac{1-\beta}{\beta} - \frac{1}{1+E}\left(\frac{\partial E}{\partial p}\right)_T\right], \tag{5.24}$$

$$\left(\frac{\partial \rho}{\partial \theta}\right)_p = \rho\left[-1 - \frac{4(1-\beta)}{\beta} - \frac{1}{1+E}\left(\frac{\partial E}{\partial \theta}\right)_p\right]. \tag{5.25}$$

The internal energy per unit mass may be written as equation (5.15), but the ionization energy is no longer constant. It may be expressed as

$$U_{ion} = \frac{R}{\mu_n k}\sum_i \nu_i \chi_i y_i \tag{5.26}$$

where χ_i is the ionization potential. Thus U becomes

$$U = \frac{3}{2}\frac{RT}{\mu} + \frac{aT^4}{\rho} + \frac{R}{\mu_n k}\sum_i \nu_i \chi_i y_i \ . \tag{5.27}$$

This may be rewritten as

$$U = \frac{R}{\mu_n}\left\{\left[\frac{3}{2} + \frac{3(1-\beta)}{\beta}\right](1+E)T + \frac{1}{k}\sum_i \nu_i \chi_i y_i\right\}, \tag{5.28}$$

and its derivative with respect to temperature becomes

$$\left(\frac{\partial U}{\partial T}\right)_p = \left[\frac{3}{2} + \frac{3(4+\beta)(1-\beta)}{\beta^2}\right](1+E) + \left[\frac{3}{2} + \frac{3(1-\beta)}{\beta}\right]\left(\frac{\partial E}{\partial \theta}\right)_p + \frac{1}{kT}\sum_i \nu_i \chi_i \left(\frac{\partial y_i}{\partial \theta}\right)_p . \tag{5.29}$$

The specific heat at constant pressure can then be written as

$$C_p = \frac{R}{\mu_n}\left\{\left[\frac{5}{2} + \frac{4(4+\beta)(1-\beta)}{\beta^2}\right](1+E) + \sum_i \nu_i \Phi_i \left(\frac{\partial y_i}{\partial \theta}\right)_p\right\} \tag{5.30}$$

where

$$\Phi_i = \frac{5}{2} + \frac{4(1-\beta)}{\beta} + \frac{\chi_i}{kT} \ . \tag{5.31}$$

To evaluate these quantities one still needs to know the partial derivatives of E and y_i. If only one stage of ionization is important at a time, then y_i=1 for all lower stages and y_i=0 for all higher stages. The quantity E may then be written as

$$E = C_i + \nu_i y_i \tag{5.32}$$

where

$$C_i = \sum_{j \neq i} \nu_j y_j \ . \tag{5.33}$$

Under the assumption of independent ionization C_i is a constant. Thus the derivatives of E become

$$\left(\frac{\partial E}{\partial \theta}\right)_P = \nu_i \left(\frac{\partial y_i}{\partial \theta}\right)_P , \qquad \left(\frac{\partial E}{\partial p}\right)_T = \nu_i \left(\frac{\partial y_i}{\partial p}\right)_T . \tag{5.34}$$

The problem is now reduced to finding the derivatives of y_i. The y_i's are found from the Saha equation. It may be written as

$$\frac{y_i}{1 - y_i} \frac{E}{1 + E} = e^{\zeta} \left(\frac{T^{5/2}}{\beta P}\right) e^{-\chi_i / kT} \tag{5.35}$$

where ζ is an appropriate constant. This equation may be written in the form

$$\frac{y_i}{1 - y_i} \frac{E}{1 + E} = e^{K_i(P,T)} \tag{5.36}$$

where K_i is given by

$$K_i(P,T) = \zeta + 2.5\theta - p - \ln \beta - \chi_i / kT \ . \tag{5.37}$$

Equation (5.36) can be differentiated with respect to p or θ. Then from equations (5.34) and (5.35) the derivatives of y_i are given as

$$G_i \left(\frac{\partial y_i}{\partial p}\right)_T = \left(\frac{\partial K_i}{\partial p}\right)_T , \qquad G_i \left(\frac{\partial y_i}{\partial \theta}\right)_P = \left(\frac{\partial K_i}{\partial \theta}\right)_P \tag{5.38}$$

where

$$G_i = \frac{1}{y_i(1-y_i)} + \frac{\nu_i}{E(1+E)} . \tag{5.39}$$

From equation (5.37) the derivatives of K_i may be evaluated, then

$$\left(\frac{\partial y_i}{\partial p}\right)_T = - \frac{1}{\beta G_i} , \qquad \left(\frac{\partial y_i}{\partial \theta}\right)_P = \frac{\Phi_i}{G_i} . \tag{5.40}$$

The density, its derivatives, and the specific heat finally become

$$\rho = \frac{\mu}{R} \frac{\beta P}{T} , \tag{5.41}$$

$$\left(\frac{\partial \rho}{\partial p}\right)_T = \frac{\rho}{\beta} \left(1 + \frac{1}{1+E} \sum_i \frac{\nu_i}{G_i} \right), \tag{5.42}$$

$$\left(\frac{\partial \rho}{\partial \theta}\right)_P = \rho \left(\frac{3\beta - 4}{\beta} - \frac{1}{1+E} \sum_i \frac{\nu_i \Phi_i}{G_i} \right), \tag{5.43}$$

$$C_p = \frac{R}{\mu_n} \left\{ \left[\frac{5}{2} + \frac{4(1-\beta)(4+\beta)}{\beta^2} \right](1+E) + \sum_i \frac{\nu_i}{G_i} \Phi_i^2 \right\}. \tag{5.44}$$

The derivatives of C_p do not need to be known accurately. They can be evaluated numerically or by various approximations and simplifications.

V-4. Weak degeneracy

Near the centers of the stars the density may be high enough so that the electrons become degenerate. The ions still behave as a perfect gas, but the electrons must obey the Fermi-Dirac statistics.

The integrals describing the density, pressure, and internal energy of the electron gas (Chandrasekhar 1939) may be written as

$$\frac{\rho}{\mu_e} = m_H \int_0^\infty p \frac{\partial \varepsilon}{\partial p} \, w(p) \, dp \, , \tag{5.45}$$

$$P_e = \frac{1}{3} \int_0^\infty w(p) \, dp \, , \tag{5.46}$$

$$U_e \rho = \int_0^\infty \varepsilon \, w(p) \, dp \tag{5.47}$$

where p is the electron momentum and w(p) is the Fermi-Dirac distribution taken to be

$$w(p) = \frac{8\pi}{h^3} \frac{p^2}{e^{-\psi} e^{\varepsilon/kT} + 1} \tag{5.48}$$

where ψ is the degeneracy parameter and ε is the electron kinetic energy given by

$$\varepsilon = m_e c^2 \left[(1 + p^2/m_e{}^2 c^2)^{\frac{1}{2}} - 1 \right] . \tag{5.49}$$

The quantities m_H and m_e are the masses of the proton and the electron respectively.

Values of ψ run from $\psi=-\infty$ for no degeneracy to $\psi=+\infty$ for complete degeneracy. In practice the transition region between a perfect gas and the totally degenerate gas runs roughly between $\psi=-7$ and $\psi=+7$. This is the region of weak degeneracy.

It is convenient to use an approximation for each of the integrals in equations (5.45) through (5.46). Kippenhahn and Thomas (1964) have devised a series approximation involving twelve terms. Define the two quantities

$$\Lambda = e^{\psi} \, , \tag{5.50}$$

$$\gamma = kT/m_e c^2 . \tag{5.51}$$

Then for the transition region, $0.001 < \Lambda < 1000$, the integrals become

$$\frac{\rho}{\mu_e} = C_1 \gamma^{3/2} \sum_{i=1}^{12} a_i \frac{(1+\frac{1}{2}\gamma u_i)^{\frac{1}{2}} (1+\gamma u_i)}{\Lambda^{-1} + \alpha_i}, \tag{5.52}$$

$$P_e = C_2 \gamma^{5/2} \sum_{i=1}^{12} a_i u_i \frac{(1+\frac{1}{2}\gamma u_i)^{3/2}}{\Lambda^{-1} + \alpha_i}, \tag{5.53}$$

$$U_e \rho = C_3 \gamma^{5/2} \sum_{i=1}^{12} a_i u_i \frac{(1+\frac{1}{2}\gamma u_i)^{\frac{1}{2}} (1+\gamma u_i)}{\Lambda^{-1} + \alpha_i} \tag{5.54}$$

where the constants are given by

$$C_1 = 8\pi (2)^{\frac{1}{2}} m_H \left(\frac{m_e c}{h}\right)^3, \tag{5.55}$$

$$C_2 = \frac{2}{3} \frac{m_e c^2}{m_H} C_1, \tag{5.56}$$

$$C_3 = \frac{3}{2} C_2. \tag{5.57}$$

The coefficients a_i, u_i, and α_i are taken from a table given by Kippenhahn and Thomas (1964) and Kippenhahn, Weigert, and Hofmeister (1967).

As with the ionization case it is necesary to iterate to obtain the correct value of the pressure. With an estimated value of Λ equations (5.52) and (5.53) will give P_e and ρ. From these results the total pressure is evaluated and will in general be different from the given pressure. A Newton-Raphson method is used to correct Λ until the given and the computed pressures are equal.

For the iteration to find Λ, the evaluation of the density derivatives, and the evaluation of the specific heat it is necessary to obtain derivatives of equations (5.52) through (5.54) with respect to temperature and with respect to the degeneracy parameter. From the polynomial

form of these expressions the derivatives may be obtained in a straightforward manner. From these results and equations (5.5) and (5.11) the derivatives of the total pressure with respect to θ and Λ may be computed.

It is necessary to obtain the derivatives of the density with respect to pressure and temperature. These may be found by means of the relations (Kippenhahn, Thomas, and Weigert 1965)

$$\left(\frac{\partial\rho}{\partial p}\right)_T = P \left(\frac{\partial\rho}{\partial\Lambda}\right)_T \left(\frac{\partial P}{\partial\Lambda}\right)^{-1}, \tag{5.58}$$

$$\left(\frac{\partial\rho}{\partial\theta}\right)_P = T \left(\frac{\partial\rho}{\partial T}\right)_\Lambda - \left(\frac{\partial\rho}{\partial\Lambda}\right)_T \left(\frac{\partial P}{\partial T}\right)_\Lambda \left(\frac{\partial P}{\partial\Lambda}\right)_T^{-1}. \tag{5.59}$$

The specific heat at constant pressure may be written as

$$C_p = \frac{3}{2}\frac{R}{\mu_n} + \left(\frac{\partial U_e}{\partial T}\right)_P + \frac{P}{\rho^2 T}\{3[4\rho - \left(\frac{\partial\rho}{\partial\theta}\right)_P](1-\beta) - \left(\frac{\partial\rho}{\partial\theta}\right)_P\} \tag{5.60}$$

where U_e is the electron internal energy. This derivative may be evaluated by using equation (5.59) with ρ replaced by U_e. The factor of T on the right hand side cancels when the derivative is taken with respect to T rather than ln T.

V-5. High degeneracy

For values of $\psi > +7$ the series approximations of equations (5.45) through (5.47) as given by Chandrasekhar (1939) become more appropriate. These are written in terms of a new degeneracy parameter defined by

$$z = [\,(1 + \gamma\psi)^2 - 1\,]^{\frac{1}{2}}. \tag{5.61}$$

Then

$$\frac{\rho}{\mu_e} = C_1\,(2)^{-\frac{1}{2}}\left[\,\frac{z^3}{3} + \frac{\pi^2}{6}\frac{\gamma^2}{z}(1 + 2z^2) + \ldots\,\right], \tag{5.62}$$

$$P_e = C_2 \frac{(2)^{-\frac{1}{2}}}{2} \left[\frac{f(z)}{8} + \frac{\pi^2}{6} \frac{\gamma^2}{z^3} f_2(z) + \ldots \right], \tag{5.63}$$

$$U_e\rho = C_3 (2)^{-\frac{1}{2}} \left[\frac{g(z)}{8} + \frac{\pi^2}{6} \frac{\gamma^2}{z^3} g_2(z) + \ldots \right] \tag{5.64}$$

where

$$f(z) = z(2z^2 - 3)(1 + z^2)^{\frac{1}{2}} - 3 \ln[(1+z^2)^{\frac{1}{2}} - z], \tag{5.65}$$

$$f_2(z) = 3z^4 (1 + x^2)^{\frac{1}{2}}, \tag{5.66}$$

$$g(z) = \frac{8}{3} z^3 [(1 + z^2)^{\frac{1}{2}} - 1] - \frac{1}{3} f(z), \tag{5.67}$$

$$g_2(z) = (3z^4 + z^2)(1 + z^2)^{\frac{1}{2}} - 2z^4 - z^2 . \tag{5.68}$$

As with the weak degeneracy case it is necessary to iterate to obtain the correct value of z. The iteration is done in the same way.

The derivatives of equations (5.62) through (5.64) are needed. They are evaluated quite easily. The density derivatives with respect to temperature and pressure are obtained from these results and equations (5.58) and (5.59) except with Λ replaced by z. The specific heat is also still obtained from equation (5.60) but the U_e derivative is evaluated from equation (5.59) with Λ replaced by z and ρ replaced by U_e as described above.

The derivatives of C_p used are those obtained from equation (5.17) for the perfect gas case. This equation is valid as long as the electrons are non-relativistic. Under cases of extreme degeneracy this is no longer true, but since the derivatives need only be known approximately it suffices to use the derivatives of equation (5.17) in all cases except ionization.

V-6. Limits and pressure derivatives

It is most convenient to evaluate the equation of state for each shell proceeding inward from the surface of the star. The ionization solutions are used until a point is reached such that $y_3 > 0.98$ or $T > 5\times10^5$ °K. The perfect gas solutions are then used until the density and temperature are high enough so that $2.5 \ln T - \ln P < 6.546$, which roughly corresponds to $\psi = -7$, at which point the solutions of weak dengeneracy are used. Whenever these solutions give $\psi > +7$, the high degeneracy solutions are adopted for the rest of the star down to the center.

The transition shells from the ionization solutions to the perfect gas solutions and from the perfect gas solutions to the degeneracy solutions are fixed during the first iteration of the Henyey method. This prevents non-convergence due to one shell being evaluated by different methods at every other iteration. If one shell switches from one method to another, the computed corrections may change sign without decreasing in magnitude at each iteration.

Since many of the auxiliary variables are expressed as functions of the density and the temperature and the solutions of the structure equations require the derivatives with respect to pressure and temperature, it is necessary to obtain expressions whereby these derivatives can be obtained from the derivatives with respect to density. These relations may be expressed as (Sears 1953, p. 55)

$$\left(\frac{\partial w}{\partial p}\right)_T = \left(\frac{\partial w}{\partial \rho}\right)_T \left(\frac{\partial \rho}{\partial p}\right)_T , \tag{5.69}$$

$$\left(\frac{\partial w}{\partial \theta}\right)_P = \left(\frac{\partial w}{\partial \theta}\right)_\rho + \left(\frac{\partial w}{\partial \rho}\right)_\theta \left(\frac{\partial \rho}{\partial \theta}\right)_P \tag{5.70}$$

where w is any of the auxiliary variables expressed as

$$w = w(\rho, \theta) \ . \tag{5.71}$$

CHAPTER VI

OPACITIES AND NEUTRINO COOLING

VI-1. Opacities

The radiative opacities used in this work are taken from tables published by Cox and Stewart (1965). These tables include the effects of bound-bound transitions, bound-free transitions, free-free transitions, and electron scattering. Each table is computed for a specific composition. Since the composition changes during the evolution of a star, it is necessary to interpolate between tables. The compositions of the tables used are given in Table 6-1.

Table 6-1. Opacity tables.

	X	Y	X_C	Z
Kippenhahn 1.	0.602	0.354		0.044
Weigert 1.	0.000	0.956		0.044
Weigert 2.	0.000	0.000	0.956	0.044

During the latter stages of core helium burning considerable oxygen may be present and a fourth table must be considered. However, the opacity table for the Weigert 3. composition which contains equal amounts of carbon and oxygen differs very little from the Weigert 2. table. Hence, it suffices to use just the three tables given in Table 6-1, and a considerable simplification is realized since only two tables need to be considered at any one time. Carbon is present only

when hydrogen is completely absent. Interpolation is linear in Y.

The tables cover a range in temperature from 3000 °K to 10^9 °K and a range in density from 10^{-10} to 10^9 gm/cm^3. The temperature-density plane is divided into rectangular boxes by the grid points of the tables. A four-point interpolation scheme is used with the values of the opacity at the four corners of the box which contains the given temperature and density. Interpolation is linear in log T and log ρ, since the opacity is nearly linear in these variables over much of the range of interest. Radiative opacity derivatives are evaluated by numerical differentiation in the tables.

In electron degenerate regions the heat transport may occur by electron conduction. The equations that describe the transport are identical to those for radiative transport except the opacity must now include the effects of conduction.

Conductive opacities are evaluated from a formula given by Bodenheimer, et al. (1965). This is a modified version of one given by Haselgrove and Hoyle (1959) which was a fit to the tabular values of Mestel (1950). The conductive opacity is given by

$$\frac{1}{\kappa_c} = \frac{T_7}{301.8} \{1 + [0.004364\ (1+X)\ \frac{\rho}{T_7^{3/2}}]^{5/3}\}. \qquad (6.1)$$

Recent work by Hubbard and Lampe (1969) indicate that this formula gives values of κ_c that are up to three times too small. However, since conduction is important only in those regions of extremely high degeneracy, and helium burning takes place in regions of weak degeneracy in the more massive stars, equation (6.1) will suffice for the present investigation. It is a much simpler formula than that of Hubbard and Lampe, and hence is much faster to compute .

The total opacity in degenerate regions is then given by

$$\frac{1}{\kappa} = \frac{1}{\kappa_r} + \frac{1}{\kappa_c} \tag{6.2}$$

where κ_r is the radiative opacity obtained from the tables.

VI-2. Neutrino cooling

There are three thermal neutrino processes that are believed important in the late evolution of stars. At the present there is no experimental evidence that verifies the existence of these processes, but they may be considered fairly possible on theoretical grounds. Since the entire star is quite transparent to neutrinos, they escape without interacting with the rest of the star. Hence the neutrino emission serves as a local energy sink, a cooling mechanism.

The thermal neutrino processes arise from the "universal Fermi interaction" which predicts a direct electron-neutrino coupling. In stellar interiors the conditions of composition, density, and temperature are such that three processes dominate: Photoneutrino, plasma neutrino, and pair-annihilation neutrino reactions.

The photoneutrinos are created when a photon is converted into a neutrino-antineutrino pair by scattering off an electron. The plasma neutrinos are created when a plasmon, a quantum of plasma oscillation, spontaneously transforms itself into a neutrino-antineutrino pair. Pair-annihilation neutrinos arise from the decay of an electron-positron pair directly into a neutrino-antineutrino pair. The electron-positron pairs exist in equilibrium with the radiation field at very high temperatures.

Since the energy losses due to these neutrino processes are "local",

they may be simply treated as a negative energy generation rate in equation (2.1). Beaudet, Petrosian, and Salpeter (1967) have calculated the rate of the neutrino energy loss and derived an analytical interpolation formula.

Define the two quantities

$$\lambda = kT/m_e c^2 \ , \tag{6.3}$$

$$\xi = 10^{-3} \ (\rho/\mu_e)^{1/3} \ \ \lambda^{-1}. \tag{6.4}$$

The quantity λ is the same as γ as defined by equation (5.51). The notation used in this section corresponds to that of Beaudet, Petrosian, and Salpeter (1967).

Also define a function f with seven coefficients by

$$f(\lambda,\xi) = \frac{(a_o + a_1\xi + a_2\xi^2) \ e^{-c\xi}}{\xi^3 + b_1\lambda^{-1} + b_2\lambda^{-2} + b_3\lambda^{-3}} \tag{6.5}$$

and a function g by

$$g(\lambda) = 1 - 13.04\lambda^2 + 133.5\lambda^4 + 1534.0\lambda^6 + 918.6\lambda^8 \ . \tag{6.6}$$

The neutrino emission is then given by

$$\epsilon_\nu = \frac{1}{\rho} \ [(\rho/\mu_e)^3 \ f_{pl} + (\rho/\mu_e) \ \lambda^5 f_{ph} + g \ e^{-2/\lambda} \ f_{pa} \ ] \tag{6.7}$$

where f_{pl}, f_{ph}, and f_{pa} are the form of equation (6.5) but with the appropriate coefficients for the plasma, photo, and pair neutrino rates respectively. These coefficients are tabulated by Beaudet, Petrosian, and Salpeter (1967).

This formula was derived by a least squares fit to correct numerical

values of the neutrino emission rates. The accuracy of the interpolation formula is 5-15 percent in the temperature range 10^8-10^{10} °K for all relevant densities.

For the range of temperatures and densities that may be found in the centers of low and intermediate mass stars during the helium burning phase, the photoneutrino and the plasma neutrino reactions will dominate, but the pair-annihilation rate becomes important in the higher masses near the end of the helium burning (Iben 1966c). Neutrino cooling is calculated for $T > 35\times10^6$ °K in regions where the hydrogen abundance is zero. This temperature is somewhat lower than the ignition point of the helium burning reactions.

CHAPTER VII

COMPUTATIONAL PROCEDURES

VII-1. Envelope integrations

The rapid variation of pressure and temperature near the surface of the star would require a large number of shells and hence a large amount of computation time to adequately cover the region. The calculation of these regions can easily be done separately for given values of the luminosity and the effective temperature, and then the appropriate envelope model is matched to the interior as described in section II-3. The procedure used is that of Zimmermann (1970) which is similar to that of Hofmeister, Kippenhahn, and Weigert (1964).

The photosphere is constructed by assuming a grey atmosphere. The rest of the envelope is integrated using the stellar structure equations until the fitting point is reached. In the photosphere it is convenient to use as the independent variable the optical depth. This is defined as

$$d\tau = -\kappa\rho \, dr \, . \tag{7.1}$$

Then from stellar atmosphere theory, the temperature variation with optical depth is given by

$$T^4 = \frac{3}{4} T_e^4 \, [\tau + q(\tau)] \tag{7.2}$$

where T_e is the effective temperature. The $q(\tau)$ is taken from a table of Chandrasekhar's sixth approximation to the grey atmosphere as given

in Kourganoff (1963, p. 138).

For the photosphere it may be assumed that M_r, r, and L_r are constant. Then the equation of hydrostatis equilibrium may be expressed as

$$\frac{dP_g}{d\tau} = \frac{g_{eff}}{\kappa} \tag{7.3}$$

where g_{eff} is the effective acceleration due to gravity and is given by

$$g_{eff} = \frac{GM}{R^2} - \frac{\kappa\sigma T_e^4}{c} . \tag{7.4}$$

The second term on the right is the correction due to the radiation pressure. It is more realistic to handle the radiation pressure in this way. The total radius of the star is obtained from the given luminosity and effective temperature by the relation

$$L = 4\pi\ \sigma R^2 T_e^4 \tag{7.5}$$

where σ is the Stefan-Boltzmann constant.

Equation (7.3) is integrated down to an optical depth of 2/3. The temperature is given by equation (7.2). The equation of state includes the effects of ionization as well as the perfect gas solutions. The opacities are taken from the same tables by Cox and Stewart (1965) as used for the interior, except that for the envelope only the first two tables listed in Table 6-1 are needed. The integration is started at an optical depth of $\tau = 0.01$ by assuming that the pressure and the optical depth are small enough so that equation (7.3) may be written as

$$\frac{P_g}{\tau} = \frac{g_{eff}}{\kappa} . \tag{7.6}$$

Since the opacity is also a function of the pressure via the density, it is necessary to iterate to find the starting pressure.

Below the photosphere it is no longer a good assumption that r and M_r are constant. The luminosity is still assumed to be a constant throughout the photosphere and the envelope down to the fitting point. The structure equations can now be written with pressure as the independent variable:

$$\frac{d \ln r}{d \ln P} = - \frac{1}{G} \frac{Pr}{M_r \rho} , \tag{7.7}$$

$$\frac{d \ln M_r}{d \ln P} = -\frac{4\pi}{G} \frac{r^4 P}{M_r^2} , \tag{7.8}$$

$$\frac{d \ln T}{d \ln P} = \nabla . \tag{7.9}$$

The temperature gradient is more involved than in the interior. In the outer layers of a star convection may be quite inefficient; thus instead of an adiabatic gradient in the convection zone there may arise regions where the temperature gradient is superadiabatic. These are handled by the mixing-length theory of Böhm-Vitense (1958).

The radiative gradient is given by

$$\nabla_r = \frac{3}{16\pi acG} \frac{\kappa L P}{M_r T^4} . \tag{7.10}$$

The adiabatic gradient is

$$\nabla_a = \frac{\delta}{C_p} \frac{P}{\rho T} \tag{7.11}$$

where δ is defined by equation (2.11).

In the case where the convective gradient is superadiabatic, it is

given by the solution of the cubic equation (Kippenhahn 1963)

$$\nabla_c - \nabla_r + \frac{9}{8U_k}\left[(\nabla_c - \nabla_a + U_k^2)^{\frac{1}{2}} - U_k\right]^3 = 0 \qquad (7.12)$$

where the quantity U_k is defined by

$$U_k = \frac{12\sigma T^3}{C_p \rho^2 \alpha^2 H_p}\left(\frac{8}{gH_p\delta}\right)^{\frac{1}{2}} \qquad (7.13)$$

with g the acceleration due to gravity at the point under consideration, and the pressure scale height H_p is defined as

$$H_p = -P\frac{dr}{dP}\,. \qquad (7.14)$$

The mixing length is taken to be αH_p where α is of the order of unity. For the present work it is chosen to be 1.5.

Equation (7.12) can be solved analytically for ∇_c (Kippenhahn, Weigert, and Hofmeister 1967). The temperature gradient is then evaluated by

$$\nabla = \begin{cases} \nabla_r & \nabla_r < \nabla_a\,, \qquad (7.15a) \\ \nabla_c & \nabla_r > \nabla_a \text{ and } \ln U > -8 - \ln(\nabla_r - \nabla_a), \qquad (7.15b) \\ \nabla_a & \nabla_r > \nabla_a \text{ and } \ln U < -8 - \ln(\nabla_r - \nabla_a). \qquad (7.15c) \end{cases}$$

If ∇_c is only slightly superadiabatic, it suffices to use the adiabatic gradient. In the interior convection is adiabatic.

Equations (7.7) through (7.9) are integrated down to the fitting point. This gives the values of the radius, the luminosity, the temperature, and the pressure at the fitting point. A grid of envelopes is computed that covers the expected luminosity and effective temperature. These are then used to compute the coefficients in equations (2.33) and

(2.34), the interpolation formulas for the outer boundary.

The grid is chosen by the following criteria:

$$\Delta \log L/L_{\odot} = 0.1 \qquad \text{for all } L\,, \tag{7.16}$$

$$\Delta \log T_e = \begin{cases} 0.05 & \log T_e > 3.9, \quad (7.17a) \\ 0.02 & 3.9 > \log T_e > 3.8, \quad (7.17b) \\ 0.01 & 3.8 > \log T_e > 3.6, \quad (7.17c) \\ 0.005 & 3.6 > \log T_e. \quad (7.17d) \end{cases}$$

The values of $\log T_e$ are chosen to keep the changes in radius between one grid point and the next reasonably small.

VII-2. Composition changes

The composition changes are due to two causes: nuclear burning and mixing by a growing convection zone. The situation may be complicated by the presence of nuclear burning in a convection zone.

First consider only the changes due to nuclear burning. The rate of change of a given element is

$$\frac{dX_i}{dt} = \sum_j \epsilon_j E_j - \sum_k \epsilon_k E_k \tag{7.18}$$

where the summation in the first term is over all reactions that produce X_i and the second term includes all reactions that destroy X_i. The quantity E_j is the reciprocal of the energy released per gram of interacting nuclei.

The nuclear burning splits into two phases: hydrogen burning and helium burning. In the hydrogen burning phase only X and Y, the fractional abundances by mass of hydrogen and helium, will change. The rate

equations are:

$$\frac{dX}{dt} = -\epsilon_{pp}E_{pp} - \epsilon_{CNO}E_{CNO} , \tag{7.19}$$

$$\frac{dY}{dt} = -\frac{dX}{dt} \tag{7.20}$$

where

$$E_{pp} = \frac{4m_H}{Q_{pp}}\frac{\phi}{\Phi} \quad \text{and} \quad E_{CNO} = 4m_H/Q_{CNO} \tag{7.21}$$

with Q_{pp} the energy released per reaction in the proton-proton chains and Q_{CNO} the energy released per reaction in the CNO cycle. These are not equal due to different neutrino losses. The quantities ϕ and Φ give the branching for the different pp chains and are defined in section IV-1.

The energy generation rate for the pp chains is proportional to X^2, but the energy generation rate for the CNO cycle is only proportional to X. In the upper main sequence stars the CNO cycle will dominate so the rate equations may be simply integrated by assuming X is constant throughout the time step. The values of X and Y at the new time are:

$$X(t_1) = X(t_o) + \Delta X, \tag{7.22}$$

$$Y(t_1) = Y(t_o) - \Delta X \tag{7.23}$$

where

$$\Delta X = -(\epsilon_{pp}E_{pp} + \epsilon_{CNO}E_{CNO})\Delta t \tag{7.24}$$

with

$$\Delta t = t_1 - t_o . \tag{7.25}$$

The helium burning phase is slightly more complicated. The rate

equations for helium burning are:

$$\frac{dY}{dt} = - \varepsilon_{3\alpha}E_{3\alpha} - \varepsilon_{C\alpha}E_{C\alpha} - \varepsilon_{O\alpha}E_{O\alpha} - \varepsilon_{Ne\alpha}E_{Ne\alpha}, \tag{7.26}$$

$$\frac{dX_C}{dt} = - 3\varepsilon_{C\alpha}E_{C\alpha} + \varepsilon_{3\alpha}E_{3\alpha}, \tag{7.27}$$

$$\frac{dX_O}{dt} = - 4\varepsilon_{O\alpha}E_{O\alpha} + 4\varepsilon_{C\alpha}E_{C\alpha}, \tag{7.28}$$

$$\frac{dX_{Ne}}{dt} = - 5\varepsilon_{Ne\alpha}E_{Ne\alpha} + 5\varepsilon_{O\alpha}E_{O\alpha} \tag{7.29}$$

where

$$E_{3\alpha} = \frac{12m_H}{Q_{3\alpha}}, \quad E_{C\alpha} = \frac{4m_H}{Q_{C\alpha}}, \quad E_{O\alpha} = \frac{4m_H}{Q_{O\alpha}}, \text{ and } E_{Ne\alpha} = \frac{4m_H}{Q_{Ne\alpha}}. \tag{7.30}$$

The triple-alpha reaction is proportional to Y^3. Hence the rate is drastically affected by the helium abundance, and it is not a good approximation to assume that Y is constant during the time step. The rate equations may be written in the form:

$$\frac{dY}{dt} = - AY^3 - BY, \tag{7.31}$$

$$\frac{dX_C}{dt} = - 3CY + AY^3, \tag{7.32}$$

$$\frac{dX_O}{dt} = - 4DY + 4CY, \tag{7.33}$$

$$\frac{dX_{Ne}}{dt} = - 5BY + 5CY \tag{7.34}$$

where

$$A = \frac{1}{Y^3}\ \varepsilon_{3\alpha}E_{3\alpha}\ , \tag{7.35a}$$

$$B = \frac{1}{Y}\ (\varepsilon_{C\alpha}E_{C\alpha} + \varepsilon_{O\alpha}E_{O\alpha} + \varepsilon_{Ne\alpha}E_{Ne\alpha}), \tag{7.35b}$$

$$C = \frac{1}{Y}\ \varepsilon_{C\alpha}E_{C\alpha}, \tag{7.35c}$$

$$D = \frac{1}{Y}\ \varepsilon_{O\alpha}E_{O\alpha}\ . \tag{7.35d}$$

The quantities A, B, C, and D are independent of Y so the rate equations can be integrated.

Integrating equation (7.31) the new value for Y is

$$Y(t_1) = Y(t_o)\left[AY(t_o)^2\ \left(\frac{e^{2B\Delta t} - 1}{B}\right) + e^{2B\Delta t}\right]^{-\frac{1}{2}} \tag{7.36}$$

for $B \neq 0$. If only the triple-alpha reaction is present, then $B = 0$ and the limit of the quantity in parenthesis must be used. Then equation (7.36) becomes

$$Y(t_1) = Y(t_o)\ [2A\Delta tY(t_o)^2 + 1]^{-\frac{1}{2}}. \tag{7.37}$$

Equation (7.32) may be integrated by using equation (7.31) to replace the AY^3 term. It then becomes

$$\frac{dX_C}{dt} = -\frac{dY}{dt} - (B + 3C)Y. \tag{7.38}$$

This equation now contains only a term proportional to Y which can be replaced by the average value of Y during the time step. Then the change in X_C may be written as

$$X_C = - \Delta Y - (B + 3C) Y_m \Delta t \tag{7.39}$$

where

$$\Delta Y = Y(t_1) - Y(t_o), \tag{7.40}$$

$$Y_m = \tfrac{1}{2}[Y(t_1) + Y(t_o)]. \tag{7.41}$$

Then

$$X_C(t_1) = X_C(t_o) + \Delta X_C . \tag{7.42}$$

In like manner the remaining rate equations may be integrated. Thus

$$X_O(t_1) = X_O(t_o) + (4C - 4D) Y_m \Delta t, \tag{7.43}$$

$$X_{Ne}(t_1) = X_{Ne}(t_o) + (10D + 5C - 5B) Y_m \Delta t. \tag{7.44}$$

The abundance of magnesium is then simply found from the conservation of mass:

$$X_{Mg}(t_1) = 1 - Y(t_1) - X_C(t_1) - X_O(t_1) - X_{Ne}(t_1) - Z. \tag{7.45}$$

The composition may also change by a growing convection zone. The convection zone will homogenize the composition. Only full convective mixing is considered in the present work. Semi-convection is not introduced. If the convection zone moves into a region which previously had a different composition, it will average that region in with the rest of the zone. If nuclear burning is present in the convection zone, the composition change will affect the entire region equally. To account for this the nuclear burning must be averaged over the zone. The more accurate method is to average the energy generation and then calculate an average change in the composition (Kippenhahn, Weigert, and

Hofmeister 1967), which is then applied to each shell in the convective region.

The average energy generation for the zone is taken to be

$$\bar{\varepsilon}_i = \frac{1}{q_{j1} - q_{j2+1}} \sum_{j=j1}^{j2} \left(\varepsilon_{ij}\varepsilon_{i,j+1}\right)^{\frac{1}{2}} (q_j - q_{j+1}) \tag{7.46}$$

where $\bar{\varepsilon}_i$ is the average energy generation rate for the i-th reaction, ε_{ij} is the energy generation rate for the i-th reaction at shell j with mass fraction q_j, and j1 and j2 are the outer and inner shells of the convection zone.

This average energy generation rate is substituted into equations (7.19) and (7.35) in place of the unaveraged energy generation rate. The resultant changes in the composition are then applied to each shell in the convection zone. For the helium abundance this becomes

$$Y_j(t_1) = Y_j(t_o) + \overline{\Delta Y}\ , \quad j = j1, \ldots, j2. \tag{7.47}$$

Even if the convection zone does not contain a nuclear burning region, the composition may change if the convection zone moves into a previously radiative region. The composition must be averaged over the convection zone. The average abundance of the i-th element is

$$\bar{X}_{ij} = \frac{1}{q_{j1} - q_{j2+1}} \sum_{j=j1}^{j2} X_{ij}(q_j - q_{j+1}). \tag{7.48}$$

In practice the nuclear burning is first averaged over the convection zone, and then the composition is averaged by equation (7.48). This covers the situation where nuclear burning is taking place in a portion of the convection zone and the zone is growing.

VII-3. Initial Models

The Henyey method requires an approximate model which is then iterated to convergence. Once an evolutionary sequence is underway the approximate model is extrapolated from the previous two models. For the first model an initial approximate model must be supplied.

The evolution is begun with a chemically homogeneous model, which is taken to represent the zero-age main sequence. The initial models are generated by the fitting method of Sears and Brownlee (1965). The equation of state includes ionization but not degeneracy. The outer boundary is treated simply by obtaining the effective temperature from the given radius and luminosity and iterating to find the pressure. The composition is that given in section I-3.

The Henyey method then converges the initial approximation with all the time derivatives in the energy equation set to zero. This model is then model number one of the evolutionary sequence. The initial guess for the structure of model number two is just the converged first model. Succeeding initial guesses are extrapolated from the previous two models.

VII-4. Time steps

For most of an evolutionary sequence it is desirable for the program to select an appropriate time step. The criterion must be such that the composition or the structure variables do not change by a large amount.

The first step is to obtain the energy generation rates for the individual reactions. The maximum rate of change of helium is computed,

and a time step is chosen to keep the maximum change in the element that is being burned small. If burning occurs in a convective core, it is appropriate to compute an average change for the convective core. The maximum permissible change allowed is 20 percent unless the abundance of the burning element is less than 10^{-4}, then the change is fixed at a small quantity to allow burnout in a few more models.

During the helium burning phase a hydrogen burning shell source may be present. If so, the inner and outer limits are found. The maximum change in the composition is also computed. It is also possible that a luminosity inversion may occur if the temperature maximum in the star is not at the center. Any inversion is also found.

The maximum rate of change of each of the structure variables is computed from the present model and the previous one. If a shell source is present the temperature and pressure changes in the shell are ignored in finding the maximum changes in these variables. The profiles of temperature and pressure as a function of mass fraction are quite steep in this region. They tend to move out through the star. The gravitational contribution to the luminosity is small, hence large changes may be allowed in these variables without introducing noticeable error. If only small changes were allowed, then unreasonably short time steps would be necessary. Similarly the criteria for the maximum rate of change of the luminosity near an inversion point is also relaxed.

From the maximum rate of change of the structure variables a time step is computed to allow no more than a 20 percent change. The smaller of the composition time step and the structure time step is chosen as the calculated time step, τ_{cal}. The new time step τ_{new} is then chosen to be

$$\tau_{new} = 2^{n}\tau_{old} \tag{7.49}$$

where n is an integer such that

$$-4 \leq n \leq 1, \tag{7.50}$$

$$2^{n-1}\tau_{old} < \tau_{cal} < 2^{n}\tau_{old} . \tag{7.51}$$

Equation (7.50) is always satisfied, and equation (7.51) is used to determine n within the limits of equation (7.50). The quantity τ_{old} is the time step for the previous model to the present model.

Once the time step is chosen the composition is changed by the method described in section VII-2. If the helium abundance is less than 10^{-5}, then

$$X_C(t_1) = X_C(t_o) - 3Y(t_o), \tag{7.52a}$$

$$X_O(t_1) = X_O(t_o) + 4Y(t_o), \tag{7.72b}$$

$$Y(t_1) = 0. \tag{7.52c}$$

The new model is extrapolated from the previous two models except in the region of a thin shell source. If the shell source is sufficiently thin, the entire shell is moved bodily out through the star by the shell profile method. The profiles of the structure variables are kept constant, but the mass fraction of each shell is changed corresponding to how much the shell has burned in the interval.

The luminosities are interpolated in the region of an inversion point. Finally the track in the H-R diagram is extrapolated. If the star has moved outside the previous box in the atmosphere table, a new box is selected and the coefficients for the outer boundary interpolation formula are calculated.

At times it is convenient to select the time step manually. In this case the program merely mixes the composition and extrapolates to the new

model using the preset time step.

VII-5. Rezoning

The necessary zoning in a star varies from one part of the star to another. It is desirable to keep the changes in the structure variables and the composition small from one shell to the next. In certain regions of the star the zoning must be very fine since the structure variables are changing quite rapidly with the mass fraction. In other regions where the changes are slow the zoning may be quite coarse. If a fine zoning is used throughout the star, an unreasonable number of shells would be required and a large amount of computing time would be used in regions where nothing is happening. So it is desirable to adjust the zoning to keep the total number of shells as small as possible and also adequately handle those regions where large changes are occuring. As the star evolves these regions move in the star so shells must be continually inserted and deleted.

It is desirable to make the rezoning automatic; however, to write a program that would anticipate all possible situations would take large amounts of time. In many cases manual control may be used to a good advantage. Normally the composition variables should not change by large amounts from one shell to the next, but at the edge of a growing convection zone there is physically a composition discontinuity. This should be allowed to exist, and shells should not be inserted to decrease the discontinuity. If the convection zone then retreats, there is no way for the program to realize that it should not insert shells at that point.

The model is rezoned after it has been extrapolated to the new

model but before any corrections have been applied. Shells are first deleted and then other shells are inserted by a linear interpolation scheme. A check is made to prevent deletion of a particular shell and then an immediate insertion of a shell at that point.

VII-6. Core evolution

For helium burning investigations it is only necessary to repeat the evolution from the point at which the triple-alpha process ignites. Further, since helium burning occurs only in a small region of the star, it is desirable to compute only that region. As previously discussed in chapter I and in section II-6, the structure of the star is relatively insensitive to the actual reaction rate parameters used. The outer portions of the stars will be essentially the same for different evolutionary sequences using different values of the reaction rate parameters. The values of the structure variables at a specific point in the star obtained from one evolutionary sequence of the entire star may be used as an outer boundary of an evolutionary sequence of the core alone. The procedure by which these are applied to the core is discussed in section II-6.

The largest changes in the outer boundary of the core occur near the beginning of the helium burning phase and near the end. It is necessary to choose the core boundary conditions to match the evolutionary state of the interior.

As noted in chapter I, the time scales for the helium burning phase will be altered for different values of the reaction rate parameters. Thus if the age of the core is used to select the outer boundary conditions, then the large changes in the structure variables at the outer

edge of the core that are associated with core burnout may occur later or earlier than the actual burnout. This may have little effect on the final abundances of carbon and oxygen. The alteration in the time scale is not large,and near burnout when the helium abundance is small the triple-alpha process is smaller by a factor of Y^2 than the carbon-alpha reaction. Thus the carbon-alpha reaction dominates, and there is little competition between the two reactions.

Instead of age, a possible independent variable is Y_c , the central value of the helium abundance. Because of the extreme temperature dependence of the helium burning reactions, most of the energy is released in a very small region of the star. Radiative transfer is unable to transport the energy out and a convection zone develops. Thus the central value of the helium abundance is given by the helium abundance of the convection zone. As the zone changes size, the helium abundance at the center may change. As the zone increases there is more helium mixed into the central region. If the zone decreases, then there is less volume for the helium to mix into. For a given rate of energy generation at the center, there will be a larger rate of change of helium abundance in the region. The exact value of the central value of the helium abundance is dependent on the precise zoning near the edge of the convective core and may not always be a smooth function.

A third possible independent variable to use is the average helium content in the core. This is expressed as

$$\overline{Y} = \frac{1}{q_k} \sum_{j=k}^{m-1} Y_j (q_j - q_{j+1}) \tag{7.53}$$

where Y_j is the fractional abundance by mass of helium at shell j, and q_j is the mass fraction of that shell. The index k is the shell number

of the edge of the core in the complete star. For different models in an evolutionary sequence the value of k will change but the mass fraction of the shell q_k will be a constant. For the core itself, the shells are renumbered so that the outer boundary is at j=1.

If the outer boundary is chosen so that it is interior to all hydrogen burning, then $\overline{Y}$ will be a monotonically decreasing function of the time. Also all reference to hydrogen can be deleted from the program, resulting in another simplification. It is also desirable to make the core as large as possible. This will make any errors in the outer boundary conditions to have the least effect on the center of the core where most of the nuclear burning is taking place.

The burning occurs in a convective zone. Unfortunately, this convective region grows as the helium burning progresses and only decreases again when the helium abundance in the center becomes very low. Full convective mixing is assumed so that the composition is fully homogenized over the region. This leads to a very drastic composition discontinuity at the edge of the convective region. Thus a slight difference in the location of this discontinuity may have a major effect on $\overline{Y}$ for a given central helium abundance.

The region just outside the nuclear burning region is almost neutrally stable against convection, thus small errors in the temperature gradient may result in large differences in the location of the convective boundary. If the temperature that is forced onto the outer core boundary is slightly too small for what the star would really like, then the temperature gradient is steepened and the size of the convection zone will increase.

In the complete evolutionary sequences of the stars there is little

difference in the size of the convective zone even with rather large differences in the reaction rate parameters. Thus to provide a more realistic situation and force consistency between model cores, the size of the convective zone is also specified as a function of $\overline{Y}$,and full mixing is only done over this region. The program is allowed to use either the convective or radiative transport equation in solving the structure equations. Only for the mixing is a convective region of a specified size forced on the core.

Mixing in this way also makes $\overline{Y}$ a good independent parameter. The core burnout will now always occur at a specific value of $\overline{Y}$, and the outer boundary conditions will follow the evolution of the interior.

The procedure for the core evolution is first to pick a starting model and an edge of the core. This is to be below the hydrogen burning shell, but it is to be as large as possible. Then for each model in the evolutionary sequence for the entire star obtain the averaged helium abundance of the core, the size of the convective core, and the values of the temperature and the pressure at the specified point.

The core evolution program then determines the time step as described in section VII-4. An additional constraint is set to limit the change in Y to 0.02. This was unnecessary for the evolution of the entire star where changes in the envelope limit the time steps even more. The average helium abundance for the present model is determined. This is used to set the size of the convective region by a linear interpolation scheme in the outer boundary tables. The composition is then advanced and the structure of the core is extrapolated. The values of the temperature and the pressure at the outer boundary are fixed by linear interpolation in the outer boundary tables. The Henyey method then

converges the model. A very small error is introduced by using the boundary conditions for the present model as the appropriate boundary conditions for the new model. The error is very small since only near the beginning of the helium burning and near the end are the changes in the boundary conditions large, and at those times the time step must be relatively short since large changes are occuring near the center of the core. The boundary conditions between any two subsequent models are almost identical.

CHAPTER VIII

EVOLUTION AT 7.0 SOLAR MASSES

VIII-1. Introduction

A mass of 7.0 solar masses is a reasonable choice for a typical upper main sequence star. The evolution at this mass has been previously investigated by Hofmeister, Kippenhahn, and Weigert (1964a, 1964b, and 1964c). This mass is sufficiently high to give a relatively rapid evolution but is not so large as to encounter difficulties with semi-convection in the envelope. It is a reasonably well behaved star.

The triple-alpha rate is fairly well determined, but the carbon-alpha rate is very uncertain. Rather arbitrarily the value chosen for the carbon-alpha reaction rate is the parameter $\gamma_{1\alpha}{}^2 = 0.01$ MeV. This is near the lower end of the possible range for this parameter.

The evolution is repeated from the point at which the helium burning reactions ignite for another value of the carbon-alpha reaction rate parameter, namely $\gamma_{1\alpha}{}^2 = 0.1$ MeV, which is the largest value used in the present work. From each of the two evolutionary sequences values of the core boundary conditions are obtained. These are first used to check the validity of the core evolutions, and then they are used to investigate other values of the reaction rates.

The convergence criterion is set so that the maximum correction is less than 10^{-4} for the model to be considered converged. For the giant models this is relaxed to 3×10^{-4}.

VIII-2. Hydrogen burning phase

The star spends most of its lifetime near the main sequence burning hydrogen in the center. A moderate convective core is present due to the fairly high temperature dependence of the CNO reaction rate. The changes in the star are quite slow and relatively large time steps may be taken.

The track in the H-R diagram is given in Figure 8-1. The small letters label the local extrema in the luminosity or in the effective temperature. The data for these points are given in Table 8-1. The value for the luminosity of the sun is taken to be 3.79×10^{33} erg/sec. The age is in units of millions of years, and all other quantities are in cgs units. The quantity q_{cc} is the mass fraction at the edge of the convective core, if one is present. Additional points are given that correspond to important conditions in the interior and are labeled in the last column.

The structure of the interior during the hydrogen burning phase is shown in Figure 8-2. The "bubbly" regions denote convective regions, and the hatched areas show where the energy generation rate is large.

The evolution of the center of the star in the log ρ-log T plane is given in Figure 8-3. Contour lines for constant values of the degeneracy parameter are also shown.

Both the convective core and the region of energy generation slowly shrink as the star evolves from a to b, but the central value of the energy generation rate increases, as does the central value of the temperature and the density. The total luminosity of the star increases, but the effective temperature decreases as the envelope expands. At b

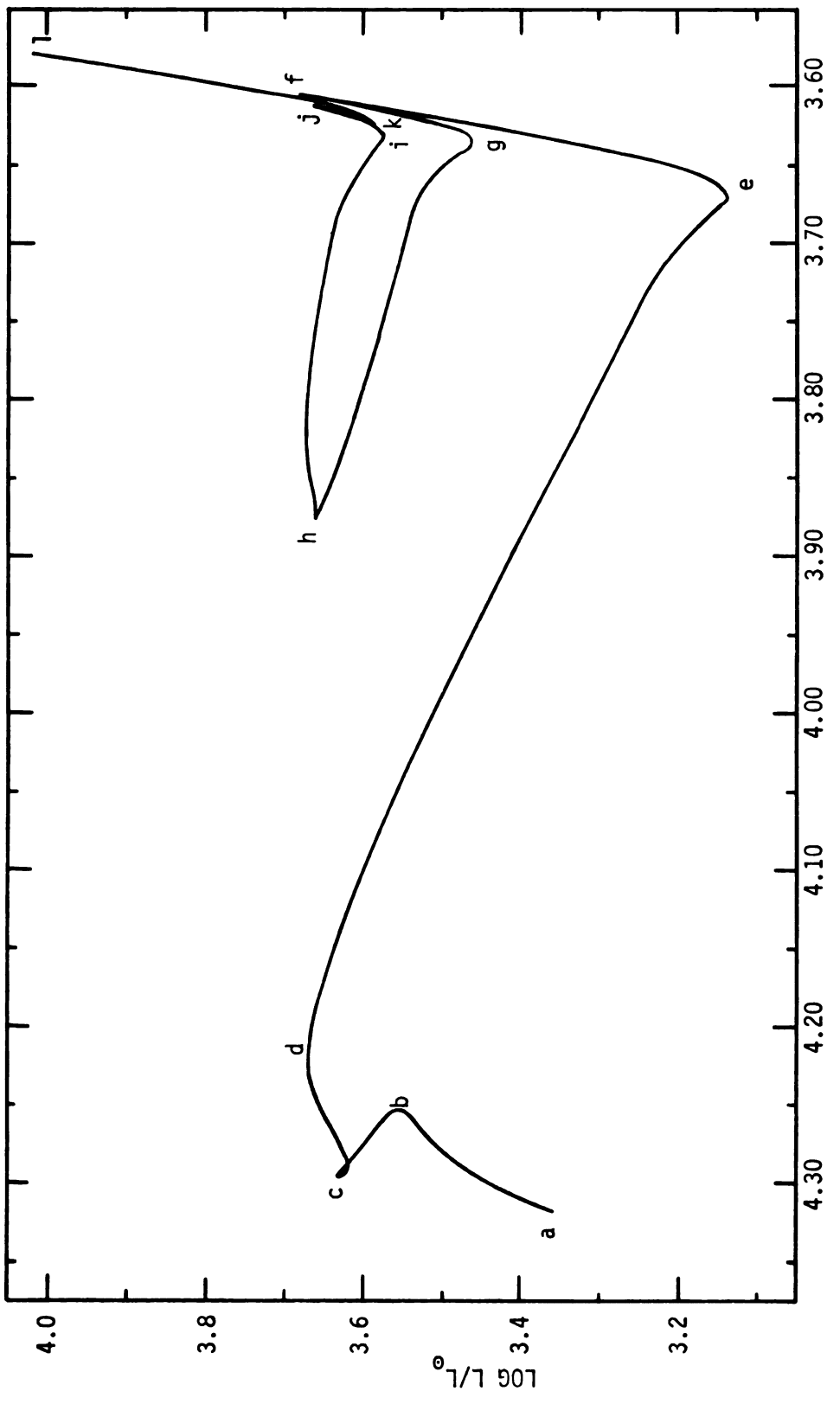

Figure 8-1. H-R diagram for the evolution of the 7.0 $M_\odot$ star.

Table 8-1. Parameters for the 7.0 $M_\odot$ evolution.

	Model	Age	log T_e	log $L/L_\odot$	log R	Y_c	ϵ_c	log T_c	log ρ_c	q_{cc}	comment
a	1	0.	4.316	3.352	11.406	0.3540	2.2E+4	7.4453	0.9981	0.224	initial model
b	20	25.408	4.257	3.575	11.636	0.9384	7.1E+4	7.5594	1.2842	0.116	
c	45	25.776	4.295	3.636	11.590	0.9558	2.5E+4	7.6344	1.6140	0.040	
	53	25.788	4.290	3.624	11.595	0.9560	0.	7.6128	1.8123		burnout at center
d	58	25.852	4.254	3.659	11.685	0.9560	0.	7.6013	2.2983		
	71	26.108	4.025	3.540	12.082	0.9560	1.9E-5	7.9101	3.5281		3α ignition
e	94	26.174	3.669	3.136	12.592	0.9560	3.7E+1	8.0380	3.8480		
	106	26.186	3.625	3.456	12.842	0.9559	2.9E+2	8.0596	3.9006		
	111	26.196	3.613	3.586	12.929	0.9556	1.8E+3	8.0800	3.9385		$\epsilon > 10^3$
	114	26.206	3.610	3.624	12.954	0.9550	1.6E+4	8.1081	3.9551	0.005	maximum ρ_c
f	126	26.274	3.604	3.682	12.995	0.9477	5.3E+4	8.1355	3.8172	0.043	
g	185	28.902	3.635	3.463	12.825	0.6035	8.7E+4	8.1766	3.6420	0.058	
h	288	30.148	3.872	3.664	12.452	0.3990	1.0E+5	8.1994	3.6435	0.065	
i	396	32.400	3.629	3.577	12.893	0.0518	1.0E+5	8.2893	3.7997	0.079	
j	430	32.794	3.611	3.669	12.976	0.0002	1.0E+5	8.3714	4.1292	0.010	
	437	32.801	3.612	3.662	12.970	0.	0.	8.3586	4.1784		burnout at center
k	495	32.929	3.623	3.584	12.909	0.	0.	8.3329	4.6657		
	504	32.994	3.615	3.620	12.942	0.	0.	8.3460	4.8105		H shell < 10^3
l	541	33.396	3.579	4.023	13.217	0.	0.	8.5425	5.9050		

Age in 10^6 years.

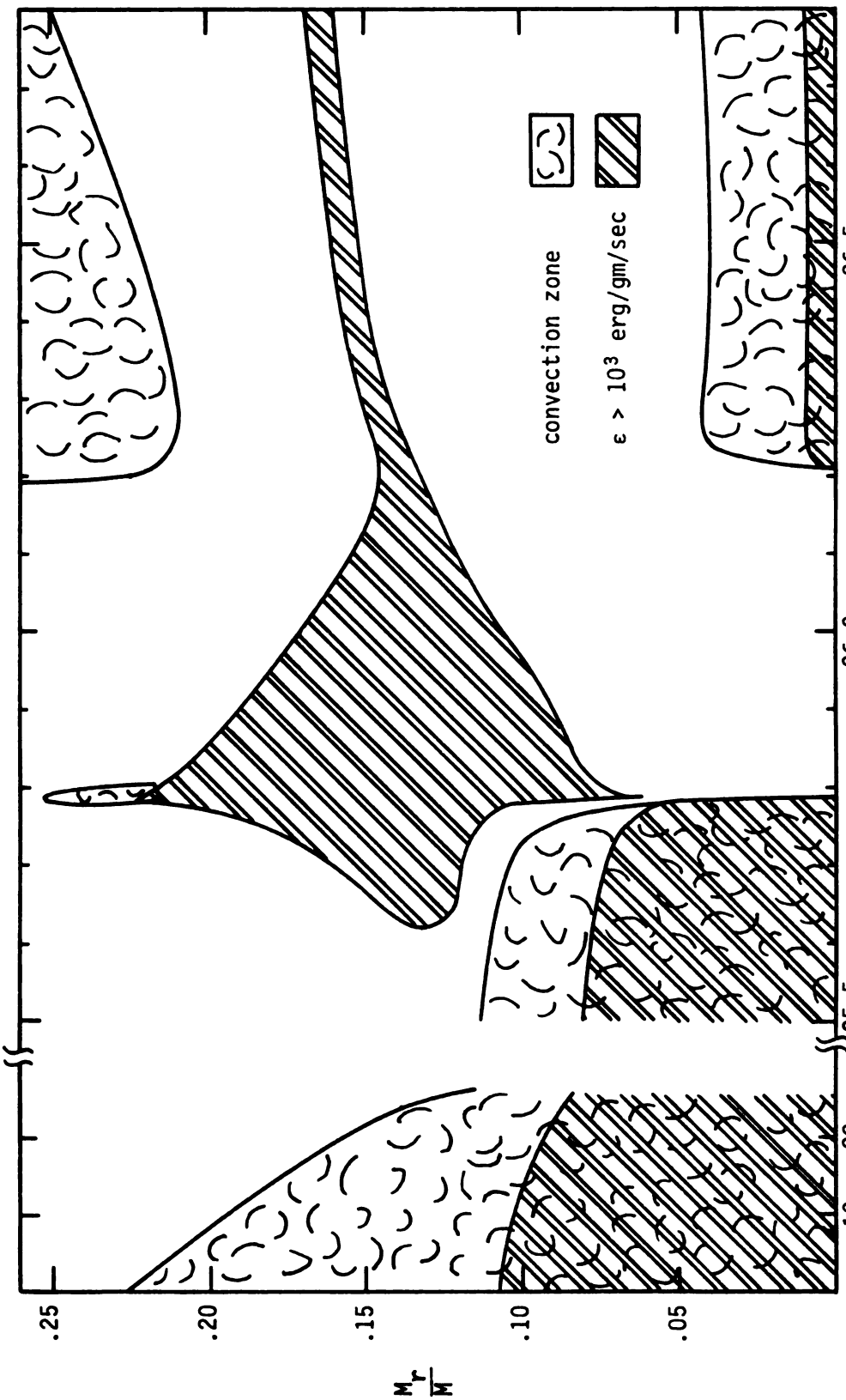

Figure 8-2. Interior conditions during the early evolution of the 7.0 $M_\odot$ star.

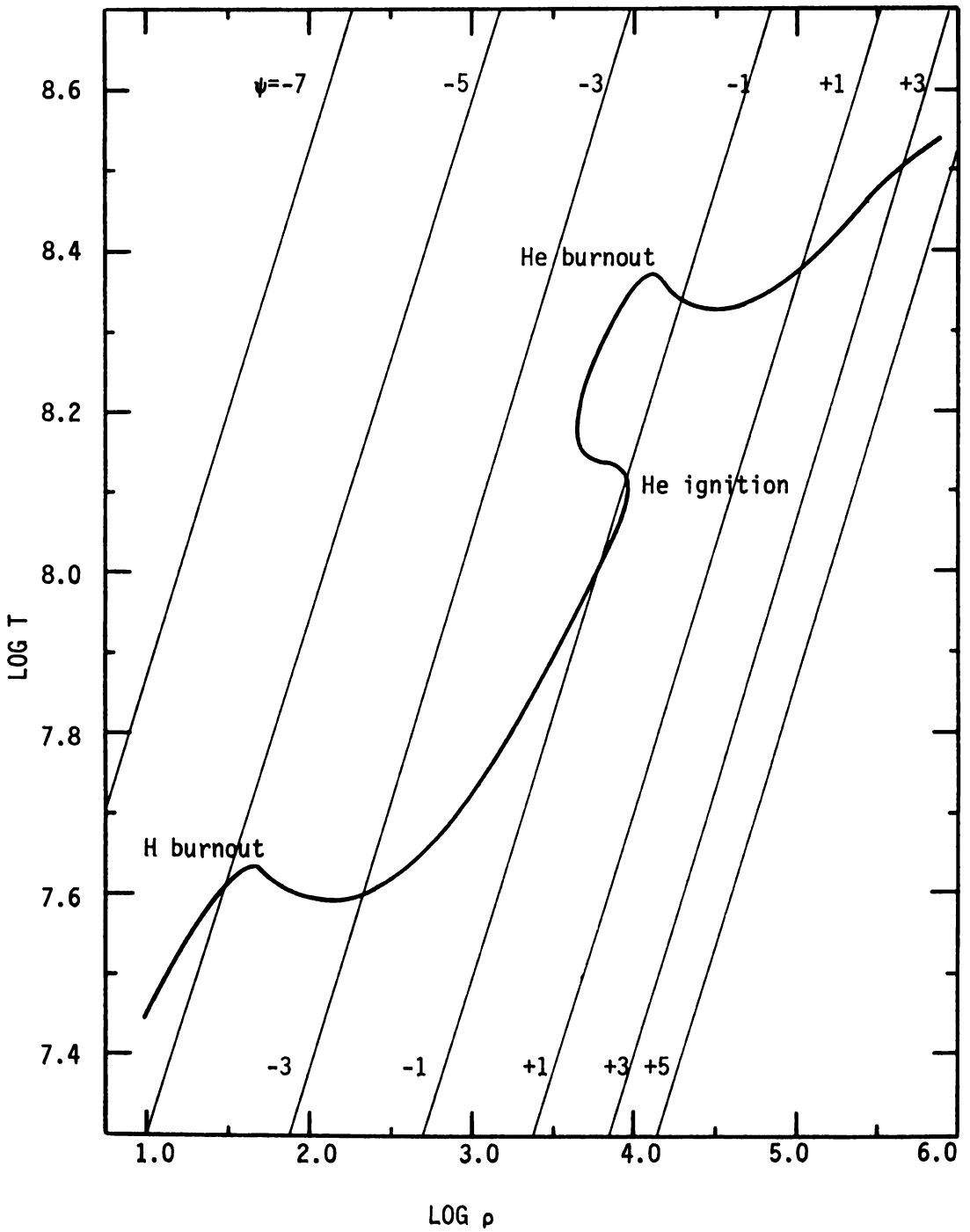

Figure 8-3. Evolution of the center of the 7.0 $M_\odot$ star.

the radius begins to decrease so the star moves toward the left as the effective temperature rises. The shrinking convective core leaves behind a fairly smooth composition gradient. The dependence on X of the energy generation rate is small as compared to the dependence on T, but as burnout approaches, a shell begins to develop due to the greater abundance of hydrogen further out in the star as compared to the central value.

As the shell source begins to grow in importance, the star reverses its track in the H-R diagram at c and begins to expand. The shell grows quite rapidly, and the convective region shrinks suddenly to zero a short time before the actual burnout occurs. For awhile the energy is generated over a very large region but with a low generation rate at any point. The core burns out,and the shell source begins to shrink from both the outer and inner edges. Since there is no longer any energy being liberated in the center and the center is somewhat degenerate, the central value of the temperature decreases after burnout. The core is contracting so the density increases quite rapidly. Soon sufficient thermal energy is liberated from the gravitational potential energy that the temperature begins to rise.

At the maximum extent of the shell source a small convection zone appeared near the outer edge. This was not observed by Hofmeister, Kippenhahn, and Weigert (1964b). The difference may be due to the different opacity tables that they used. The appearence of the convection zone may be indication that semi-convection is trying to occur. In the 5.0 $M_\odot$ star no convection zone appeared, and in the 15.0 $M_\odot$ star a large convection zone developed that had a major effect on the evolution of the envelope. This will be discussed in detail below. There is no major

effect on the envelope of the 7.0 $M_\odot$ star. The size of the convection zone is quite small, and no large discontinuities in the composition appeared.

The shell source narrows very rapidly as the star moves to point e. This portion is covered in a fairly short time. The triple-alpha process ignites at model 71. This is the first time that $\epsilon_{3\alpha} > 10^{-5}$, which is the smallest non-zero value that the program allows for the energy generation rate. The nuclear energy generation rate at this point is still several orders of magnitude below the gravitational energy source. It has no effect on the evolution of the star until it has grown much stronger.

VIII-3. Helium burning phase

At point e a large convective envelope develops,and the star begins to move up the red giant branch. At model 111 the energy generation rate becomes greater than 1000 erg/gm/sec, and shortly afterwards, the central density reaches a maximum and begins to decrease as the additional energy being liberated in the region forces an expansion. The center of the star is slightly degenerate, so the ignition of the triple-alpha process is mildly explosive. Both the convective core, which develops at this time, and the region of energy generation reach a maximum and then decrease slightly as the core adjusts to the helium burning.

As the helium burning core begins to dominate the structure of the entire star, the rapid increase in luminosity as the star moves up the red giant branch is halted at point f, and the track is reversed. There follows a relatively long period in which the convective envelope slowly retreats. The hydrogen burning shell is stabilized in size and is

burning its way out through the star. It is still in the composition gradient left over from the shrinking convective core during the core hydrogen burning phase. As it moves into regions of higher hydrogen abundance, it slows its rate of movement outward but remains approximately the same size.

The interior evolution during the helium burning phase is shown in Figure 8-4. The central convection zone, after contracting slightly following the ignition of the triple-alpha process, begins to increase in size. A fairly large composition discontinuity develops at its outer edge as the helium is destroyed in the center. At point g the convective envelope has almost disappeared, and the star begins to move away from the red giant branch.

The star evolves moderately fast to its maximum effective temperature at point h. The envelope is decreasing in size, and the helium burning is proceeding at a fairly uniform rate with only a small increase in the central density. From point h to point i the core begins to contract more rapidly and the envelope once again expands. The star slowly moves back toward the red giant branch. The evolution from f to g and from h to i comprises most of the helium burning phase.

As the star approaches the red giant branch a convective envelope once again develops. The star evolves up the red giant branch until the core contraction becomes sufficiently rapid to halt the expansion of the envelope at point j. The convective core reached a maximum shortly before this at mass fraction q=0.079000, and as a shell source of helium burning begins to establish itself, the temperature gradient near the outer edge is decreased until the convection zone is forced to retreat. The helium abundance in the center is quite low, but the rising density

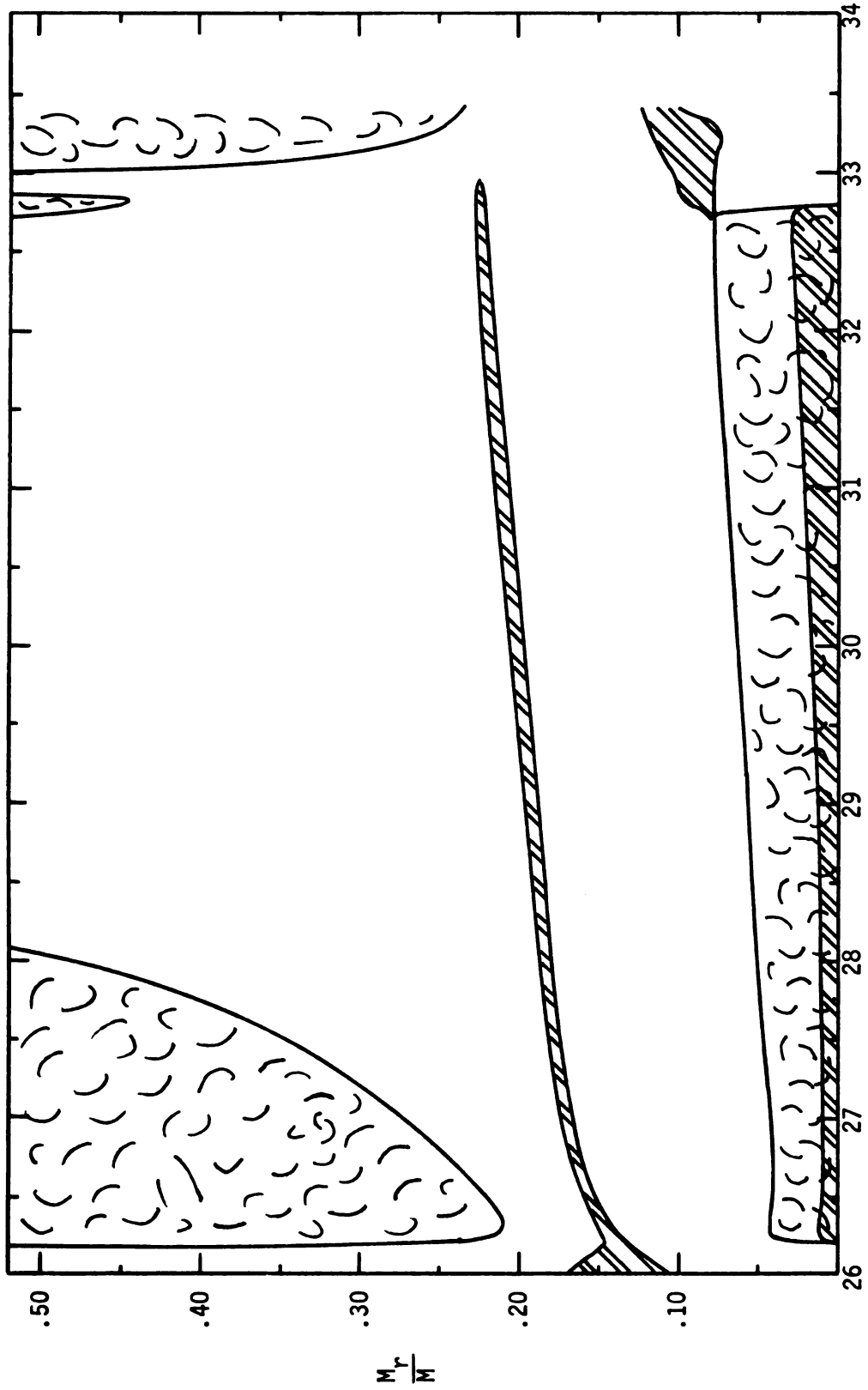

Figure 8-4. Interior conditions during helium burning of the 7.0 $M_\odot$ star.

and temperature keep the energy generation fairly large until burnout occurs. The abundance of carbon at the center is 0.564. As with the core hydrogen burnout, the central temperature decreases as the central density increases.

As the helium burning shell adjusts itself the luminosity of the star begins to increase again from point k. The convective envelope, which had retreated to mass fraction q=0.70, once again grows. The decreasing temperatures and densities in the hydrogen burning shell decrease the energy generation rate until the shell source is completely quenched.

As the density of the center increases, the neutrino cooling begins to have a major effect on the core. During the entire phase of core helium burning the neutrinos have had a very small effect on the star. The maximum cooling rate was a small fraction of the nuclear energy generation rate. Now the core beneath the narrowing helium burning shell becomes isothermal and finally a luminosity inversion appears as the temperature maximum moves away from the center.

The effects of the neutrino cooling may be seen in the evolution of the center in the log ρ- log T plane. The temperature at the center is always increasing after the initial decrease following the helium core burnout just as it did following the hydrogen burnout. The rate of increase is slowed substantially by the neutrino cooling, as seen by the way the track begins to turn horizontal in Figure 8-3.

The evolution was halted soon after the luminosity inversion developed. At this time the inner edge of the helium burning shell is at mass fraction q = 0.10. The profile of carbon is shown in Figure 8-5. The composition discontinuity occurs at the point where the convective core

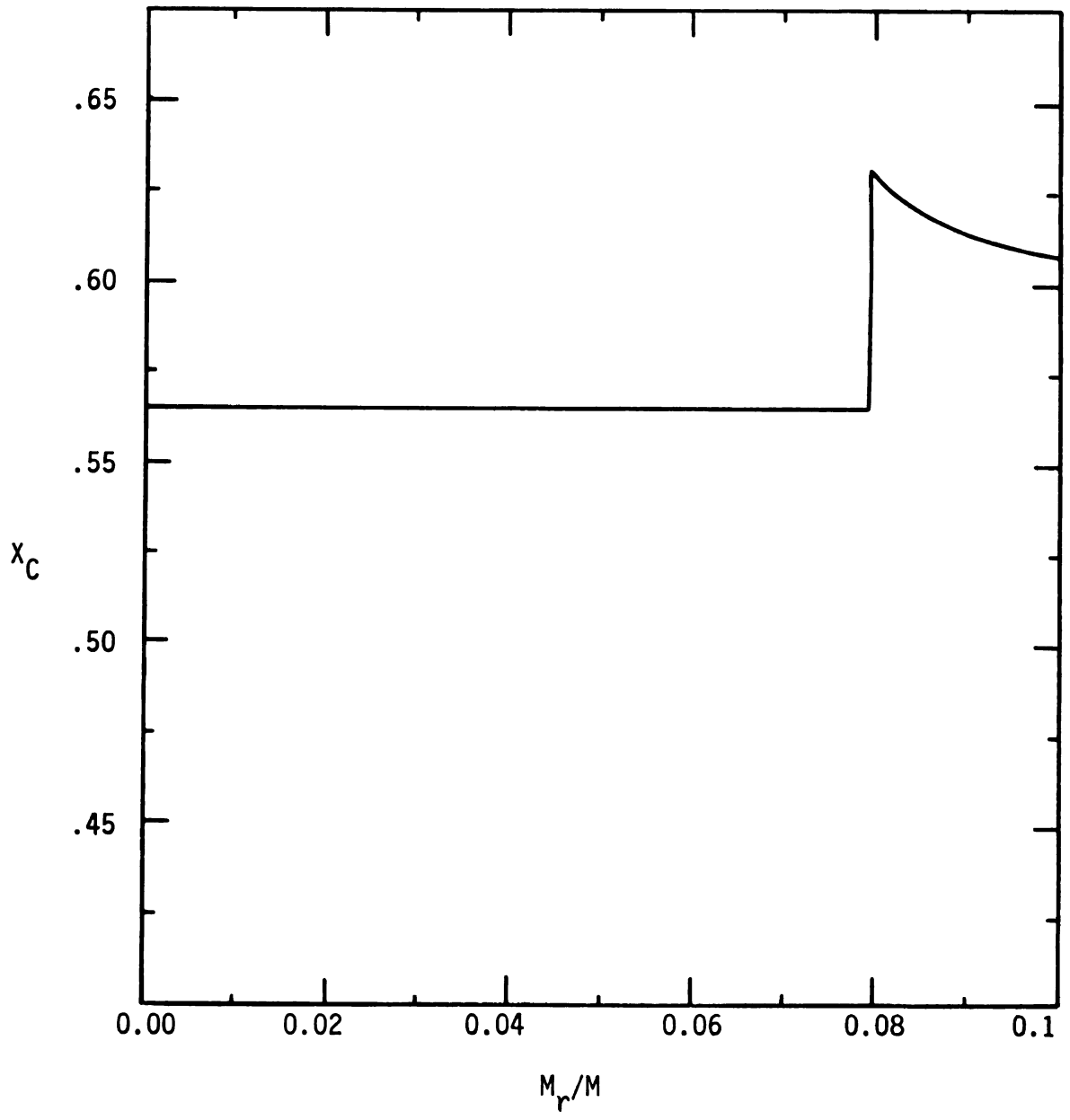

Figure 8-5. Carbon profile in the core of the 7.0 $M_\odot$ star.

reached its maximum extent during the core helium burning. Interior to that point the carbon abundance is uniform to within ±0.0005.

The discontinuity in the composition is probably due to the manner in which convection was handled. In all regions where the radiative temperature gradient is larger than the adiabatic gradient full convective mixing is done. The region just outside the convective core is almost neutrally stable against convection. It is likely that a semi-convective transition region should occur between the fully mixed convective core and the radiative region just outside. In such a region there is a slow exchange of material to produce a composition gradient that is just neutrally stable. The semi-convection does not contribute significantly to the energy transport.

This problem has been studied in regard to the envelope structure in massive stars (Chiosi and Summa 1970), and also concerning the core structure during the helium burning phase (Paczynski 1970b). At the moment there seems to be no straightforward way to treat such a region. The technique used in the present investigation allows the composition to be computed explicitly. It would be necessary to iterate on the composition in some fashion to produce an adequate treatment of a semi-convective region.

Unfortunately, a convective core that grows near the end of the helium burning may have a large effect on the composition at the center. There is a large composition discontinuity at the edge. A small increase in the size of the mixed region may change the center abundance of helium by an appreciable amount. The immediate effects on the ratio of the carbon and the oxygen abundances will be small. Both will be decreased. However, since the helium content of the core is small, the carbon-alpha

reaction rate is dominant. Hence any helium mixed into the region will serve to burn the carbon into oxygen rather than produce more carbon by the triple-alpha process.

The maximum effect may be estimated from the composition profile shown in Figure 8-5. At the edge of the convective core the difference in the carbon abundance is 0.066, which is about 12 percent of the value at the center. As the shell source moves outward, the abundance of carbon decreases and seems to be approaching a value of about 0.60. The composition discontinuity is most probably caused by not considering semi-convection at the outer edge of the convective core. The effect on the abundances at the center is not easily estimated accurately. This would involve knowing the detailed composition gradient that was built up during the early portions of the helium burning and the exact growth of the fully convective region as the helium content became small. Any convective region that grows when the central helium content is low will have a major effect on the end abundances.

The time steps that were derived from the criteria given in section VII-4 during the helium burning phase between point g and i were too long for the models to converge. A typical time step based on maximum allowed changes in the structure and the composition was of the order of 2×10^5 years. The models would diverge unless the time step was held to approximately 3×10^4 years. A dcrease of 20 percent in the time step would reduce the number of iteractions by roughly a factor of two. In the interest of minimizing the total computing time, the time steps were set fairly small.

The above problem suggests that the algorithm for extrapolating from one model to the next is inadequate for these models with complex

structures. Most of the divergence difficulties seemed to be associated with the hydrogen burning shell source, although previously in the evolutionary sequence, as the star moved from point f to g, much longer time steps were used with no problems of convergence. Since the convective core was growing during this phase, the small time steps combined with the fine zoning in the core probably allowed greater accuracy in following its growth.

VIII-4. Effects of an increased carbon-alpha reaction rate

The evolution for the second value of the carbon-alpha reaction rate, which is a factor of 10 larger than the value used in section VIII-3, is repeated from model 106. At this time the carbon-alpha reaction had ignited but was still extremely small. The total amount of helium that had been previously burned by the triple-alpha reaction is less than 10^{-4}. The core of the star is still radiative, and the helium burning reactions are just beginning to affect the structure of the core. Any error in the final oxygen abundance will be less than 10^{-8} when compared with starting the evolution previous to the triple-alpha ignition. This model was chosen because it was previous to the time when the helium burning reactions become important, and a fairly large core is free of hydrogen.

The evolutionary track in the H-R diagram for this sequence is given in Figure 8-6. Also plotted is the track for the helium burning phase of the previous sequence with the points labeled as in Figure 8-1. The important parameters for the star are given in Table 8-2. The primed letters refer to the points labeled in Figure 8-6. The units and symbols are the same as those in Table 8-1.

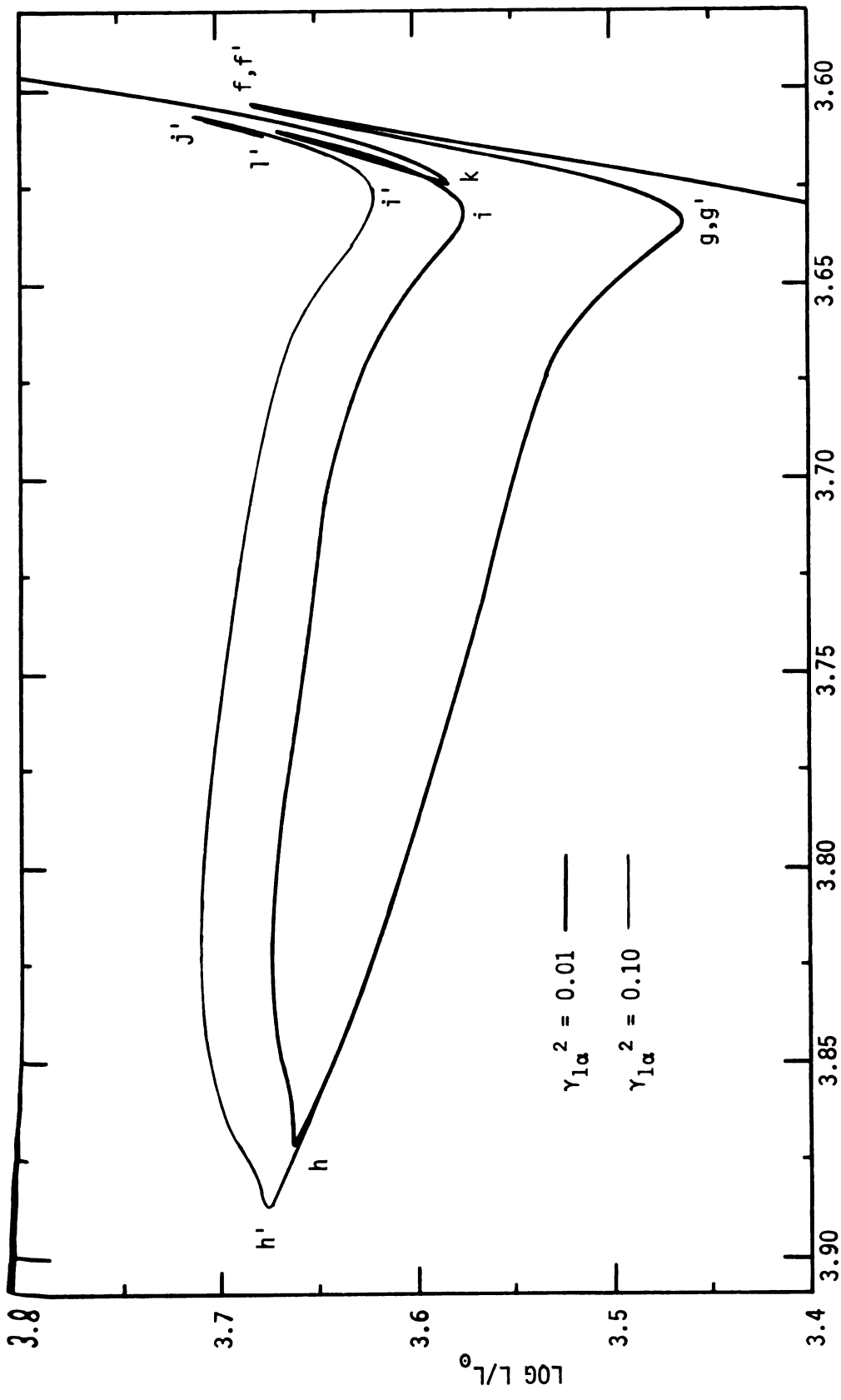

Figure 8-6. H-R diagram for the helium burning phase for the two 7.0 $M_\odot$ sequences.

Table 8-2. Parameters for the helium burning phase of a 7.0 $M_\odot$ star.

	Model	Age	log T_e	log $L/L_\odot$	log R	Y_c	ε_c	log T_c	log ρ_c	q_{cc}	comments
	106	26.186	3.625	3.456	12.842	0.9559	2.9E+2	8.0596	3.9006		
	111	26.194	3.614	3.578	12.924	0.9557	2.2E+3	8.0749	3.9319		$\varepsilon_c > 10^3$
	116	26.206	3.610	3.624	12.954	0.9550	1.5E+4	8.1073	3.9559	0.005	maximum ρ_c
f'	131	26.297	3.603	3.681	12.997	0.9451	4.9E+4	8.1353	3.8040	0.043	
g'	181	28.849	3.634	3.463	12.826	0.6436	7.9E+4	8.1710	3.6273	0.059	
h'	280	30.261	3.887	3.677	12.427	0.4316	9.2E+4	8.1915	3.6159	0.064	
i'	430	33.404	3.628	3.620	12.916	0.0476	1.1E+5	8.2921	3.7643	0.084	
j'	461	33.734	3.607	3.710	13.003	0.0007	2.1E+4	8.3817	4.1160	0.018	
	473	33.750	3.611	3.682	12.982	0.	0.	8.3622	4.2319		burnout
l'	475	33.752	3.612	3.679	12.979	0.	0.	8.3601	4.2467		

Age in 10^6 years.

The evolution of the star is very similar to the previous evolutionary sequence. The maximum effective temperature at the blue end of the helium burning loop is somewhat higher, and the rest of the loop back to the red giant branch is at larger luminosities than previously encountered. The major differences occur toward the end of the helium burning phase, as was expected. The triple-alpha process, which was unchanged, is dominant until an appreciable amount of helium has been destroyed.

The convective core reached a mass fraction of q = 0.083739 which is somewhat larger than the previous evolution. At burnout the central carbon abundance is 0.0343. The evolution was halted soon after the core helium burnout occured. The star was still descending the red giant branch. The evolution takes almost one million years longer than in the previous case. This is about 14 percent greater if the helium burning phase is considered to begin at model 106. Due to the slightly larger size of the convective core, approximately 6 percent more helium is burned. The alteration in the time scale for the helium burning phase is small but significant.

The exact age of the star at this point is somewhat arbitrary. It depends not only on the reaction rates used but on the size of the convective core, which depends on the method for mixing the composition. A semi-convection zone at the outer boundary may change the size of the fully convective core by a substantial amount. This would affect the time for the helium burning phase. The exact structure of the convective core during the hydrogen burning phase can have a large influence on the age of the star when the helium burning reactions ignite.

The size of the loops in the H-R diagram during the helium burning

phase seems to be largely dependent on the computational method (Paczynski 1970b). Robertson (1971) showed that the hydrogen profile in the envelope has a major effect on the loop. Thus the particular choice of zoning and time steps used during the hydrogen burning phase may greatly affect the track in the H-R diagram at a much later time. The core of the star where the helium burning reactions are taking place should be influenced very little by the hydrogen burning phase.

VIII-5. Tests of the core evolution

In order to determine the feasibility of the core evolutions it is necessary to compute several test cases and check them against the results of the two evolutionary sequences for the entire stars. Such calculations showed the necessity for handling the outer boundary conditions as described in section II-6 and the mixing in the convective core as given in section VII-6.

Table 8-3. End abundances in the 7.0 $M_\odot$ stars.

case	Cα	q_{max}	X_C	X_O	X_{Ne}	X_{Mg}	N_r
A	0.01	0.079000	0.564	0.392	1.2E-6	5.6E-8	1.9184
B	0.10	0.083739	0.0343	0.922	1.0E-5	7.3E-7	0.0496

The relevant data from the two evolutionary sequences at 7.0 $M_\odot$ is given in Table 8-3. The abundances are those found in the center of the star after helium burnout has occured. The quantity N_r is the number ratio of carbon to oxygen and is defined as

$$N_r = \frac{4}{3}\frac{X_C}{X_O} . \qquad (8.1)$$

The designation for the carbon-alpha reaction rate is the reduced level width as given in Table 4-5. The triple-alpha reaction rate is the rate labeled "mean" in Table 4-2. The maximum size of the convective core is given as q_{max}.

From each of these two sequences values of the boundary conditions are obtained with a value of the mass fraction at the core edge chosen to be q = 0.128471. The evolution is repeated from model 106 with just the core of the star. A maximum of 100 shells is allowed. Typically burnout is reached in 130-140 additional models.

There are several checks that may be made. The evolution of the core with the same values of the reaction rate parameters as used to produce the boundary conditions will give an estimate of the accuracy of the method. A more stringent check is to determine how well an evolutionary sequence, using different values of the reaction rate parameters from those used to produce the boundary conditions, will agree with the sequence of the entire star.

Table 8-4. Results of the core evolution tests.

3α	Cα	b.c.	X_C	X_O	X_{Ne}	X_{Mg}	N_r
mean	0.01	A	0.548	0.408	1.3E-6	5.9E-8	1.7909
mean	0.01	B	0.531	0.425	1.8E-6	8.8E-8	1.6659
mean	0.10	A	0.0374	0.919	7.5E-6	9.7E-7	0.0543

The results of the tests of the core evolutions are presented in Table 8-4. The boundary condition designation is given in Table 8-3. The first result is for the same energy generation rate parameters as used for the boundary conditions. The other results are for the

different values.

The first two results are to be compared to the first entry in Table 8-3. The agreement is reasonably good. The nature of N_r makes it quite sensitive to small changes in the end abundance of carbon as the amount of carbon gets large. The agreement in the abundance of carbon is only about 3 percent for the first case and 5 percent for the second case. The differences are probably due to differences in the time steps and the exact zoning in the region where the maximum convective core is reached. The time at which a given amount of helium is mixed down is significant to the final carbon abundance since the ratio of the triple-alpha reaction rate to the carbon-alpha reaction rate is changing quite rapidly near the end of helium burning.

The last case agrees quite well in the carbon abundance. The percentage difference is less than 10 percent, which is very good since the abundance of the carbon is so very low.

The results of the test cases indicate that the use of the core evolution as an approximation to an evolutionary sequence of the entire star is quite feasible. In order to isolate the causes of the differences in the end abundances, only the core evolutions will be compared.

Thus for other masses it is necessary to first do a complete evolutionary sequence to obtain the boundary conditions. Then repeat the evolution with just the core using the same values of the reaction rate parameters to provide a "standard". Finally do various sequences with the core for a range of reaction rates. Only one evolutionary sequence of the entire star needs to be done.

VIII-6. Effect of the uncertainties in the triple-alpha rate

The triple-alpha reaction is fairly well determined. The energy generation rate for the maximum and minimum values of the parameters as given in Table 4-2 differs by about 60 per cent from the mean value. Although this uncertainty is much less than the uncertainty in the carbon-alpha reaction rate, it is necessary to determine its effect on the end abundances of helium burning.

The evolution is repeated from model 106. The amount of carbon produced prior to this is less than 10^{-4}. This has a negligible effect on the end abundances. The energy generation rate still has a minor effect on the structure.

Table 8-5. Results of varying the triple-alpha rate.

3α	Cα	b.d.	X_C	X_O	X_{Ne}	X_{Mg}	N_r
maximum	0.01	A	0.629	0.327	6.9E-7	2.5E-8	2.5647
mean	0.01	A	0.548	0.408	1.3E-6	5.9E-8	1.7908
minimum	0.01	A	0.430	0.526	2.9E-6	1.8E-7	1.0900
maximum	0.1	A	0.117	0.839	1.4E-6	4.1E-8	0.1859
mean	0.1	A	0.0374	0.919	7.5E-6	4.7E-7	0.0543
minimum	0.1	A	est 0.0	0.953	2.2E-4	1.9E-4	0.0

The results are summarized in Table 8-5. The quantities are the same as those in Table 8-5. Two different values of the carbon-alpha reaction rate are used. For the last entry the abundances of carbon and oxygen are estimated. With Y_c=0.0018 the amount of carbon left is $X_C=4\times10^{-4}$. At this point the core requires excessively small time steps to converge due to a drastic discontinuity in the energy generation rate at the maximum extent of the convective core. Due to the

small triple-alpha rate and the large carbon-alpha rate the composition discontinuity is not smoothed sufficiently to decrease the discontinuity in the energy generation rate to a reasonable amount. The evolution of the core is stopped at that point. The amounts of neon and magnesium given in Table 8-5 are those that are present at $Y_c = 0.0018$.

Thus the uncertainty in the triple-alpha rate leads to an uncertainty in the final abundance of carbon of about 20 per cent for the small value of the carbon-alpha reaction rate. If the carbon-alpha reaction rate is large and the triple-alpha reaction at its minimum, then there may be no carbon left after the helium burning phase. Also in this case, since both the triple-alpha rate, because of small helium abundance, and the carbon-alpha rate, because of the small carbon abundance, are quite small the alpha captures on oxygen and neon become important and relatively large amounts of heavier elements may be produced, perhaps of the order of 2×10^{-3}.

VIII-7. Effect of the uncertainties in the carbon-alpha rate

The carbon-alpha reaction rate has a very large uncertainty. Several core sequences are evolved with different values of carbon-alpha reaction rate as given in Table 4-5. There is no need to consider larger values of the reduced level width than $\gamma_{1\alpha}^2 = 0.1$, since this produces such a small amount of carbon. The minimum amount of carbon that can be produced is zero.

The results are given in Table 8-6. The quantities are the same as given in the previous two tables. For this given range of the reaction rate there is a very large range in the amount of carbon produced. The amount of elements heavier than oxygen is negligible.

Table 8-6. Results of varying the carbon-alpha rate.

3α	Cα	b.c.	X_C	X_O	X_{Ne}	X_{Mg}	N_r
mean	0.005	A	0.663	0.293	1.5E-6	8.1E-8	3.0171
mean	0.010	A	0.548	0.408	1.3E-6	5.9E-8	1.7908
mean	0.020	A	0.400	0.556	1.4E-6	5.2E-8	0.9592
mean	0.040	A	0.227	0.729	1.7E-6	6.0E-8	0.4152
mean	0.060	A	0.134	0.822	2.5E-6	9.6E-8	0.2174
mean	0.100	A	0.0374	0.919	7.5E-6	4.7E-7	0.0543

Perhaps the only definite conclusion that may be reached is that carbon will be found in significant quantities and that the elements heavier than oxygen are negligible. Thus the next burning phase will be that of carbon burning. It is likely that carbon will ignite in a carbon flash (Thomas 1968) or very explosively in a carbon detonation (Arnett 1969). The neutrinos may cool the center, as was noted just before the evolution was halted, and the resulting flash could occur in a shell as in the helium flash problem with neutrinos (Zimmermann 1970). Since the composition varies with mass fraction the details of the ignition could depend on the point in the star where it occurs. However, the composition profile, as shown in Figure 8-5, is probably due in part to the method in which the convective core was handled, and the exact nature of the carbon ignition must remain in the realm of speculation.

CHAPTER IX

EVOLUTION AT OTHER MASSES

IX-1. Introduction

The conditions under which the helium burning reactions are taking place vary with the mass of the star. In general the central temperature increases and the central density decreases as the mass of the star increases. Since the triple-alpha and the carbon-alpha reaction rates have a different temperature and density dependence, the conditions at the center may have a large effect on the end abundances of the helium burning. It is desirable to repeat the evolution for a range of masses to determine what the general effect of the mass will be.

IX-2. Evolution of a 5.0 $M_\odot$ star

The 5.0 $M_\odot$ star has been previously considered by a number of investigators (Iben 1966a, Weigert 1966, Hofmeister 1967, Robertson 1971). The center is not so degenerate that the triple-alpha process ignites in the "helium flash" that is characteristic of lighter stars (Zimmermann 1970). Thus there is no need for very short time steps and large amounts of computer time to evolve the star to the burning phase of interest.

The evolution is done with the "mean" value of the triple-alpha rate, and the reduced level width for the carbon-alpha reaction set to

$\gamma_{1\alpha}^2$ = 0.01 MeV. This value is chosen, even though it is near the lower end of the range of allowed values, since it is expected to produce approximately 50 per cent carbon. From the results of section VIII-5 it should be relatively unimportant which value of the carbon-alpha reaction is used for the evolution of the entire star.

The track in the H-R diagram for the 5.0 $M_\odot$ star is given in Figure 9-1. The points are labeled in the same way as Figure 8-1 except point k is the end of the evolution. The data are given in Table 9-1. The quantities are the same as those in Table 8-1. The evolution of the interior of the star is given in Figure 9-2 and Figure 9-3. The evolution of the center in the log ρ-log T plane is given in Figure 9-4. The early evolution of the star agrees very well with that given by Hofmeister (1967) which uses the same opacity tables and other "physics".

The structure and evolutionary track is similar to that found at 7.0 $M_\odot$. The first difference is the lack of any convection zone at the maximum extent of the hydrogen burning shell. The shell also remains fairly thick for a much longer time before it begins to narrow rapidly just prior to the ignition of the triple-alpha process.

The ignition of the triple-alpha process is somewhat more violent than in 7.0 $M_\odot$ since the core is more degenerate. The large changes in the density and temperature at the center associated with burnout and ignition of a nuclear burning phase are much more pronounced. There is a slight temperature decrease following the ignition of the triple-alpha which was not observed in the 7.0 $M_\odot$ star. The maximum extent of the convective core is q_{max} = 0.061421. The neutrinos played no significant role before or during the helium burning phase even though the

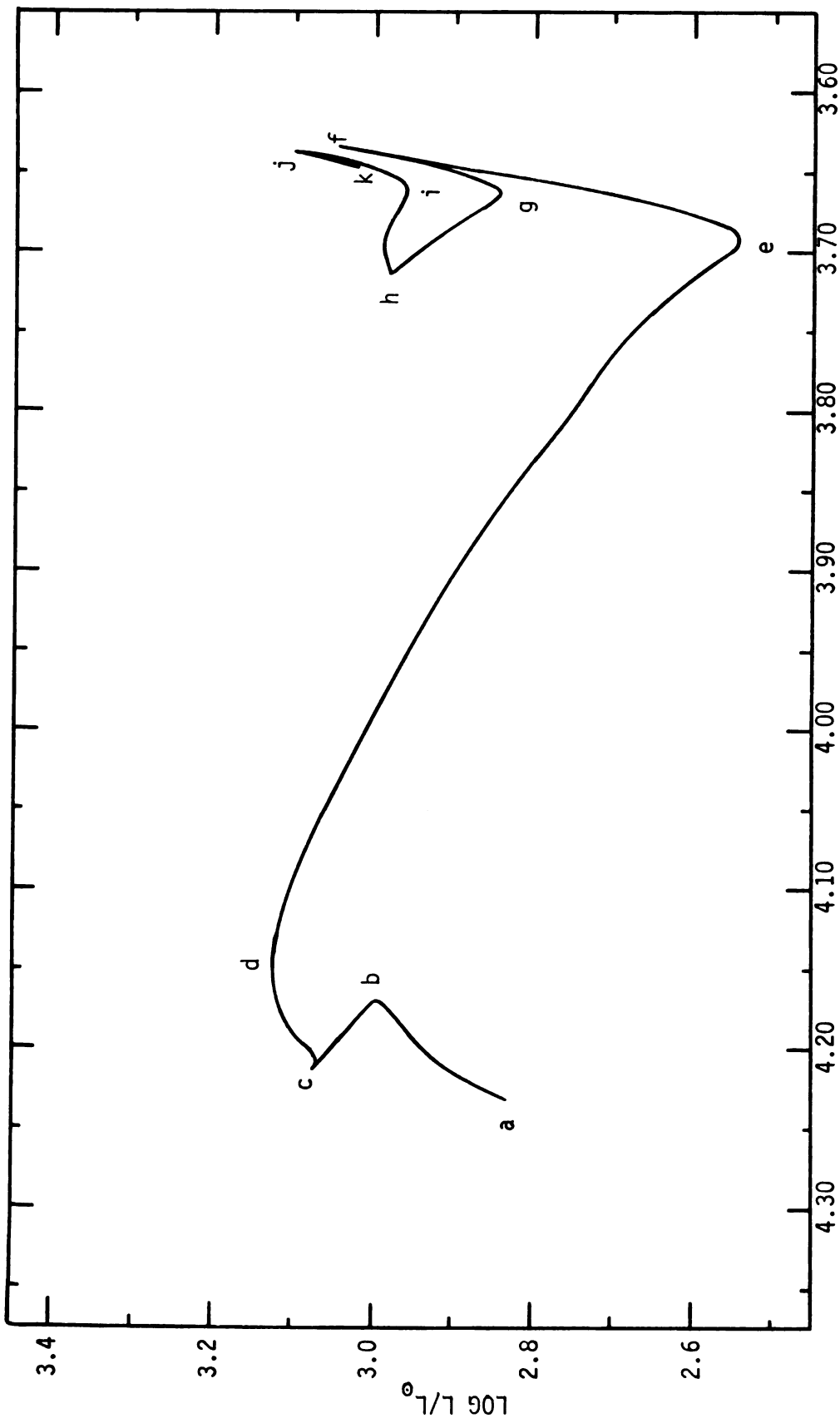

Figure 9-1. H-R diagram for the evolution of the 5.0 $M_\odot$ star.

Table 9-1. Parameters for the 5.0 $M_\odot$ star.

	Model	Age	log T_e	log $L/L_\odot$	log R	Y_c	ε_c	log T_c	log ρ_c	q_{cc}	comments
a	1	0.	4.230	2.832	11.319	0.3540	1.0E+4	7.4132	1.1764	0.179	initial model
b	15	47.104	4.170	2.992	11.518	0.8995	3.0E+4	7.4939	1.3834	0.089	
c	41	49.648	4.211	3.076	11.478	0.9556	8.6E+3	7.5753	1.7955	0.018	
	44	49.680	4.206	3.070	11.486	0.9560	0.	7.5356	1.9750		burnout
d	54	51.008	4.145	3.121	11.633	0.9560	0.	7.5561	2.9492		
	69	51.712	3.887	2.878	12.027	0.9560	4.0E-5	7.9000	3.9182		3α ignition
e	81	51.844	3.694	2.551	12.250	0.9560	7.1E-1	7.9806	4.1185		
	104	51.980	3.640	2.998	12.581	0.9550	1.6E+3	8.0578	4.2815	0.001	$\varepsilon_c > 10^3$
	106	51.996	3.638	3.017	12.594	0.9552	5.0E+3	8.0713	4.2874	0.005	maximum ρ_c
f	112	52.060	3.635	3.049	12.617	0.9531	2.9E+4	8.0996	4.2126	0.029	
g	196	59.468	3.661	2.842	12.462	0.6615	2.7E+4	8.1307	3.9596	0.043	
h	310	65.500	3.714	2.983	12.426	0.3684	3.7E+4	8.1630	3.9331	0.053	
i	438	70.552	3.662	2.962	12.520	0.0809	3.9E+4	8.2274	4.0304	0.060	
j	518	72.628	3.636	3.096	12.638	0.0001	7.9E+2	8.3135	4.4079		
	525	72.642	3.638	3.082	12.628	0.	0.	8.2940	4.4387		burnout
k	550	72.732	3.646	3.016	12.579	0.	0.	8.2571	4.5879		

Age in 10^6 years.

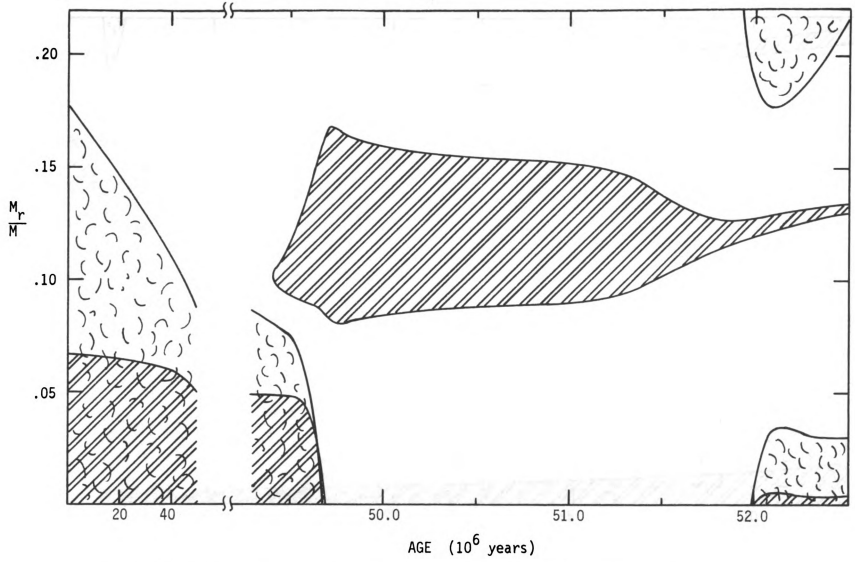

Figure 9-2. Interior conditions during the early evolution of the 5.0 $M_\odot$ star.

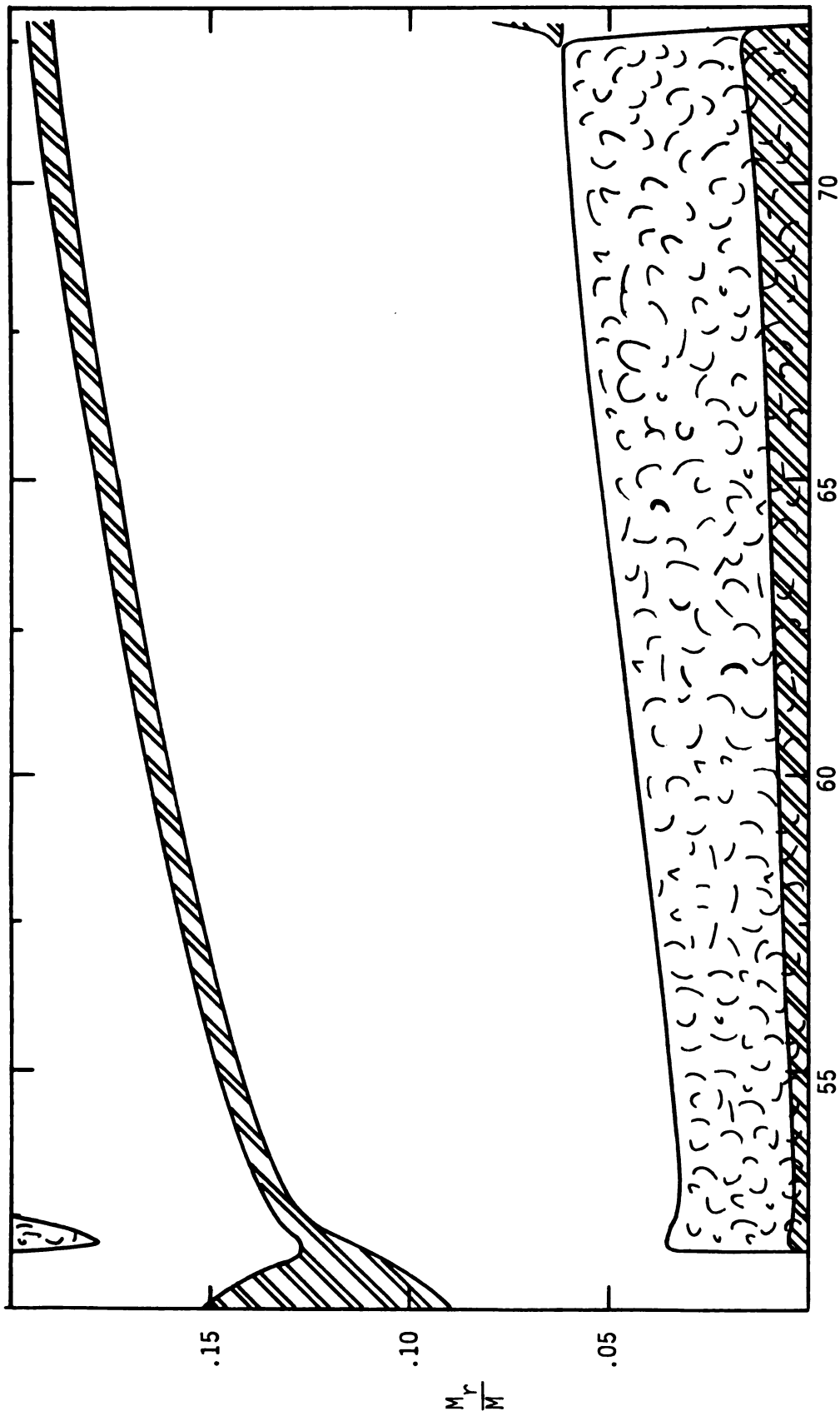

Figure 9-3. Interior conditions during helium burning of the 5.0 $M_\odot$ star.

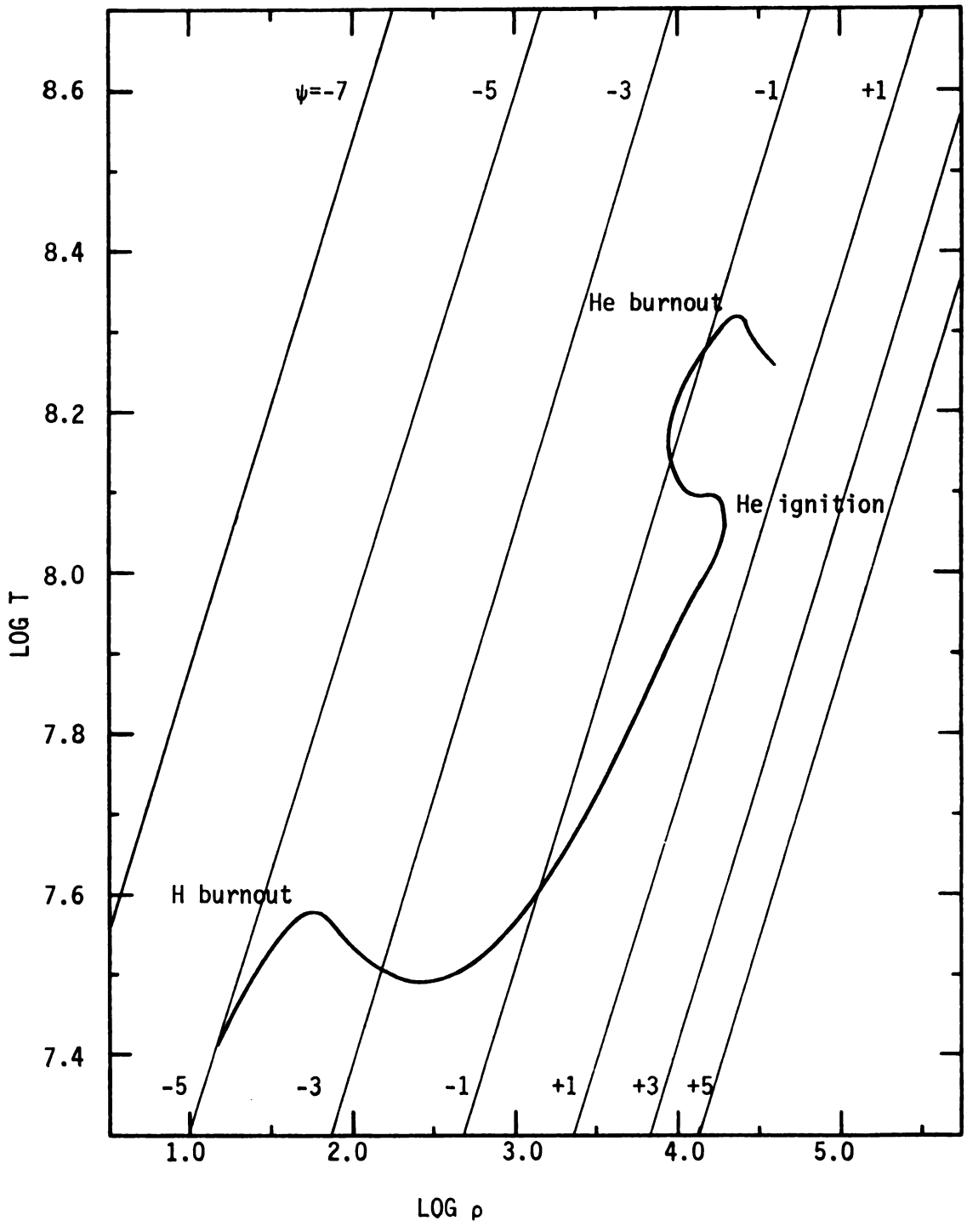

Figure 9-4. Evolution of the center of the 5.0 $M_\odot$ star.

core is more dense than the 7.0 $M_\odot$ core. Many of the comments concerning the uncertainties in the age and the track in the H-R diagram of the 7.0 $M_\odot$ star presented in section VIII-4 also apply to the 5.0 $M_\odot$ star.

Table 9-2. Results of 5.0 $M_\odot$ star and core evolutions.

case	3α	$C\alpha$	X_C	X_O	X_{Ne}	X_{Mg}	N_r
star	mean	0.01	0.547	0.409	2.7E-7	9.5E-9	1.7832
core	mean	0.01	0.528	0.428	2.9E-7	1.1E-8	1.6449

The mass fraction at the boundary of the core is chosen to be $q = 0.117134$ and values of the temperature and pressure are obtained. The evolution is repeated from model 96 with just the core using the same values of the reaction rates. Approximately 150-160 core models are required. The results for the end abundances are presented in Table 9-2. The first entry is for the entire star, and the second is for the core.

The amount of carbon in the core after burnout is slightly less than that found in the 7.0 $M_\odot$ star. This may be due in part to the exact zoning around the maximum extent of the convective core. In both stars a very fine zoning was inserted just above the edge of the growing convective core, but slight differences may be important. The hydrogen free models of Cox and Salpeter (1964) and Deinzer and Salpeter (1964) also found that the abundance of carbon produced was at a maximum around one solar mass. The size of the helium core in the 5.0 $M_\odot$ star varies from 0.65 $M_\odot$ at the start of the helium burning phase to 0.95 $M_\odot$ near the helium core burnout. Thus the smaller amount

of carbon may be realistic rather than an effect of the programming technique.

IX-3. Effects of varying the carbon-alpha reaction

The evolution of the cores is repeated using the range of carbon-alpha reaction rate parameters as given in Table 4-5 to determine the effect of the carbon-alpha reaction rate. No further tests of the core evolutions or sequences using different values of the triple-alpha are computed.

Table 9-3. Effects of varying the carbon-alpha reaction rate.

3α	$C\alpha$	X_C	X_O	X_{Ne}	X_{Mg}	N_r
mean	0.005	0.647	0.309	2.5E-7	1.1E-8	2.7918
mean	0.010	0.528	0.428	2.9E-7	1.1E-8	1.6449
mean	0.020	0.371	0.585	3.5E-7	1.1E-8	0.8456
mean	0.040	0.155	0.801	5.7E-7	1.9E-8	0.2580
mean	0.060	0.107	0.849	6.0E-7	2.1E-8	0.1680
mean	0.100	0.0219	0.934			0.0313

The results are given in Table 9-3. The quantities are the same as previously described. The last entry is estimated with $Y_c = 0.0013$ by assuming that only the carbon-alpha reaction is significant. By comparing the estimates obtained for various values of $Y_c < 0.01$, which is after the time when the convective core reached its maximum extent, this assumption can be shown to be quite valid. Any uncertainty in the abundance of carbon is less than $\pm$ 0.0001.

The results seem to agree very well with the end abundances as found in the 7.0 $M_\odot$ case. Typically the abundance of carbon is 2-3 per cent less than the corresponding amount in the heavier star. However,

the abundance of carbon for the $\gamma_{1\alpha}{}^{2}$ = 0.04 MeV case seems to be rather low. On the basis of comparison with the results from 7.0 $M_{\odot}$ one would expect a value of about 0.20.

A possible explanation is that fairly long time steps were taken in the evolution, especially near the latter part of helium burning. Since comparison between the evolution of the star and the core indicates that increasing the time steps decreases the abundance of carbon, this effect is in the right direction to help explain the above anomaly. Also the zoning was somewhat coarse and any mixing would tend to occur at a later time, which would also have the effect of decreasing the end abundance of carbon. It should be noted that in all the other core evolutions the time steps and zoning were done more carefully.

IX-4. Evolution of a 15.0 $M_{\odot}$ star

The 15.0 $M_{\odot}$ has also been previously investigated (Iben 1966, Paczynski 1970a, 1970b). The tracks in the H-R diagram are quite different. In Iben's model most of the helium burning phase occurred before the star first reached the red giant branch, whereas Paczynski found that most of the helium burning occurred after it reached the red giant branch, but no loops were present as found in the less massive stars.

In a slightly more massive star, 20.0 $M_{\odot}$, Chiosi and Summa (1970) showed that the relation of the track in the H-R diagram to the helium burning in the core is influenced by the method by which semi-convection is treated in the envelope. In the present work full convective mixing is assumed. In any case, the structure of the envelope should have a small effect on the core of the star.

The track in the H-R diagram is given in Figure 9-5. The extrema are labeled in like manner to Figure 8-1. Since the helium burning loop is not present, points f through i are not equivalent to the same letters on the previous tracks. The data are given in Table 9-4. The quantities are the same as given for Table 8-1. The early interior evolution is presented in Figure 9-6.

The early evolution of the star is remotely similar to that given in section VIII-2 for the 7.0 $M_\odot$ star. The small convection zone that appeared at the maximum extent of the hydrogen burning shell source in that star also appears in the 15.0 $M_\odot$ star, but now grows quite large. Soon after it develops, another convective region appears further out in the envelope. The entire region seems to be neutrally stable against convection. These zones create fairly large composition discontinuities. The last isolated region to appear remains fairly small in thickness at any given time but moves down through the envelope and very effectively smooths the composition gradient. Perhaps the effect is similar to what a semi-convection region would do.

In a previous test run the envelope was zoned much more coarsely with about a third as many shells in the interval q = 0.40-0.60 as in the case presented above. Soon after forming, the first two convection zones merged. There followed a rather rapid readjustment of the convective region. After this large zone died out no other convective zones appeared in the envelope. The star began helium burning long before it reached the red giant branch and presumably would have done the major part of the core helium burning before it had evolved that far to the right. The cause was the difference in the hydrogen profile in the envelope due to the zoning which allowed the two zones to merge.

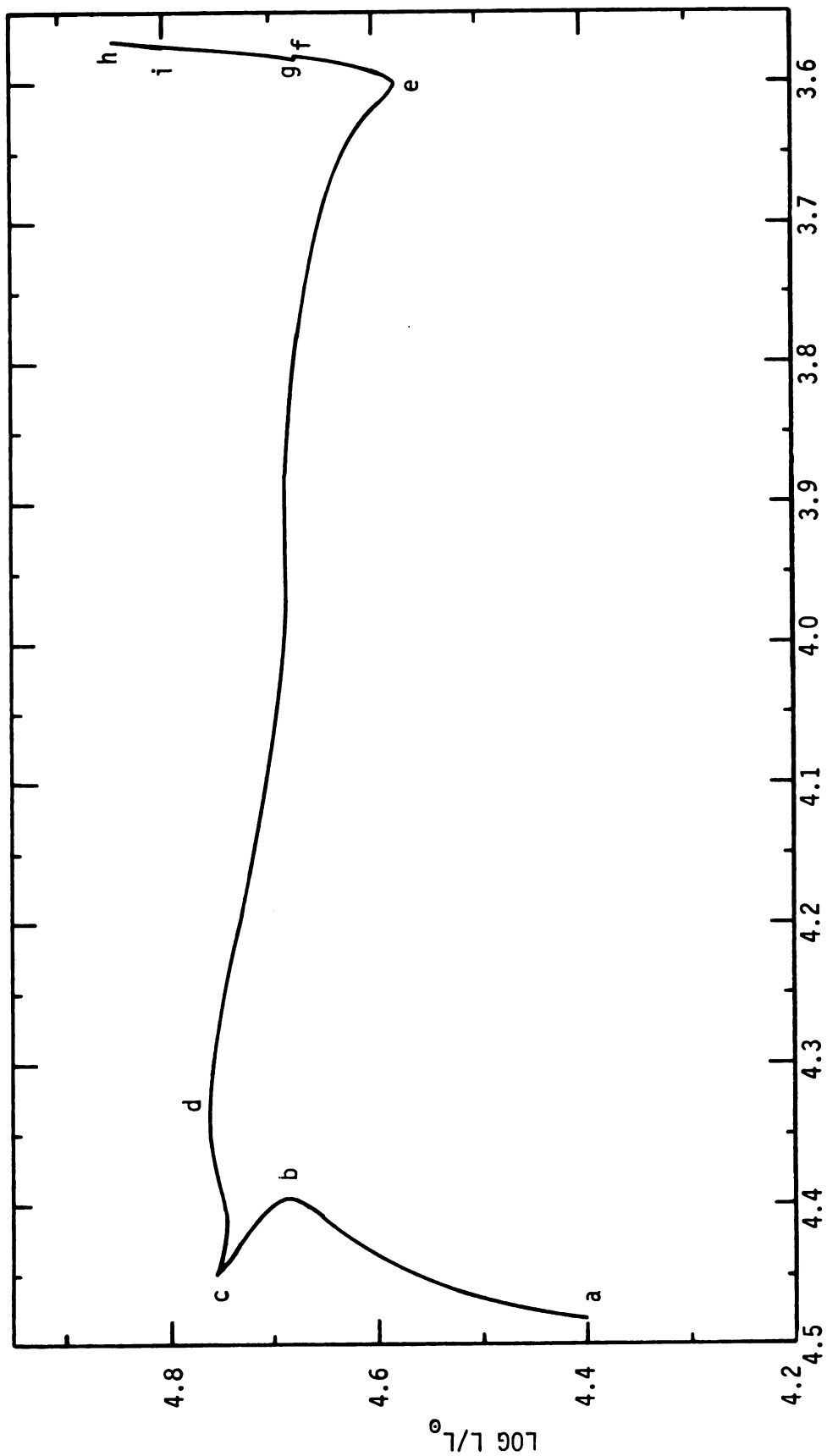

Figure 9-5. H-R diagram for the evolution of the 15.0 $M_\odot$ star.

Table 9-4. Parameters for the 15.0 $M_\odot$ evolution.

	Model	Age	log T_e	log $L/L_\odot$	log R	Y_c	ε_c	log T_c	log ρ_c	q_{cc}	comments
a	1	0.	4.483	4.397	11.594	0.3540	9.4E+4	7.5074	0.6542	0.384	initial model
b	19	7.936	4.395	4.687	11.917	0.9265	2.8E+5	7.6130	0.8938	0.223	
c	58	8.138	4.450	4.758	11.842	0.9560	0.	7.7731	1.4422		burnout
	70	8.150	4.352	4.757	12.038	0.9560	7.2E-5	7.9686	2.4471		3α ignition
d	72	8.152	4.327	4.759	12.087	0.9560	6.4E-3	8.0077	2.5895		
	80	8.159	4.228	4.737	12.276	0.9560	1.8E+3	8.1402	3.0235		$\varepsilon_c > 10^3$
	87	8.163	4.135	4.711	12.449	0.9536	4.0E+5	8.2193	3.1628	0.044	maximum ρ_c
e	122	8.184	3.600	4.567	13.445	0.9336	4.5E+5	8.2286	3.0916	0.110	
f	137	8.192	3.580	4.674	13.540	0.9259	4.5E+5	8.2293	3.0877	0.112	
g	170	8.236	3.582	4.678	13.537	0.8823	4.6E+5	8.2329	3.0819	0.116	
	225	8.524	3.580	4.711	13.559	0.5953	5.2E+5	8.2561	3.1010	0.130	
	270	8.814	3.577	4.742	13.579	0.2861	5.7E+5	8.2950	3.1702	0.138	
	325	9.025	3.574	4.771	13.600	0.0832	5.2E+5	8.3508	3.3093	0.145	
	386	9.168	3.569	4.840	13.645	0.	0.	8.5008	3.7954		burnout
h	388	9.169	3.569	4.842	13.646	0.	0.	8.5046	3.8243		
i	420	9.180	3.571	4.800	13.621	0.	0.	8.5607	4.1852		

Age in 10^6 years.

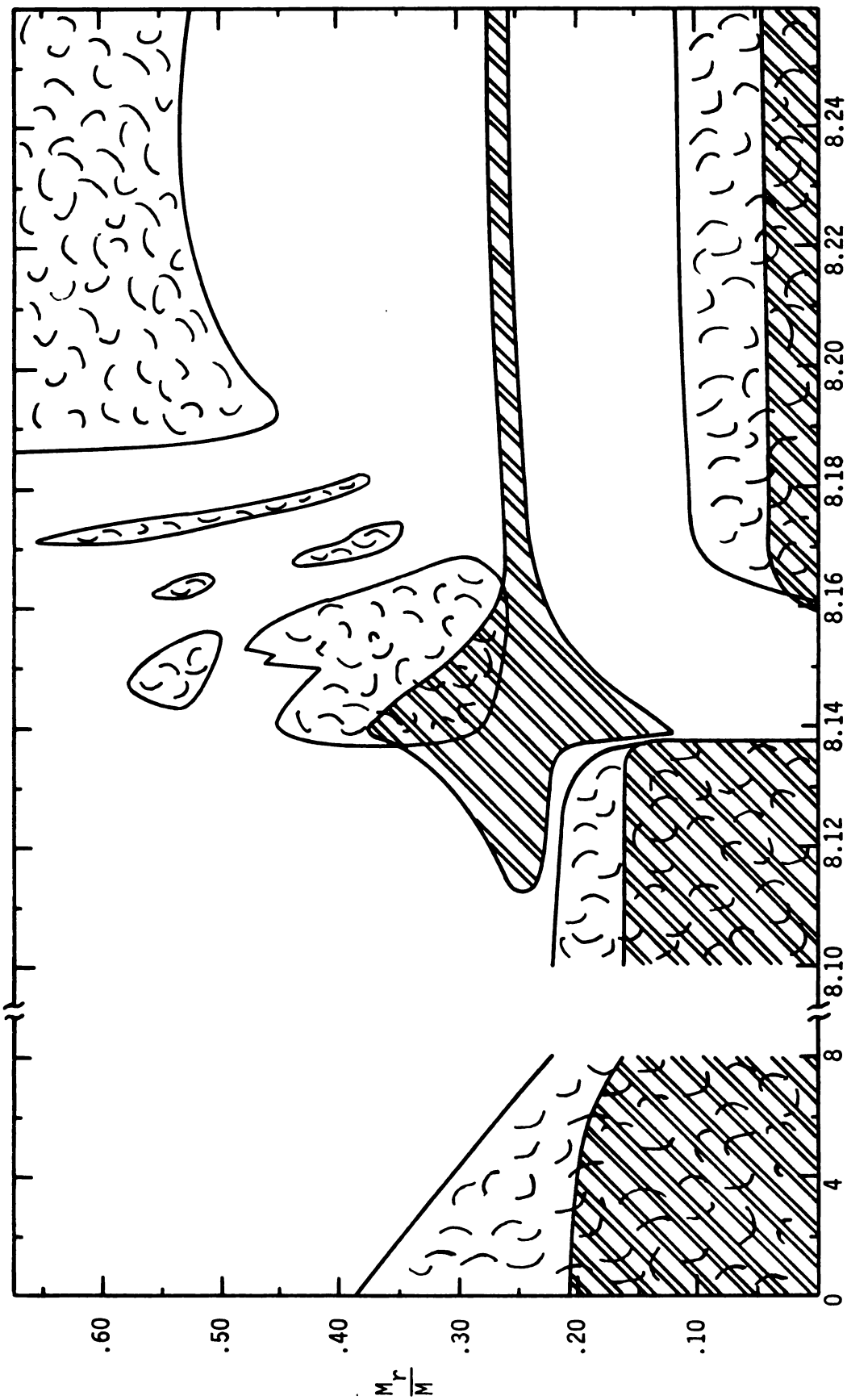

Figure 9-6. Interior conditions during the early evolution of the 15.0 $M_\odot$ star.

The interior conditions during the helium burning phase are shown in Figure 9-7. The composition discontinuity of X = 0.116 to X = 0.460 that was formed by the largest convection zone is just above the hydrogen burning shell. As the shell moves onto it the star halts its rise up the red giant branch at point f in Figure 9-5. The convective envelope retreats somewhat and the effective temperature increases slightly until the shell source adjusts itself to the increased fuel supply.

The helium burning reactions begin to dominate the star long before the red giant branch is reached. The star stays on the red giant branch for the duration of the core helium burning. The luminosity steadily increases, except for the shell adjustment between points f and g, until shortly before core helium burnout. The evolution of the center of the star in the log ρ-log T plane is shown in Figure 9-8. There are only very small changes in the temperature and density near the ignition and burnout of burning phases. The core is less degenerate than in the lighter stars. The neutrinos again play no significant role in the evolution of the core.

The maximum extent of the convective core is q_{max} = 0.147048. However, it was noted that for a fairly large range of zoning the convective core grew at the rate of one shell per model. This indicates that the programing method may have a large influence on the size of the convective core. The solution used is to set the zoning as fine as possible to minimize the effects of mixing near the end of the helium burning.

A core size of q = 0.220998 is chosen for the core evolutions. The evolution is repeated from model 81, and 120-130 core models are

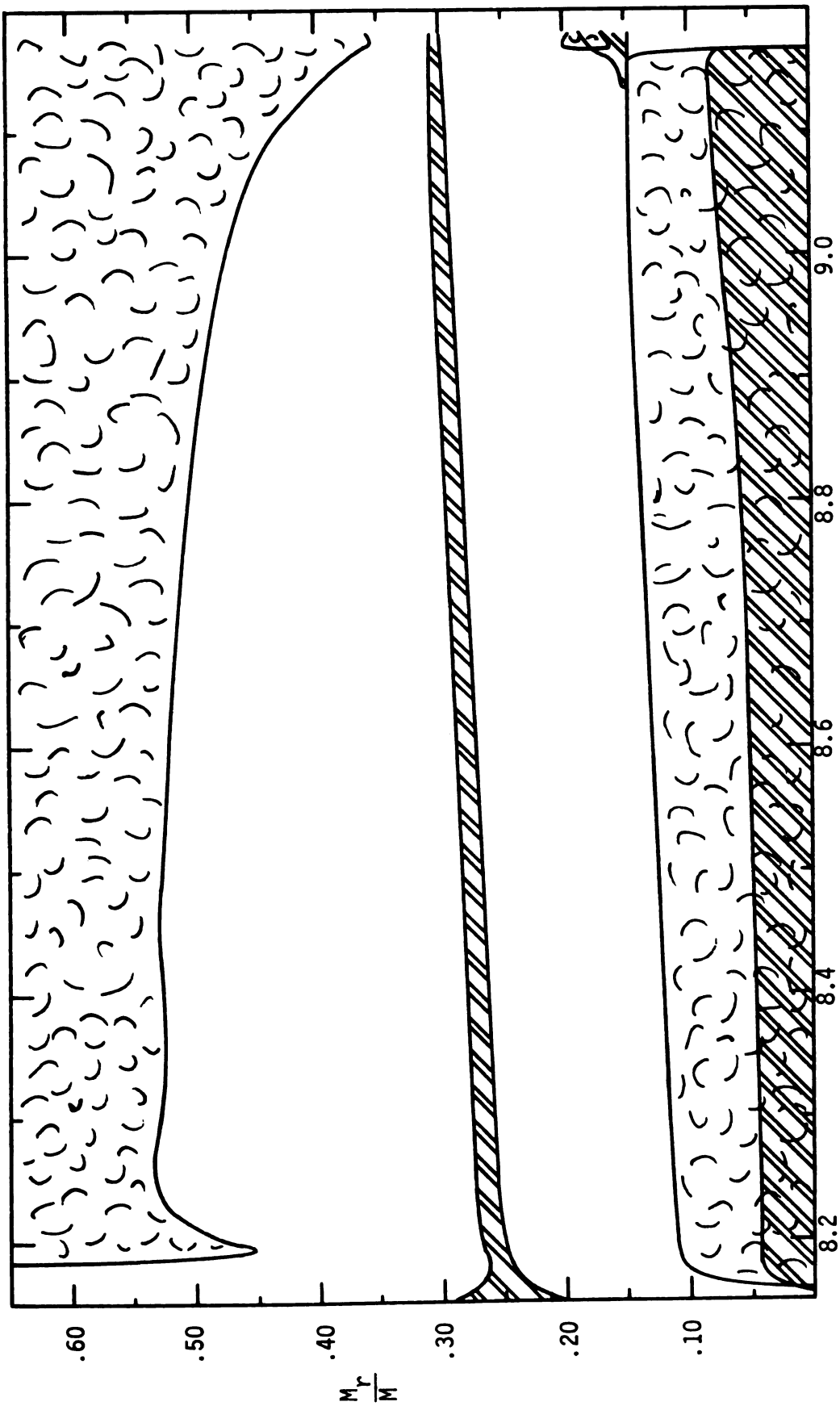

Figure 9-7. Interior conditions during helium burning of the 15.0 $M_\odot$ star.

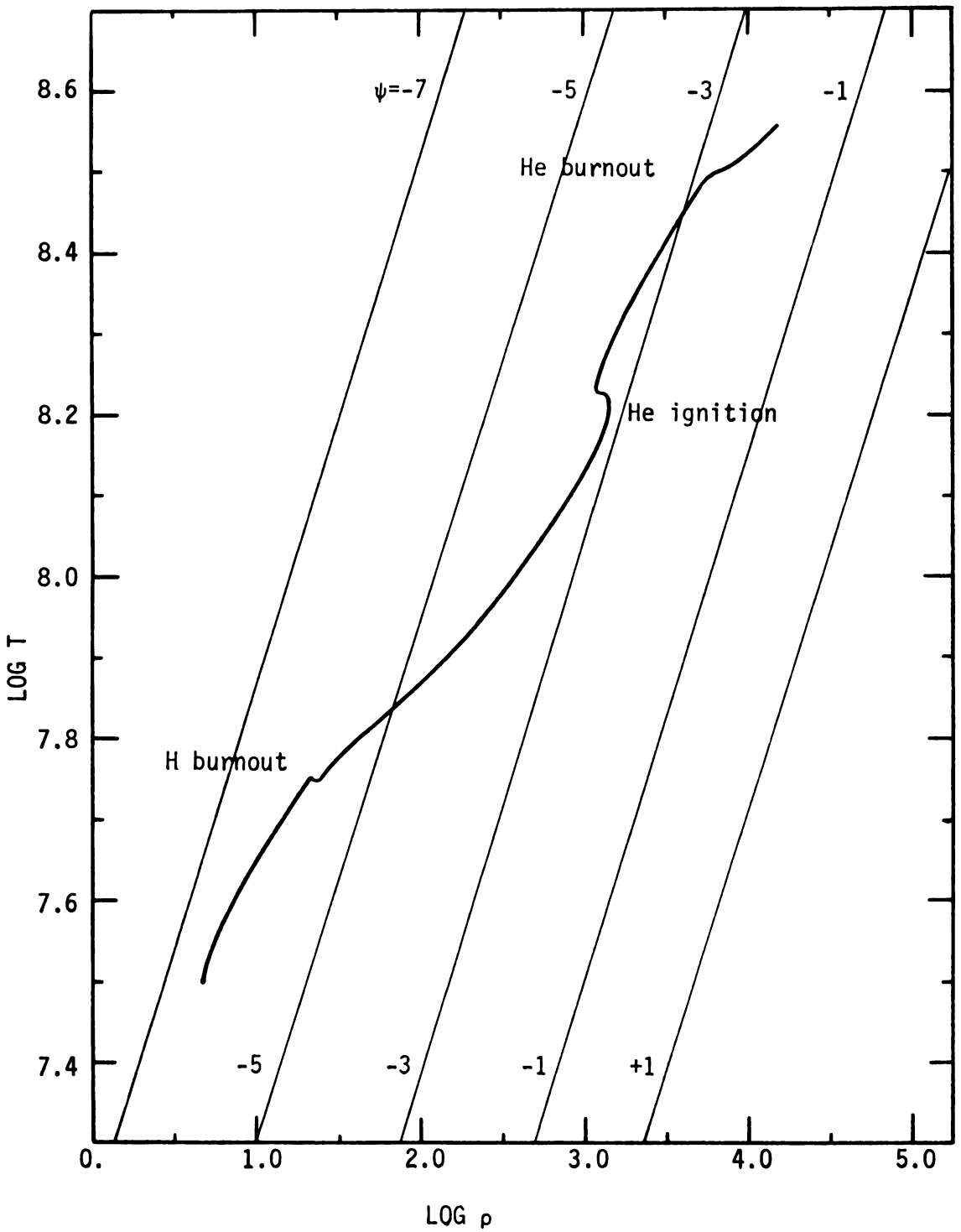

Figure 9-8. Evolution of the center of the 15.0 $M_{\odot}$ star.

needed to evolve the center to burnout. The results of the evolutionary sequence of the entire star and of the core are given in Table 9-5.

Table 9-5. Results of 15.0 $M_\odot$ star and core evolutions.

case	3α	Cα	X_C	X_O	X_{Ne}	X_{Mg}	N_r
star	mean	0.01	0.489	0.466	2.4E-4	4.7E-5	1.3991
core	mean	0.01	0.482	0.474	2.4E-4	4.8E-5	1.3558

The amount of carbon in the core is slightly less than is found in the 7.0 $M_\odot$ star. This makes it unnecessary for the present investigation to evolve any intermediate masses.

The mass at which the maximum amount of carbon is produced may be either greater or less than 7.0 $M_\odot$, but any variation in the composition due to the mass is quite small. Of course, this is only with respect to the current assumptions, of which the lack of semi-convection in the core is probably the most serious.

IX-5. Effect of the carbon-alpha reaction rate

As with the previous masses the evolution of the cores is repeated using a range of the carbon-alpha reaction rate parameters as given in Table 4-5 to determine the effect of the carbon-alpha reaction rate on the end abundances.

The results are summarized in Table 9-6. The notation is the same as previously used. The amounts of elements heavier than oxygen are considerably larger than in the lighter mass stars, but they are still quite small.

Table 9-6. Effects of varying the carbon-alpha reaction rate.

3α	$C\alpha$	X_C	X_O	X_{Ne}	X_{Mg}	N_r
mean	0.005	0.583	0.374	5.0E-4	1.2E-4	2.0784
mean	0.010	0.482	0.474	2.4E-4	4.8E-5	1.3558
mean	0.020	0.341	0.615	2.2E-4	3.0E-5	0.7393
mean	0.040	0.174	0.781	3.1E-4	4.6E-5	0.2971
mean	0.060	0.0851	0.870	6.1E-4	1.2E-4	0.1304
mean	0.100	7.3E-4	0.942	5.3E-3	7.6E-3	0.0010

CHAPTER X

APPROXIMATIONS TO HELIUM BURNING

X-1. Introduction

The use of the core evolutions is an approximation to an evolutionary sequence of the entire star. The approximation should be quite good, as shown in section VIII-5, and a considerable saving in computer time is realized. The reaction rates may be solved easily with a computer so there is no need to approximate them. Any necessary approximation involves the conditions under which helium burning takes place. Previously simplier approximations have been used. In some cases these may give additional information to the understanding of the helium burning phase. In any case, the helium burning phase should be carefully studied to determine the range of validity of various approximations.

X-2. General properties of the rate equations

The rate equations, equations (7.26) through (7.29), give the rate of change of each element as a function of the energy generation rates. These rate equations may be integrated by the method of section VII-2. This is not the most straightforward way since the energy generation rate really does not need to be known; however, it is convenient to use the same algorithm that is used in the evolutionary calculations. This prevents differences due to programing technique.

The energy generation rates may be written as

$$\varepsilon_{3\alpha} = C_{3\alpha}\, Y^3\rho^2\, f_{3\alpha}(\rho,T)\, b_{3\alpha}(T), \tag{10.1}$$

$$\varepsilon_i = C_i\, YX_i\rho\, f_i(\rho,T)\, b_i(T) \tag{10.2}$$

where ε is the energy generation rate for alpha capture on the i-th element. The function f(T) is the screening term, and the function b(T) contains the remaining temperature dependence.

In the interior of a star the total energy generation rate, the density, and the temperature change as the star evolves. Since the important variable is the amount of helium, these may be expressed as

$$\varepsilon_{tot} = \varepsilon_{tot}(Y), \tag{10.3}$$

$$\rho = \rho(Y), \tag{10.4}$$

$$T = T(Y). \tag{10.5}$$

However, only two of these are independent for a given composition, which is obtained from the initial composition and the integration of the rate equations.

Also in the core of a star a convection zone may mix a large region. The energy generation rate, and hence the rate of change of the different elements, is highly concentrated in a very small region in the center of the star. The convection zone is usually much larger than the region where all but a small fraction of the changes are occurring. The effect is to increase the time scale, and if the zone is growing near the end of helium burning, to decrease the carbon to oxygen ratio.

The approximation of the core evolutions allowed convective mixing and hopefully fixed fairly closely the total energy generation rate and the density. Any moderate differences in the reaction rates will

produce a small change in temperature. If the rate equations are simply integrated by the method of section VII-2, using only equations (7.36) through (7.45), then the effect is to assume a region with constant amount of material in it. The size of the region is unimportant since the abundances are given as fractions. Thus at the worst, simply integrating the rate equations would give a situation where the convection zone is static or shrinking. A shrinking convection zone would alter the time rate of change of a given element but would not mix additional material into a region. It would not effect the rate of change of a given element with respect to the helium abundance.

The major temperature dependence may be simply written as

$$b(T) = T^{-m} \exp(-ET^{-p}) \tag{10.6}$$

where m, E, and p are constants for the given reaction. This is written neglecting the screening contribution and other small corrections. The derivative of b(T) with respect to temperature then becomes

$$\frac{db}{dT} = \frac{b}{T} (pET^{-p} - m). \tag{10.7}$$

The quantity in parenthesis is equal to the exponent n in equation (1.1). For the triple-alpha reaction $n \simeq 40$, and for the carbon-alpha $n \simeq 20$.

X-3. Effect of a growing convection zone

From the evolutionary sequence of the 7.0 $M_\odot$ star the values of the central density and temperature as a function of the central helium abundance may be obtained. This fixes the energy generation rates for each reaction. The rate equations may then be integrated from the initial abundances of

$$Y = 0.9560 \qquad X_i = 0.0 \tag{10.8}$$

where X_i is the abundance of the i-th element which is heavier than helium. To provide a realistic time step the change in the amount of helium is required to be a small fraction of both the helium remaining and the amount burned. This provided small time steps near the beginning of helium burning, where normally the structure changes in the star would keep the time steps small, and near the end when the composition changes limit the time step.

Table 10-1. End abundances for convective and radiative centers.

case	X_C	X_O	X_{Ne}	X_{Mg}	N_r
star center	0.564	0.392	1.3E-6	5.6E-8	1.9184
edge of core	0.630	0.326	2.2E-7	8.9E-9	2.5767
core only	0.548	0.408	1.3E-6	5.9E-8	1.7909
integration	0.674	0.282	2.1E-6	9.7E-8	3.1836

The results are given in Table 10-1. The reaction rates used are: triple-alpha, "mean"; carbon-alpha, $\gamma_{1\alpha}{}^2 = 0.01$ MeV. The first entry is for the center of the 7.0 $M_\odot$ star, the second is for the shell just outside the maximum extent of the convective core, the third is for the core evolution with the same reaction rate parameters, and the last entry is for the present integration.

The amount of carbon produced is somewhat higher than previously found, even at the edge of the core. Of course the actual burning occurs over a small region in the star, and the changes in temperature and density across the region may change the relative values of the reaction rates. This probably represents a maximum value of the abundance of carbon produced. In any reasonable situation helium burning

will be accompanied by a convection zone. The details of the convection zone will affect the end abundances. The effects of a realistic semi-convective treatment will most likely be less than those of full convective mixing only. Thus the limits of the carbon abundance for the given values of the reaction rates are given in Table 10-1.

The carbon abundance as a function of helium content is given in Figure 10-1. The solid line is taken from the center of the 7.0 $M_\odot$ star and the dashed line from the present integration. The light line has a slope of +1, which would be the relation between carbon and helium if the triple-alpha process were the only helium burning reaction present. The convective core in the 7.0 $M_\odot$ star reached its maximum when the central helium abundance was about $Y_c = 0.064$. From that point on, the two lines are roughly equidistant. The portion near the end of helium burning is expanded in Figure 10-2. The light lines have a slope of -3 which is the expected relation if the carbon-alpha reaction is the only one present.

Thus for the first half of the helium burning phase the carbon-alpha reaction is almost negligible. And for the last one per cent of the helium, the triple-alpha reaction makes a very small contribution.

Between these limits the dominant reaction switches from the triple-alpha to the carbon-alpha reaction. From the nature of the dependence on the helium abundance of these two reactions, the switch-over probably occurs toward the end. This is confirmed by noting that the maximum of the carbon abundance in Figure 10-1 occurs near $Y = 0.10$. In the present integration the maximum in the carbon does occur at the point where the two energy generation rates are equal.

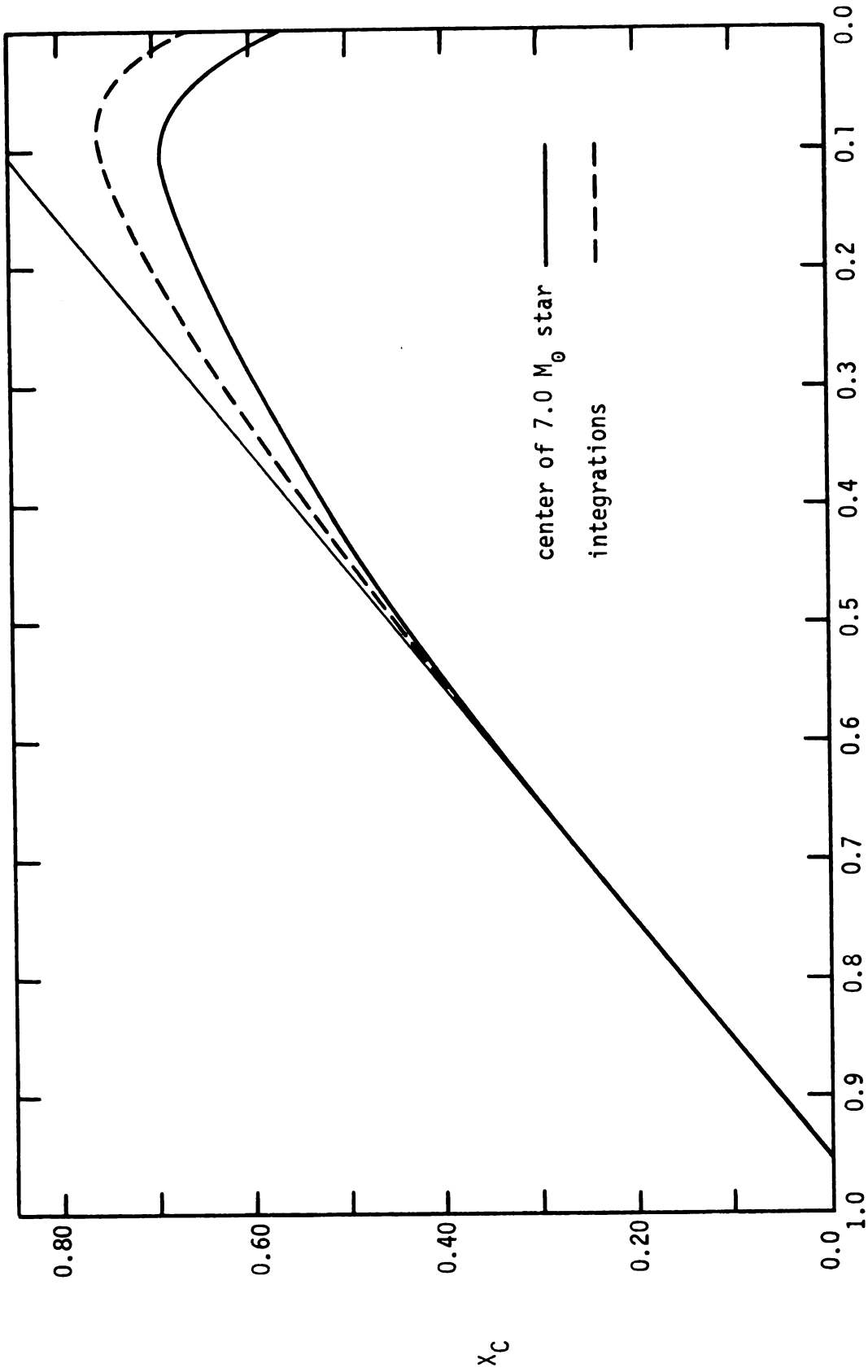

Figure 10-1. Carbon abundance versus the helium abundance.

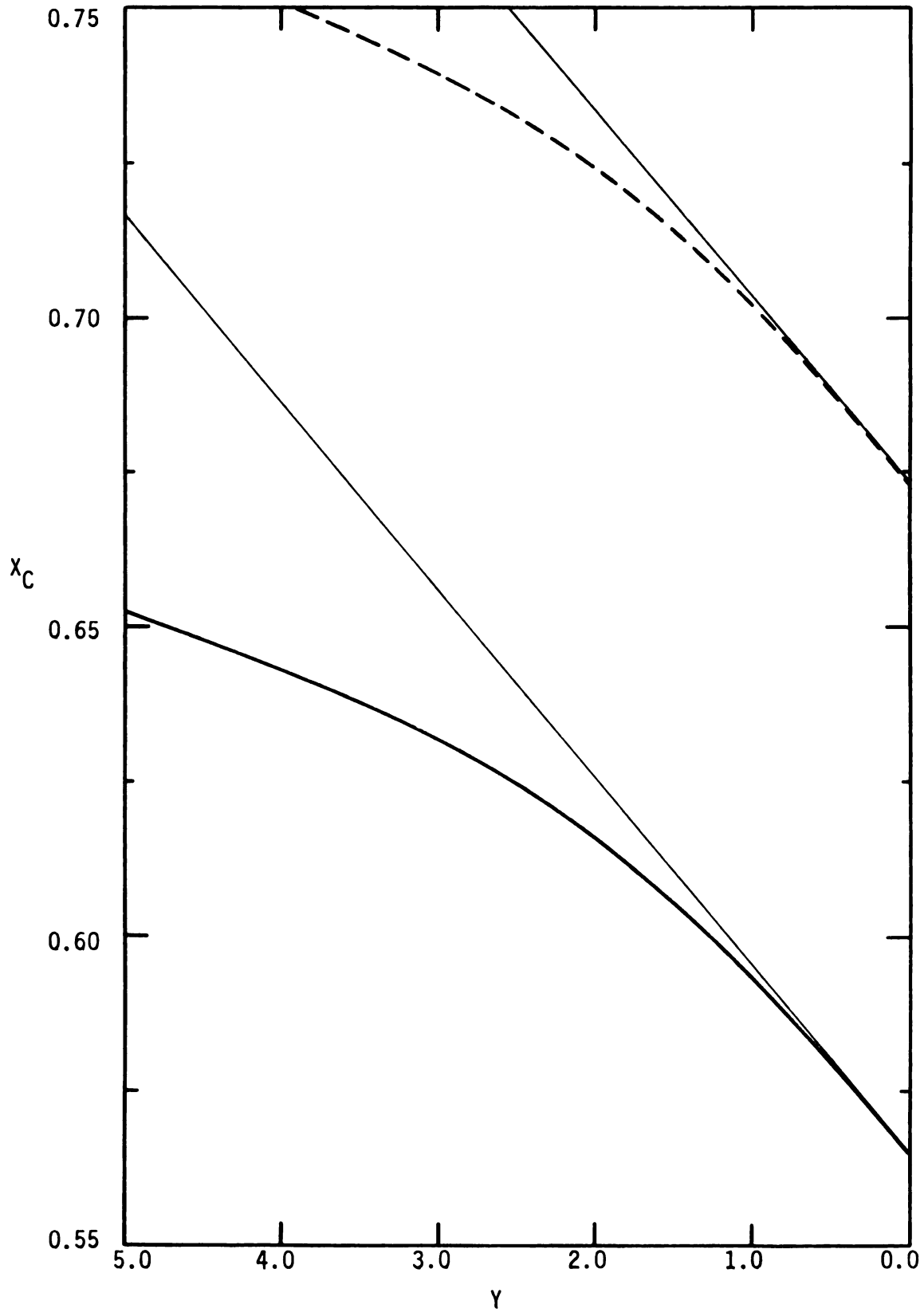

Figure 10-2. Carbon abundance near the end of helium burning.

X-4. Conditions of helium burning

During the evolution of a star through the core helium burning phase the conditions at the center slowly change. These conditions must be examined carefully to determine the effect they have on the end abundances. Figure 10-3 gives the values of the total energy generation rate, the central density, and the central temperature as a function of the helium abundance at the center of the 7.0 $M_\odot$ star described in section VIII-3.

All of these three quantities are roughly constant for most of the helium burning phase. It is not possible for all three to be exactly constant since the energy generation rate is dependent on the composition which is constantly changing. The temperature change is always increasing but the total change is small, as expected, due to the large temperature dependence of the energy generation rates.

The energy generation rate is fairly constant over much of the burning phase. The energy liberated in a star is largely determined by the luminosity of the star. The previous investigation of Cameron (1957) assumed the density and temperature were constant and then simply integrated the rate equations. This leads to very small values of energy generation rate toward the latter portion of the helium burning. This is not very realistic, but the ratio of the triple-alpha to the carbon-alpha reaction rate may be unchanged and hence the relative abundances of carbon and oxygen may be unaffected.

The results of various integrations are given in Table 10-2. In all cases the density and the temperature are fixed by some means. The term "table" refers to the central conditions as found in the 7.0 $M_\odot$

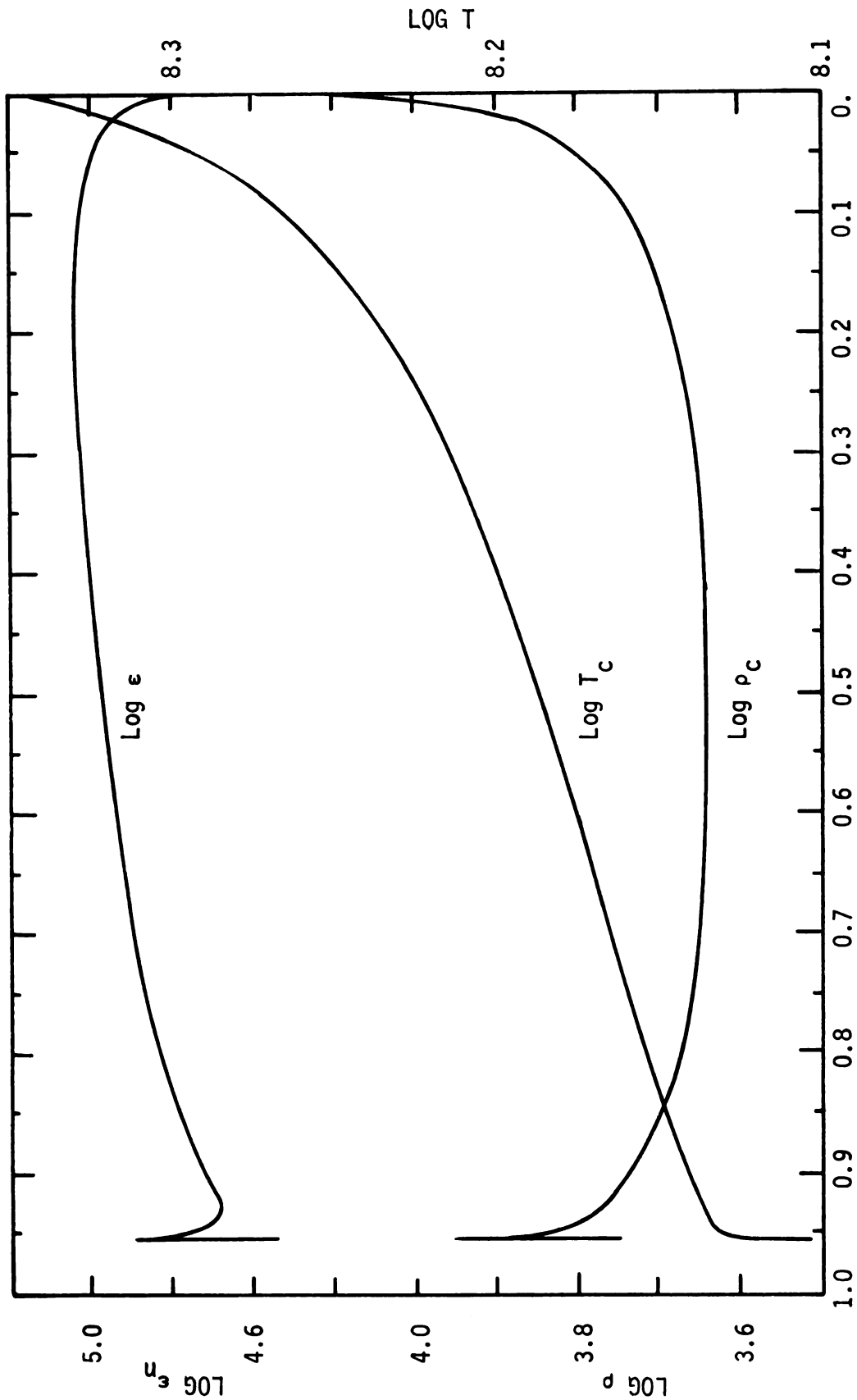

Figure 10-3. Energy generation rate, density, and temperature as a function of helium abundance.

star. Where a quantity is given by a number, it is fixed at that value.

Table 10-2. Results of integrations with constant ρ and T.

log ρ	log T	X_C	X_O	N_r
table	table	0.6738	0.2822	3.184
3.7	8.15	0.3987	0.5573	0.954
3.7	8.20	0.5681	0.3879	1.952
3.7	8.25	0.6601	0.2959	2.975
3.6	8.20	0.5304	0.4256	1.662
3.7	8.20	0.5681	0.3879	1.952
3.8	8.20	0.6030	0.3530	2.278
3.76	8.274	0.7029	0.2531	3.703

The first entry is the result for using both the temperature and density as taken from the center at 7.0 $M_\odot$ star. It is repeated from Table 10-1, for purposes of comparison. The next two sections are the results using constant temperature and density. The values of temperature and density used are those that may be found in the center of star. (See Figure 10-3.) A small change in temperature produces a large change in the end abundance. Yet the values given lie within the range of temperatures actually encountered in the star. Changing the density has a much less effect on the end abundances. Again the values used lie within the range encountered.

The significance is that a constant density may be easily chosen that will reproduce the correct abundances, but it is extremely difficult to choose a temperature that would also reproduce the correct abundances due to the rather rapid changes in the temperature. It is to be expected that the important values are those in the range where the triple-alpha and the carbon-alpha reaction rates are roughly equal.

Much before this point only the triple-alpha reaction is significant and the exact values of density and temperature are unimportant. The same is true near the end of helium burning when the carbon alpha reaction is the only significant reaction.

The last entry is for an integration using values of the temperature and density taken from the first integration, using the tables of the center of the 7.0 $M_\odot$ star, at the point when the triple-alpha and the carbon-alpha energy generation rates are equal. This occurred when $Y \simeq 0.08$. The agreement with the first entry is reasonably good.

A major problem with using this technique to investigate a range of reaction rates is that if one of the reaction rates is changed by a large amount, the point of equal energy generation rates will occur at a different value of the density and temperature. Both of these are increasing, and the effect of increasing either one is to increase the amount of carbon produced. The temperature is also changing quite rapidly which leads to a large uncertainty in the end abundances.

Another possible approximation is to assume that the energy generation rate is a constant. This has the advantage that the conditions of the helium burning are more realistic than found in the constant density and constant temperature case. Since the end abundances depend very strongly on the temperature it is a more reasonable procedure to fix the density by some means and iterate on the value of the temperature until the desired value of the energy generation rate is obtained. This is easily done by a Newton-Raphson iteration. The density may then be fixed, either by using the values obtained from the center of the 7.0 $M_\odot$ star or as a constant.

The results of several integrations with constant energy generation rate are summarized in Table 10-3. The notation is the same as given for Table 10-2. The value of the temperature is determined at each integration step by the procedure outlined above. The first section of the table shows the effects of changing the values of the energy generation with a certain form of the density dependence. The second section gives the effect of varying the density with a fixed value of the energy generation rate.

Table 10-3. Results of integrations with constant ε.

log ρ	ε_n	X_C	X_O	N_r
table	5.0E+4	0.6470	0.3090	2.792
table	7.5E+5	0.6619	0.2941	3.001
table	1.0E+5	0.6714	0.2845	3.146
table	1.5E+5	0.6835	0.2724	3.346
table	2.0E+5	0.6913	0.2647	3.482
3.4	1.0E+5	0.5885	0.3672	2.137
3.5	1.0E+5	0.6143	0.3415	2.398
3.6	1.0E+5	0.6381	0.3177	2.678
3.7	1.0E+5	0.6602	0.2958	2.976
3.8	1.0E+5	0.6805	0.2755	3.293
3.9	1.0E+5	0.6991	0.2568	3.630
4.0	1.0E+5	0.7163	0.2397	3.985

From the first section it is noted that for a wide range the value of the total nuclear burning energy generation rate has a small effect on the end abundances. Also a value of $\varepsilon_n \simeq 10^5$ gives good agreement with the calculation that used the tables of the center of the 7.0 $M_\odot$ star for both the temperature and density. This is roughly the value of the total energy generation rate at the point where the triple-alpha and the carbon-alpha energy generation rates are equal.

The last section of Table 10-3 again illustrates that the particular value of the density has a small effect on the end products. For a given percentage change in the density the effect is greater than for a corresponding change in the energy generation rate. The value of the density that most closely reproduces the "true" values of the end abundances is that value which is found when the two energy generation rates are equal.

Also to be noted are two effects: increasing the energy generation increases the amount of carbon produced and increasing the density increases the amount of carbon. As the mass of a star increases the total energy generation rate increases and the density decreases. The effect of increasing the mass of the star on the amount of carbon is to increase or decrease it depending on whether the energy generation rate increase is greater or less than the decrease in density.

In summary the approximation of constant energy generation rate and, possibly, constant density is more realistic than the constant temperature and constant density approximation. The fixed values of these parameters that best reproduce an integration using the tabular values are those that occur when the triple-alpha and the carbon-alpha energy generation rates are equal. This is true also of the constant temperature case, but specifying the correct temperature is difficult since the amount of carbon produced is quite sensitive to the value of the temperature used. The end results are much less sensitive to the value of the energy generation rate. Also the energy generation rate is very close to a constant near the point when the two reaction rates are equal. So this partially removes the difficulty discussed above in using this technique to investigate other values of the reaction rates.

These approximations are somewhat limited. If the correct values of the central conditions are chosen, then the approximate treatment reproduces the correct values of the end abundances. But a model calculation is required to specify what values of the conditions are to be expected. There is also no provision to include the effects of a growing convection zone, although it is the lack of a correct treatment for such a case that reduces the accuracy of the model calculations. In any core helium burning in a star it is very likely that there will be a convective core. If this core grows very quickly and then remains static or shrinks during the last half of the helium burning phase, then the model calculations and the approximations should give the same results.

CHAPTER XI

SUMMARY

The present investigation is concerned with the production of the alpha elements, principally carbon and oxygen, during the helium burning phase in intermediate mass stars. Three different mass stars, 5.0 $M_{\odot}$, 7.0 $M_{\odot}$, and 15.0 $M_{\odot}$, have been evolved from a homogeneous initial composition of extreme population I until core helium burnout. The solution of the time-dependent stellar structure equations is effected by a Henyey method program.

The helium burning reactions through the neon-alpha are considered. The carbon-alpha reaction rate is obtained by using a four level R-matrix theory model of the 1^- states in ^{16}O. First the carbon-alpha elastic phase shifts are fit to determine the reduced level widths and the energy eigenstates. A selection of the reduced level width for the 7.12 MeV state is made by comparison with the carbon-alpha capture cross-sections. Finally a reaction rate is obtained by numerically integrating the cross-sections over a Maxwellian distribution of energies and fitting the results to an analytic formula. The parameterization of FCZ, which neglects the contribution from the other states, is quite adequate to reproduce the given reaction rates. The resulting numbers in that formula may not be directly related to the physical quantities that entered into its derivation. The formula was used only to provide a convenient functional form of the reaction rate. The numbers were varied to give

the best fit without regard to what they "should" be.

The triple-alpha reaction rate is also considered in some detail. The relative rates of the triple-alpha and the carbon-alpha reaction rates determine the end abundances of carbon and oxygen. The oxygen-alpha reaction rate is quite small. Both the nonresonant contribution, which dominates at low temperatures, and the resonant contribution from the 5.63 MeV state, which becomes important at higher temperatures, are included in the oxygen-alpha reaction rate. The formula used for the neon-alpha reaction rate is fairly crude, and it is also quite unimportant. The nitrogen-alpha reaction is not considered.

The opacities are taken from the Los Alamos tables. The equation of state includes the effects of the ionization of hydrogen and helium and the effects of degeneracy. Conductive opacities are computed whenever degeneracy occurs. Neutrino cooling from three neutrino processes is also calculated. These are: photoneutrinos, plasma neutrinos, and pair-annihilation neutrinos. The reaction rates are modified by the screening contribution from the electron gas.

The evolution of the 7.0 $M_{\odot}$ star during the helium burning phase is repeated with a different value of the carbon-alpha reaction rate. This is used to test the feasibility of investigating the effects of the reaction rates on the end products by evolving only a portion of the star. The approximation is that the structure of the star is relatively insensitive to moderate changes in the values of the reaction rates.

The evolutions of just the core agree quite well with the evolutionary sequences of the entire star, even when the reaction rates used to obtain the boundary conditions are much different from the ones actually used in the evolution of the core. A considerable saving in computing

time is realized on several counts: fewer shells, simpler structure, certain "physics" such as ionization omitted, and longer time steps. The core evolutions take about 1/12 the computer time as do the evolutions of the entire star. Also, the storage requirements are greatly reduced.

Once the core evolutions are shown to be feasible, they may be used to investigate a variety of reaction rate values. The triple-alpha rate is fairly well determined. The effect in its uncertainty is about ±20 percent in the carbon abundance.

The carbon-alpha reaction rate is quite poorly known. A range of values of the reduced level width for the 7.12 MeV state in ^{16}O must be used. The range considered is $\gamma_{1\alpha}{}^2$ = 0.005 - 0.1 MeV. Several values within this range are computed for each mass. The abundance of carbon varies approximately from 0.03 to 0.66. The effect of the different conditions due to the mass of the star is quite small.

A large uncertainty arises from the growing convective core. The exact growth rate near the end of the helium burning is dependent on the treatment of the edge of the convective core. Unfortunately, if the zone grows when the carbon-alpha reaction dominates, the effect is to reduce the abundance of the carbon.

The maximum effect may be estimated by integrating the rate equations assuming that there is no convective mixing. This indicates that the amount of carbon produced is reduced by about 20 percent due to the growing convective core. One may expect that the actual abundance of carbon would lie within these limits. A convection zone will be present during the helium burning, but a more correct treatment would produce a composition gradient that would retard its growth.

The conditions of helium burning are such as to produce a constant density and a constant energy generation rate situation. If the temperature and the density are held constant, the end abundances are extremely sensitive to the value of the temperature used. The fixed conditions that best reproduce the results obtained by using the tabular values of the density and the temperature taken from the center of a star are those found at the point when the triple-alpha and the carbon-alpha energy generation rates are equal. This usually occurs when the abundance of helium is of the order of 0.1.

The envelope structure of the 15.0 $M_{\odot}$ star seems to suffer greatly from the lack of a semi-convection treatment. The 7.0 $M_{\odot}$ star appears to be a border-line case. A small convection zone did appear but had a negligible influence on the structure of the envelope. There is no such convection zone in the 5.0 $M_{\odot}$ star.

There is a certain amount of the "physics" that could be easily omitted without seriously affecting the results. The neutrinos play no role in the structure of the core until after core helium burnout. The center of the stars always remains in the weak degeneracy region, hence the high degeneracy code is not needed. The neon-alpha reaction is completely unimportant. There are several provisions in the code for handling special circumstances, such as a luminosity inversion, that are not needed during the helium burning phase.

However, it is only after the evolution has been completed with these included that it can be determined that they are not needed. The amount of computer time to calculate these is quite small when compared to the total time needed.

For a reasonable choice of the reaction rates, carbon will be

produced in sufficient quantities that the next burning phase will be that of carbon-carbon burning. The exact amount of carbon produced depends not only on the values of the reaction rates but on the treatment of the convective core. The details of the future evolution of the star are dependent on the exact value of the carbon left over from the helium burning, but the gross properties will be those of carbon-carbon burning.

The problem of helium burning may be investigated by using a constant density and energy generation rate approximation. This neglects the effects of the convective core. The problem then is to determine what values to use that are realistic in terms of an actual model. Changing the values of the reaction rates will change the values of the density and energy generation rate that would occur at the point of equal energy generation rate of the triple-alpha and the carbon-alpha reaction rates in an actual star. This leads to an uncertainty in the end products that is additional to the uncertainty from other causes. The only accurate solution is to do a model calculation. The core evolutions seem to be well suited to this, but they do depend on an evolutionary sequence of the entire star to obtain the values of the boundary conditions.

In view of the large uncertainties, it is desirable to investigate this problem of the helium burning phase with some sort of an approximation, unless large amounts of computer time are available. The two large remaining uncertainties are: the exact value of the reaction rates, principally the carbon-alpha reaction, and the correct treatment of a growing convective core.

The present investigation is concerned with the effects of the

uncertainties in the reaction rates. No attempt is made to develop a semi-convective treatment. Such an improvement seems to be the next logical step in improving the computational technique. If a more precise value of the carbon-alpha reaction is made available, then the results of this work may be applied. Within the context of the approximations of the model used the end products of the helium burning phase can be determined.

The fault, dear Brutus, is not in our stars,
But in ourselves, that we are underlings.
(Julius Caesar II.ii.139-140*)*

LIST OF REFERENCES

LIST OF REFERENCES

Ajzenberg-Selove, F., and Lauritsen, T. 1959, Nucl. Phys., 11, 1.

———. 1968, Nucl. Phys., A114, 1.

Arnett, W.D. 1969, Astrophys. and Space Science, 5, 180.

Austin, S.M. 1970, private communication.

Austin, S.M., Trentelman, G.F., and Kashy, E. 1971, Ap. J. Letters, 163, L79.

Bahcall, J.N. 1966, Phys. Rev. Letters, 17, 398.

Bahcall, J.H., and May, R.M. 1968, Ap. J. Letters, 152, L17.

Baker, N., and Kippenhahn, R. 1962, Z. Astrophys., 54, 114.

Barker, F.C. 1970, private communication.

———. 1971, preliminary draft.

Barker, F.C., Hay, H.J., and Treacy, P.B. 1968, Aust. J. Phys., 21, 239.

Beaudet, G., Petrosian, V., and Salpeter, E.E. 1967, Ap. J., 150, 979.

Benn, J., Dally, E.B., Müller, H.H., Pixley, R.E., Staub, H.H., Winkler, H. 1966, Phys. Letters, 20, 43.

Bodenheimer, P., Forbes, J.E., Gould, N.L., and Henyey, L.G. 1965, Ap. J., 141, 1019.

Böhm-Vitense, E. 1958, Z. Astrophys., 46, 108.

Burbidge, E.M., Burbidge, G.R., Fowler, W.A., and Hoyle, F. 1957, Rev. Mod. Phys., 29, 547.

Cameron, A.G.W. 1957, Atomic Energy of Canada Ltd. Rpt. AECL, 454.

Caughlan, G.R., and Fowler, W.A. 1962, Ap. J., 136, 453.

Chandrasekhar, S. 1939, An Introduction to the Study of Stellar Structure, (Chicago: University of Chicago Press).

Chiosi, C., and Summa, C. 1970, Astrophys. and Space Science, 8, 478.

Clark, G.J., Sullivan, D.J., and Treacy, P.B. 1968, Nucl. Phys.,A110,481.

Clayton, D.D. 1968, Principles of Stellar Evolution and Nucleosynthesis, (New York: McGraw Hill).

Cox, A.N., and Stewart, J.N. 1965, Ap. J. Supp., 11, 22.

Cox, J.P., and Salpeter, E.E. 1964, Ap. J., 140, 485.

Deinzer, W., and Salpeter, E.E. 1964, Ap. J., 140, 499.

Endt, P.M., and Van der Leun, C. 1967, Nucl. Phys., A105, 1.

Evers, D., Flügge, G., Morgenstern, J., Retz-Schmidt, T.W., Schmidt, H., Schmidt, J.W., and Skorka, S.J. 1968, Phys. Letters, 27B, 423.

Fowler, W.A. 1960, Mém. Soc. Roy. Sci. Liège, Ser. 5, 3, 207.

Fowler, W.A., Caughlan, G.R., and Zimmerman, B.A. 1967, Ann. Rev. Astron. Astrophys., 5, 525.

Gamow, G. 1928, Z. Physik, 51, 204.

Haselgrove, C.B., and Hoyle, F. 1959, M. N. R. A. S., 119, 112.

Hayashi, C., Hoshi, R., and Sugimoto, D. 1962, Supp. Prog. Theor. Phys., No. 22.

Henyey, L.G., Forbes, J.E., and Gould, N.L. 1964, Ap. J., 139, 306.

Henyey, L.G., Wilets, L., Böhm, K.H., LeLevier, R., and Levee, R.D. 1959, Ap. J., 129, 628.

Hofmeister, E. 1965, Z. Astrophys., 65, 164.

Hofmeister, E., Kippenhahn, R., and Weigert, A. 1964a, Z. Astrophys., 59, 215.

———. 1964b, Z. Astrophys., 59, 242.

———. 1964c, Z. Astrophys., 60, 57.

Hubbard, W.B., and Lampe, M. 1969, Ap. J. Supp., 18, 297.

Iben, I. 1965a, Ap. J., 141, 993.

———. 1965b, Ap. J., 142, 1447.

———. 1966a, Ap. J., 143, 483.

———. 1966b, Ap. J., 143, 505.

———. 1966c, Ap. J., 143, 516.

Jaszczak, R.J., Gibbon, J.H., and Macklin, R.L. 1970, Phys. Rev., C 2, 63.

Jaszczak, R.J., and Macklin, R.L. 1970, Phys. Rev., C 2, 2452.

Jones, C.M., Phillips, G.C., Harris, R.W., and Beckner, E.H. 1962, Nucl. Phys., 37, 1.

Kippenhahn, R. 1963, in Star Evolution, ed. L. Gratton, (New York: Academic Press), p.330.

Kippenhahn, R., and Thomas, H.-C. 1964, Z. Astrophys., 60, 19.

Kippenhahn, R., Thomas, H.-C., and Weigert, A. 1965, Z. Astrophys., 61, 241.

Kippenhahn, R., Weigert, A., and Hofmeister, E. 1967, in Methods in Computation Physics, Vol. 7, ed. B. Alder, S. Fernbach, and M. Rotenberg, (New York: Academic Press), p. 129.

Kourganoff, V. 1963, Basic Methods in Transfer Problems, (New York: Dover Publications).

Lane, A.M., and Thomas, R.G. 1958, Rev. Mod. Phys., 30, 257.

Lauritsen, T., and Ajzenberg-Selove, F. 1966, Nucl. Phys., 78, 1.

Loebenstein, H.M., Mingay, D.W., Winkler, H., and Zaidins, C.S. 1967, Nucl. Phys. A91, 481.

Mestel, L. 1950, Proc. Cambridge Phil. Soc., 46, 331.

Morris, J.M., Kerr, G.W., and Ophel, T.R. 1968, Nucl. Phys., A112, 97.

Paczyński, B. 1970a, Acta Astronomica, 20, 47.

———. 1970b, Acta Astronomica, 20, 195.

Parker, P.D. 1968, Phys. Rev., 173, 1021.

Reeves, H. 1965, in Stellar Structure, ed. L.H. Aller and D.B. McLaughlin, (Chicago: University of Chicago Press), p. 113.

———. 1966, in Stellar Evolution, ed. R.F. Stein and A.G.W. Cameron, (New York: Plenum Press), p. 83.

Robertson, J.W. 1971, Ap. J. Letters, 164, L105.

Salpeter, E.E. 1952, Ap. J., 115, 326.

———. 1954, Aust. J. Phys., 7, 373.

Schwarzschild, M. 1958, Structure and Evolution of the Stars, (Princeton, N.J.: Princeton University Press).

Sears, F.W. 1953, An Introduction to Thermodynamics, the Kinetic Theory of Gases, and Statistical Mechanics, (Reading, Mass.: Addison-Wesley Publishing Co.).

Sears, R.L., and Brownlee, R.R. 1965, in Stellar Structure, ed. L.H. Aller and D.B. McLaughlin, (Chicago: University of Chicago Press).

Stephenson, G.J. 1966, Ap. J., 146, 950.

Straka, W.C. 1971, Ap. J., 164, 125.

Swann, C.P. 1970, Nucl. Phys., A150, 300.

Swann, C.P., and Metzger, F.R. 1957, Phys. Rev., 108, 982.

Thomas, H.-C. 1967, Z. Astrophys., 67, 420.

———. 1968, private communication, quoted in Arnett (1969).

Turner, L.E., and Zimmermann, R.E. 1971, Ap. J., to be published.

Upton, E.K.L., and Bohannan, B. 1971, Ap. J., to be published.

Weigert, A. 1966, Z. Astrophys., 64, 395.

Weisser, D.C., Morgan, J.F., and Thompson, D.R. 1971, preprint.

Wigner, E.P. 1949, Am. J. Phys., 17, 99.

Wigner, E.P., and Eisenbud, L. 1947, Phys. Rev., 72, 29.

Zimmermann, R.E. 1970, unpublished dissertation, University of California at Los Angeles.

APPENDIX

APPENDIX A

THE PROGRAM

The essential computational portions of the program are contained in Chapters II through VII. This present appendix is to supplement the material presented above by illustrating the logic of the programing technique.

Figure A-1. is a flow diagram for the entire Henyey method program. "Boxes" are sections of the code that do a specific computation. Test statements are indicated by "diamonds". Several of the major sections are broken down in greater detail in the remaining figures.

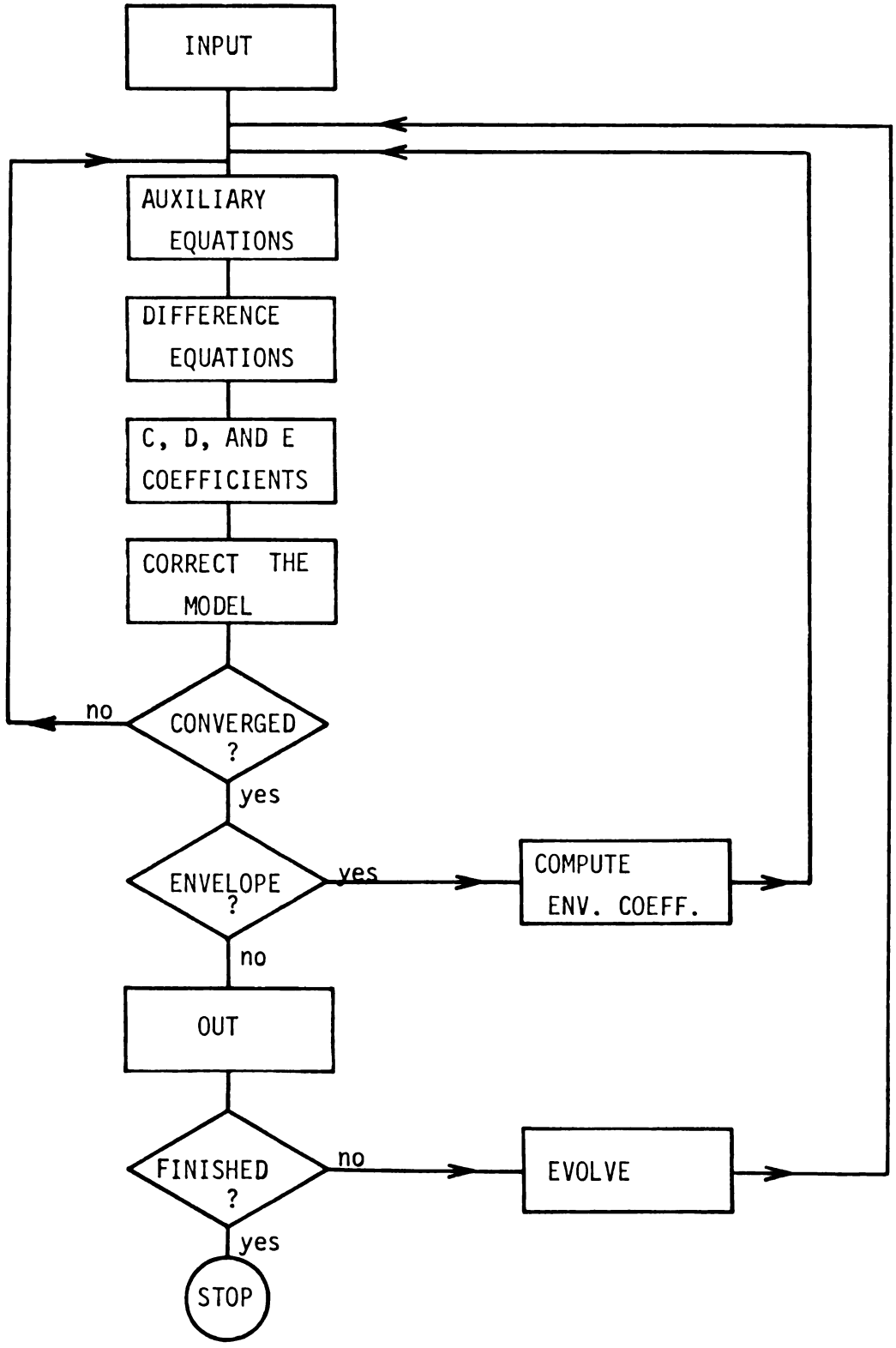

Figure A-1. Flow diagram for Henyey program.

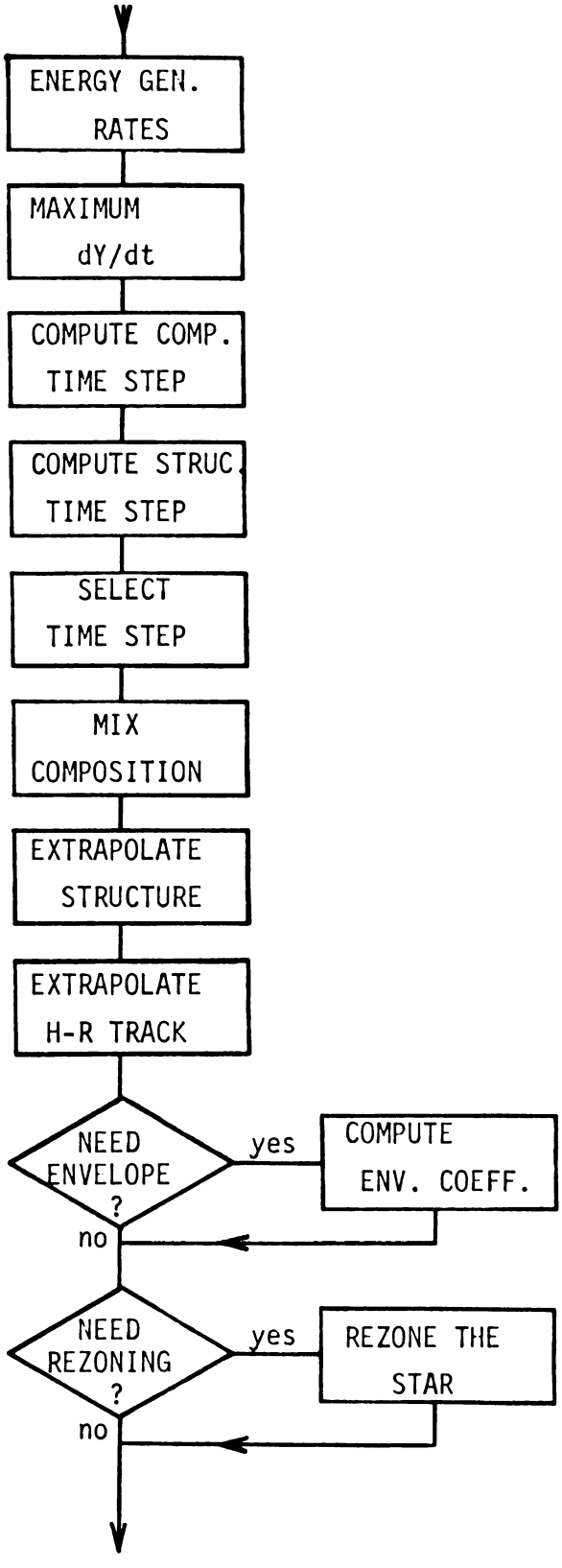

Figure A-2. Time evolution.

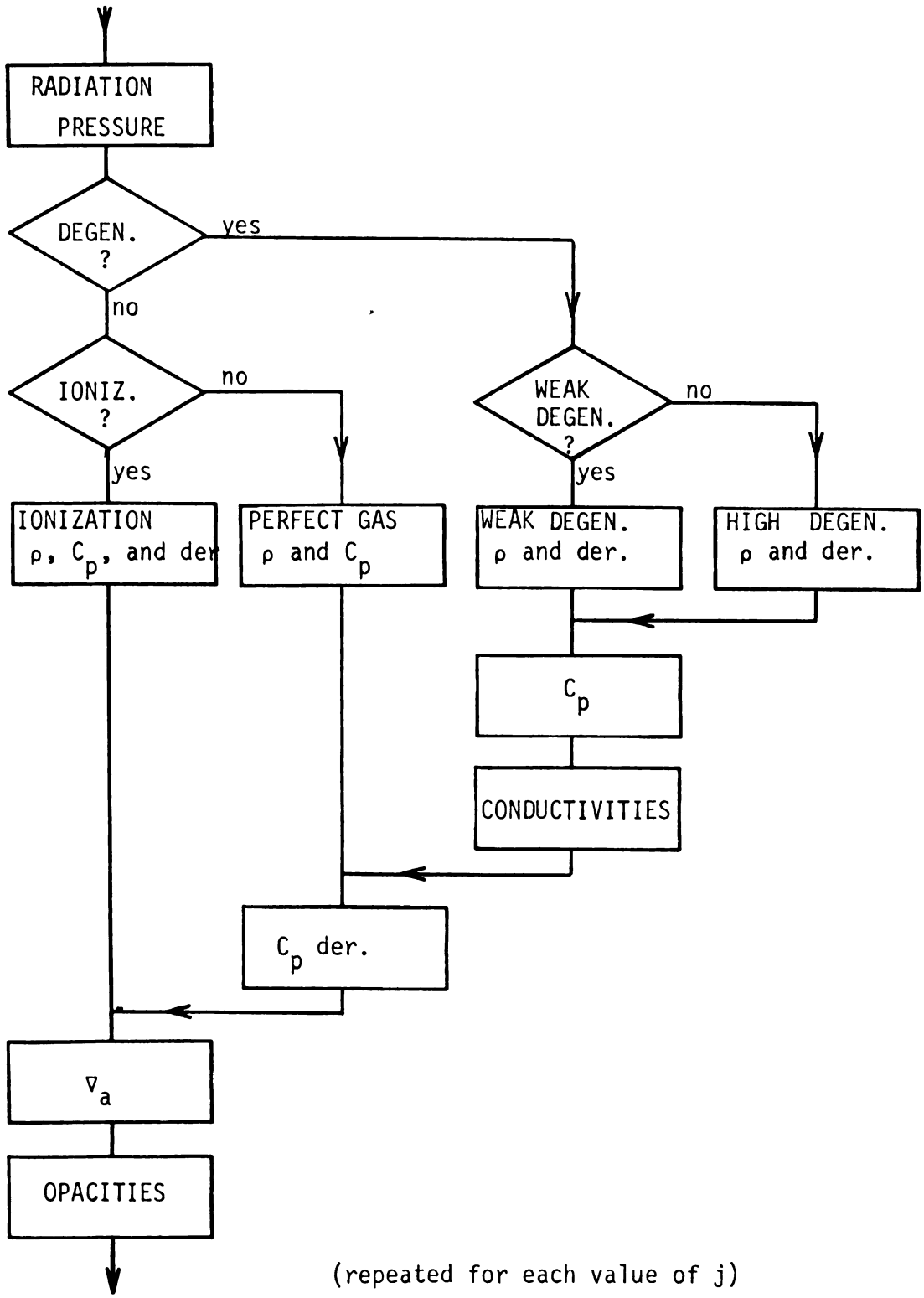

Figure A-3. Equation of state and opacities.

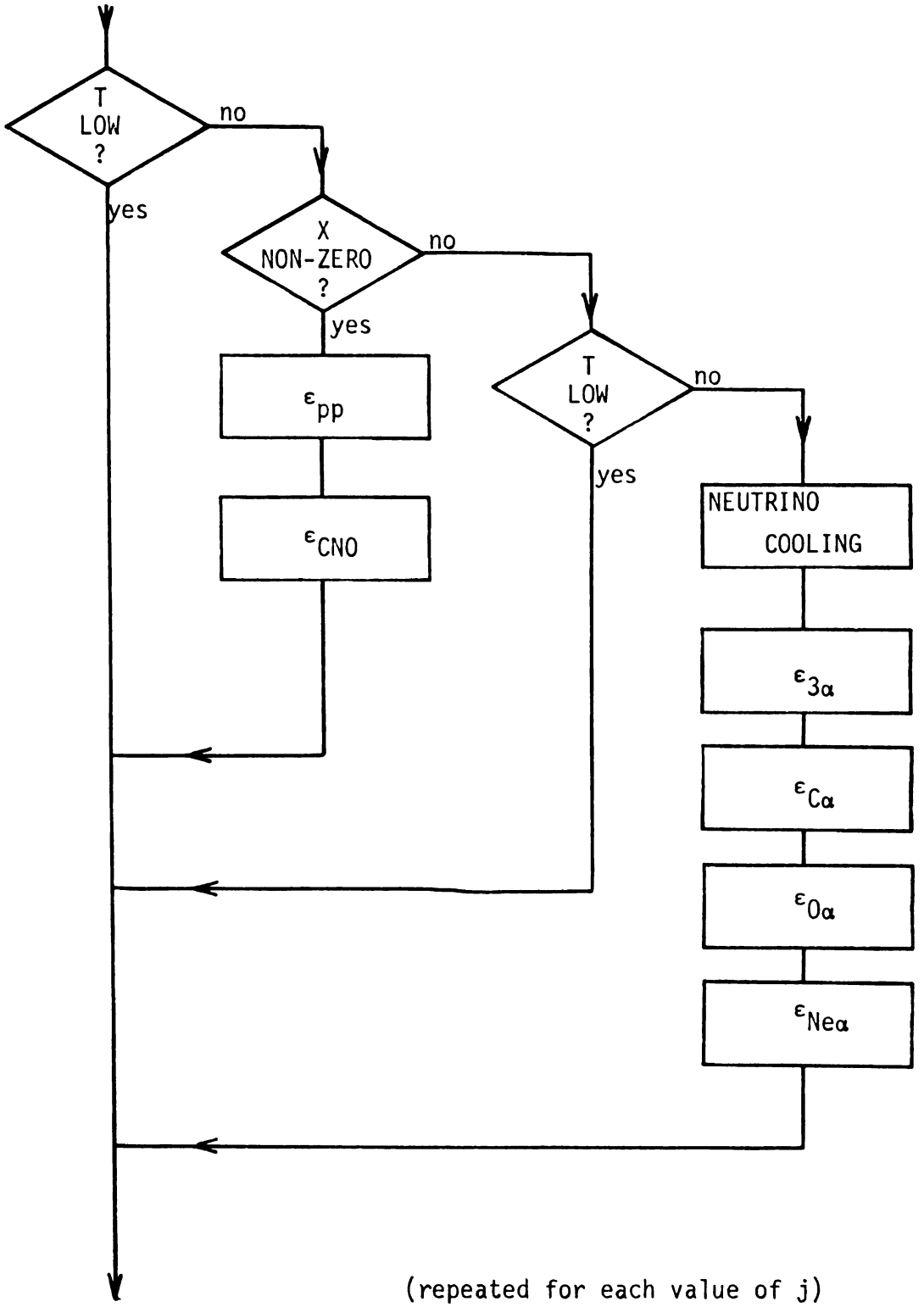

Figure A-4. Nuclear reactions and Neutrino cooling.